Coventry University
Institute for Future Transport and Cities

# Optimal Transmission System for Energy-Efficient Hybrid Electrified Powertrains


**Daizy Rajput**

A thesis submitted in partial fulfilment of the University's requirements
for the degree of Doctor of Philosophy

# Acknowledgement

I would like to express my gratitude towards my supervisors, Dr. Mauro S. Innocente, Dr. Arash M. Dizqah, and Dr. Jose M. Herreros, for their continuous support and encouragement throughout my PhD tenure. Their motivation, guidance, patience, and immense knowledge have not only helped me during my PhD, but also made it the most amazing journey so far of my life.

I would also like to thank my lab-mate at AVAILab and very dear friend Dr. Paolo Grasso, with whom I shared wonderful and challenging moments during my PhD years, bringing both warming heartfelt support and sincere friendly advice in time of need. Additionally, I would like to thank my out of PhD friends Richard Brown and Vinay Mathad for being a constant emotional support throughout this journey.

Last but not least, I would like to thank my father and my mother for their love and support throughout my life. This PhD would not be possible without countless hours of mentoring by my father. Therefore, this PhD is dedicated to my father.

# Abstract

Fuel consumption reduction in automotive vehicles is becoming a stringent norm across the world. Electrified powertrains provide a promising solution to fulfill this requirement. The transmission system is the key component responsible for increasing energy efficiency in an electrified powertrain.

The transmission system of electrified powertrains consists of a planetary gear (PG), one or two motors, battery, and an internal combustion engine. To ensure the optimal operation of the transmission system of an electrified powertrain, the optimal operation of each powertrains components is required. The PG plays a critical role by combining the output torques of different powertrain components (i.e. motors and engine) and delivering the resulting torque to the wheels. Whilst previous studies show that the number of planetary gears affects performance of hybrid electric vehicles (HEVs), there is no prior study to systematically investigate such effects on energy consumption. This thesis quantifies the energy efficiency improvement of HEVs due to increasing the number of PGs from one to two, and from two to three. This is done by comparing the minimum energy consumption for different topologies when the rest of the powertrain components –namely electric motors, batteries and engine– are the same. To calculate the minimum energy consumption, the thesis develops an optimal energy management strategy (EMS) for each topology to find the optimum sequence of clutch engagement and torque distribution. The minimum energy consumption of a vehicle with different number of PGs is then evaluated using the automotive simulation models (ASM) from dSpace. Results show that, for the same electric motors and engine, increasing the number of PGs from one to two and from two to three reduces energy consumption by 5% and 1.5%, respectively.

# Contents

# List of Figures

# List of Tables

# Chapter 1

# Introduction

## 1.1 Motivation

Fuel economy improvement is a crucial objective of the automotive industry due to limited crude oil supplies and environmental concerns. As shown in Figure 1.1, the department of transport UK has increased the fuel economy standard for both petrol and diesel vehicles up to 43% and 24% respectively, as well as reduced the $CO_2$ emissions limit by 31% in 15 years.

To meet these challenging fuel economy and emission standards, the automotive industries have studied and developed many different technologies. Amongst all of them, the electrification of automotive powertrains shows one of the most promising technologies.

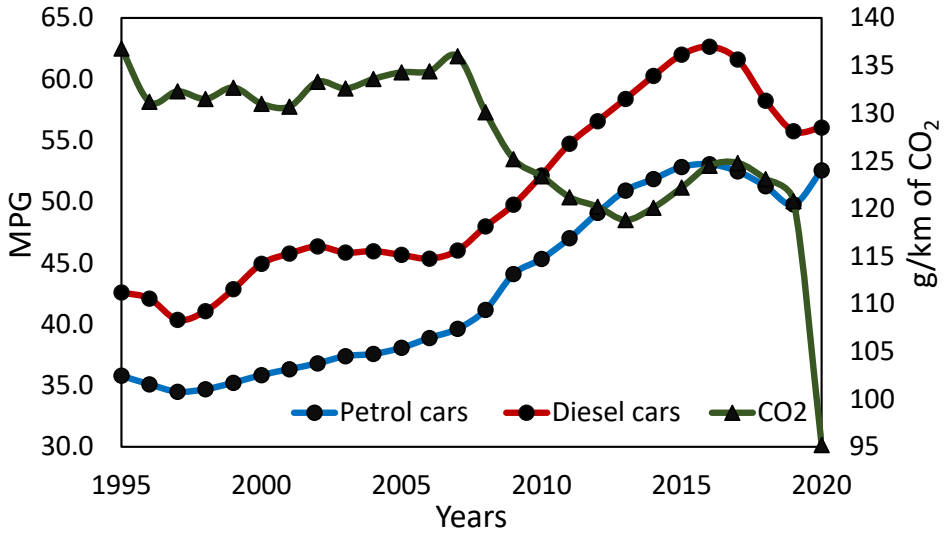


**Figure 1.1:** *Fuel economy and $CO_2$ emission for diesel and petrol vehicles by UK govt over 15 years [2]*

An electrified powertrain having more than one energy source is known as a hybrid

vehicle. There are various types of hybrid vehicle architecture, incuding - hybrid electric vehicle (HEV), mild HEV, and plug-in HEV, etc. Out of all three hybrid architectures, HEVs are the most popular.

HEVs consist of an internal combustion engine (ICE) and a battery pack as the two main energy sources. Electric Motors/Generators (MGs) are also used along with engine so that engine operation can be more fuel efficient. After more than a decade of research and improvement, HEV technologies considerably improved fuel economy for the passenger cars. Automotive companies like Toyota, General-Motors, Ford, and Chevrolet have successfully launched different HEV in the market. Table 1.1 shows the fuel economy improvement by using hybrid powertrain for the same vehicle model.

| Vehicle Models | Gasoline - MPG (city) | HEV - MPG (city) |
|---|---|---|
| Toyota Camry | 25 | 40 |
| Honda Accord | 27 | 49 |
| Chevrolet Malibu | 27 | 47 |
| Ford Fusion | 24 | 44 |
| Kia Optima | 24 | 34 |

**Table 1.1:** *Comparison of fuel economy between gasoline and HEV variants of same vehicle models [3].*

The concept of HEV has a history similar to automobile itself. The original purpose of a HEV powertrain is to improve drivability, fuel economy and efficiency of powertrain components. It also assists engine so that engine can be restricted to operated in the optimal efficiency regions and fuel consumption is reduced. HEVs also offers wide range of operation of electric motors which results in reducing equivalent fuel consumption. Therefore, improved fuel economy is the main performance metric of HEVs.

In 1899, at Paris Salon [4], the very first hybrid vehicle was launched. It was a parallel hybrid electric vehicle with a gasoline engine, a motor, and a lead-acid battery pack. In the current scenario and with the ability to charge the battery from the grid, HEVs can be categorised in to two types: the conventional self charging HEV and plug-in HEV. However, if we further categorize HEVs by mechanical connection of the powertrain components and power flow, there are four more categories namely: series hybrid vehicles, parallel hybrid vehicles, series-parallel (power-split) hybrid vehicles and multi-mode hybrid vehicles. Since there is no fundamental difference between the conventional self charging HEV and plug-in HEV in terms of mechanical connection of powertrain components, in this dissertation, we will emphasise more on the HEV powertrain in which battery is charged using engine power and different modes of operation are enables by engaging and disengaging different clutches.

Figure 1.2 shows the hierarchy of electrification of a conventional fossil fuel based powertrain to a full electric vehicle. This work focuses on the hybrid powertrains upto 70% electrification.

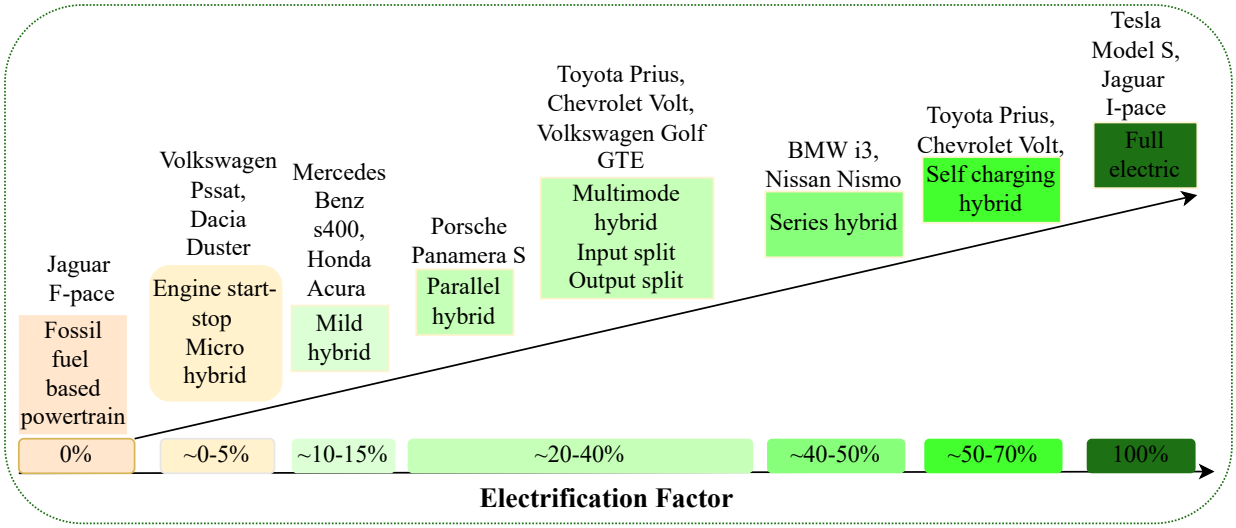


**Figure 1.2:** *Classification of powertrains based on electrification factor*

## 1.2 Aims and Objectives

The aim of this thesis is to develop an optimal transmission system for hybrid electric vehicle (HEV) powertrains, the Energy Management Strategy (EMS) of which should perform mode selection and torque distribution simultaneously. This optimal transmission system will help to investigate the effect of increasing the number of planetary gears on the fuel consumption and battery state of charge in a HEV powertrain.

In order to achieve this, the objectives of this research are:

1. To develop a novel energy management strategy (EMS) that conjointly optimises optimises mode selection, torque distribution, and components efficiencies, ensuring optimal energy consumption by the hybrid powertrain.

2. To test and validate the accuracy and adaptability of the developed EMS in the real-time scenario, hybrid powertrain models in the Software-in-loop modeling containing the EMS should be developed.

3. To analyse the effect of increasing the number of planetary gears on energy consumption and battery SoC for an HEV powertrain. The optimisation of components of a hybrid powertrain affects its energy efficiency. Therefore, this research should focus on analysing the impact of number of PGs, clutches, and different modes of operation in the hybrid powertrain.

## 1.3 Methodology

The methodology used in this study consists of four steps as described below:

1. A hybrid powertrain consists of multiple operating modes. A total of 14 modes of operation are classified, out of which only 9 modes can be used in practical application. Therefore, the modes which are fucntional in hybrid powertrains are modeled as dynamic equations of torque, speed, energy consumption, battery state of charge, modes selection, and components (i.e. engine and electric motors) efficiency.

2. Formulate the energy management strategy (EMS) as a multi-objective cost function. EMS aims to minimise three competing objectives, namely, energy consumption, modes fluctuation, and deviation of battery state of charge from initial to final. The multi-objective problem is turned into a single-objective one by a convex combinations of some quantification of each objective. This EMS simultaneously selects mode and torque distribution, hence ensuring optimal operation of powertrain components.

3. Solving the formulated EMS using KNITRO solver. To solve the mixed-integer non-linear programming type EMS, KNITRO solver is used. The solver is designed for solving large-scale, smooth nonlinear programming problems, and it is also effective for non-linear and non-convex type of problems. The KNITRO solver used for solving the optimisation problem is accessed using NEOS server, which is an open source server. The NEOS server is supported by Morgridge Institute for Research and Wisconsin Institute for Discovery.

   This open source solver only supports problems written in either AMPL (a mathematical programming language) or C language. This work uses AMPL due to its its symbolic problem representation. The AMPL code used for all five topologies is given in appendix. Local optimal solution obtained from the EMS provides optimal values of torque of MG2, torque of engine, rotational speed of MG1, and mode selection for US06 drive cycle. The US06 drive cycle is used in this work because this drive cycle has both aggressive and steady-state acceleration zones, and the efficiency of different operating modes (with engine and without engine) can be analysed together.

4. Develop simulation in loop (SIL) models of all five topologies using the automated simulation modeling (ASM) library of dSPACE. The SIL models of all five topologies differs from each other on the basis of number of planetary gearbox in the drive train models and in their electronic control unit (ECU). The real-time ECU of each topology consist of the local optimal solution from EMS as lookup table. SIL model is simulated over US06 drive cycle with a time step of 1ms. The results obtains from this simulation are presented as contribution in this work.

## 1.4 Contributions

The contributions of this study are as follows:

- Evaluation of the impact of the number of PGs on the energy consumption of HEVs. It is shown that increasing the number of PGs from one to two to three reduces the energy consumption by 5% and 1.5%, respectively.
- Development of optimal EMS optimal EMS for the multi-mode hybrid electric powertrains with different numbers of PGs. The developed EMS simultaneously controls the clutches of the gearbox as well as energy flows of components to minimise energy consumption over a driving cycle.
- Validation of results by proposed EMS using simulation in loop model developed using ASM libraries of dSPACE. The optimal EMS is integrated into the real-time ECU of SIL models. The results also shows that increasing the number of PGs from one to two and two to three reduces energy consumption by 4.7% and 1.1%, respectively. The results obtained from SIL models are slightly different to the dynamic equation based model of EMS due to added complexity and real time nature of the SIL models.

## 1.5 Layout of the Thesis

The remainder of this thesis is organised as follows: chapter 1 shows the introduction, motivation, aim and the objective for this dissertation; the literature review is presented in chapter 2; chapter 3 focuses on formulation, solution, and results of the proposed novel EMS; chapter 4 explains the test platform developed as (SIL models) to show the use of derived EMS in a real time scenario; whilst conclusions are drawn in conclusion and future work.

# Chapter 2

# Literature Review

## 2.1 Hybrid Powertrains with Multiple Planetary Gears

A key factor in reducing fuel consumption in a hybrid powertrain is its topology, which refers to how the powertrain's components (i.e., engine, motors and output) are connected with the nodes of the planetary gears (PG). Liu et al. [5] presented an exhaustive search method to analyse all possible topologies for hybrid powertrains with multiple PGs. A 2-PG powertrain has more clutches than a 1-PG powertrain, achieving multimode operation by engaging or disengaging clutches. While Toyota Prius operates in one mode only, Zhang et al. [6] introduced four modes of operation using three clutches. Results show that this reduces fuel consumption from 115.3 g to 96.2 g. In turn, 2-PG-HEV designs incorporated by Toyota Prius and Chevrolet Volt are claimed to provide improved fuel economy compared to their 1-PG counterparts [7] for the Federal Urban Drive Cycle (FUDS). In both cases, increasing the number of clutches increases the number of modes. Different types of hybrid powertrain topologies upto 3 PGs are discussed below:

### 2.1.1 Series Hybrid Powertrain

A typical series hybrid powertrain has two electric motors. One of the motors is a traction motor and is used to propel the vehicle. Another motor is used as a generator and is driven by the engine to recharge the battery, as shown in Figure 2.1. The traction motor is powered by the battery. In this type of vehicle topology, the engine is not mechanically connected to vehicle output, therefore, the engine speed is independent of vehicle speed. Due to this flexibility of engine operation, the engine can operate efficiently. Additionally, a traction motor can satisfy the torque requested by the vehicle, therefore engine operation is not required for transmission.

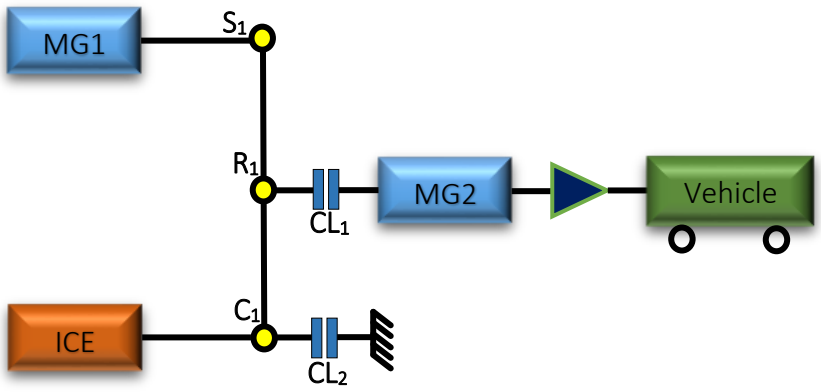


**Figure 2.1:** *Schematic diagram of series hybrid electric vehicle, where $S_1$, $C_1$, and $R_1$ are the sun, carrier, and ring gears of $1^{st}$ planetary gear.*

Since the power of motor required is determined by the driver's power request, the power management strategy of a series hybrid vehicle is comparatively simple. There are many research studies which are carried out of power management strategy for series hybrid vehicle [8–10]. These type of hybrid powertrains improves fuel economy compared to that of conventional vehicles, while keeping the power and control algorithms simple and straightforward with respect to other hybrid topologies. Heavy urban vehicles such as delivery trucks, binwagons, and buses use series hybrid powertrains [11]. There are almost no series hybrid vehicle in the market today, even though first generation of Chevrolet Volt (MY2011 - 2015) and the BMW i3 uses series mode for range-extended driving.

As discussed above, a series hybrid powertrain is simple and easy to control but it suffers highly from energy conversion losses: 100% of engine output is not converted in to electrical power some of the power is lost as heating losses. This low efficiency is more pronounced when the vehicle is running on the highway. Additionally, due to traction motor being the only power source to propel the vehicle, the motor size must be large enough to satisfy the required torque demand.

### 2.1.2 Parallel Hybrid Powertrain

A parallel hybrid powertrain, as shown in Figure 2.2, has one or two motor/generator (MG), a battery pack, an inverter, and an internal combustion engine, which parallelly can provide power required by the vehicle. If the powertrain has only one motor and the motor is relatively small, it can only start/stop the engine as well as provide some regenerative power features. However, if the MG is large, either it can drive the vehicle itself or simultaneously with the engine. The MG acts as a speed controller of the engine and engine operating points can be restricted to higher-efficiency regions, when the power requested by the vehicle is low.

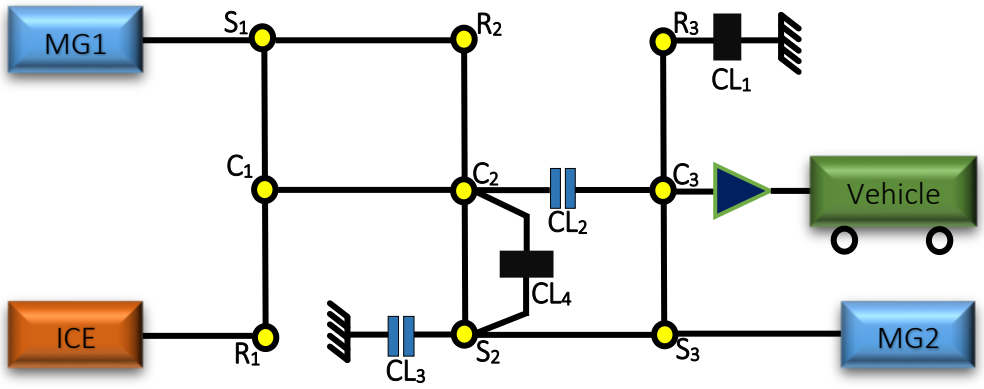


**Figure 2.2:** *Schematic diagram of parallel hybrid electric vehicle, where $S_1$, $C_1$, and $R_1$ are the sun, carrier, and ring gears of $1^{st}$ planetary gear, $S_2$, $C_2$, and $R_2$ are the sun, carrier, and ring gears of $2^{nd}$ planetary gear, $S_3$, $C_3$, and $R_3$ are the sun, carrier, and ring gears of $3^{rd}$ planetary gear.*

Honda Insight launched the first parallel hybrid vehicle in 1999 [12]. The cost involved in manufacturing a parallel hybrid powertrain is very small because it can be designed as an add-on to an existing conventional powertrain. Due to this reason, major major automotive manufactures have launched many different types of parallel hybrid vehicles, including Honda Civic hybrid [13], Volkswagen Passat hybrid and Chevy Malibu hybrid. In past 2 decades, the modeling and control of parallel hybrid vehicles are intensively investigated [13–16].

Since the motor can not be used to charge the battery and assist the engine simultaneously, the energy management strategy to assist motor operation should be controlled carefully to avoid battery discharge specifically during city driving. As city driving has frequent engine stop-start and consumes significant amount of energy from battery as well as forces engine to operate in its low efficiency regions. However, the efficiency of a parallel hybrid powertrain can be very high on highways since engine can be operated near its sweet spot and energy circulation of electrical and mechanical energy to meet vehicle energy requirement can be tremendously decreased.

### 2.1.3 Power-split Hybrid Powertrain

A twp PGs power split vehicle is shown in Figure 2.3. The typical power-split hybrid vehicle uses 2 MGs, one engine, one battery pack which are connected by one or one than one PGs [17, 18]. There are three main power split vehicle topologies : Input split, output split and compound split. In input split topology, one of the MGs is connected to the output shaft (with or without additional gears), while the other MG is neither connected to engine nor to vehicle output [19]. For an output split topology, one of the MGs is connected with engine (with or without additional gears) while the other MGs is neither connected to engine nor to vehicle output [18]. In a compound split topology, both of the MGs are neither connected to engine nor to vehicle output.

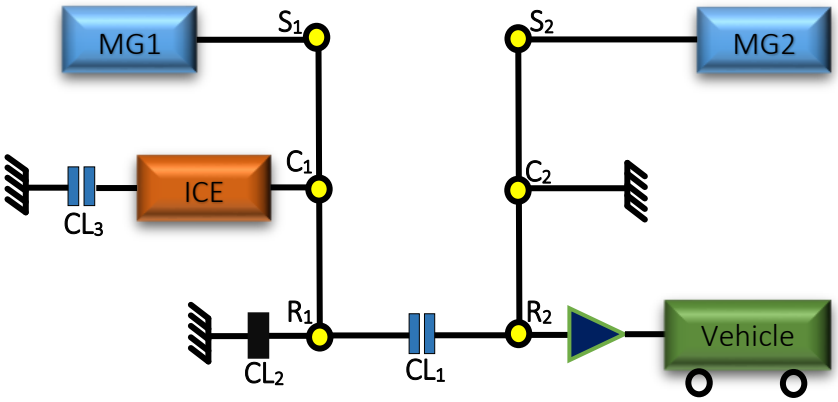


**Figure 2.3:** *Schematic diagram of power-split hybrid electric vehicle*

In a power split topology, the engine power can go to vehicle output via two paths: either through mechanical path or through the electrical path, which is known as engine-generator-motor path. The importance of using PGs in a power split topology is that the engine speed can be regulated irrespective of vehicle speed and Electric-continuous Variable Transmission (EVT) function can be realises. EVT function ensures optimal engine operation regardless of vehicle speed.

The first power split mechanism was used in lawn tractors in late 1960s [20]. Many further investigation on the use of power split mechanism followed, including flywheel transmission in hybrid powertrain [21] and planetary gear train with Continuous Variable Transmission (CVT) [22]. The first commercial car was put into mass production by Toyota Motor Corporation introduced as the Toyota Prius in Japan in 1997 [18]. This hybrid powertrain is called he Toyota Hybrid System (THS) and is the benchmark and foundation of all Toyota hybrid vehicles, as well as for many other automotive companies, including the Ford Fusion Hybrid. General Motor also launched General Motor featuring a major design of power-split hybrid powertrain, which we will discuss later in this dissertation.

The efficiency of power split vehicle is high in city driving conditions due to its EVT function. However, power split vehicles show higher energy losses compared to parallel hybrid vehicles in highway driving due to the circulation of energy from generator to motor. This gap of single mode power split hybrid powertrain can be mitigated using multi-mode hybrid designs, which is explained in the next sub-section.

### 2.1.4 Multi-mode Hybrid Powertrain

Multiple operating modes can be achieved in a power split hybrid by adding clutches. Addition of clutched enables the freedom to choose from different operating modes which can improve fuel economy and drivability.

Figure 2.4 shows an example of multi mode hybrid powertrain. This is a dual mode Allison Hybrid System HEV design patented by General Motors in 2001 [23].

This design has two operating modes which helps in achieving better drivability

and fuel economy. Additionally, this design offers flexibility in the maximum rotational speed of the MGs, resulting in cost effective and robust designs. When vehicle speed is low, CL2 is engaged and CL1 is disengaged, the engine speed can be less and still can provide high torque, resulting in lower engine fuel consumption.

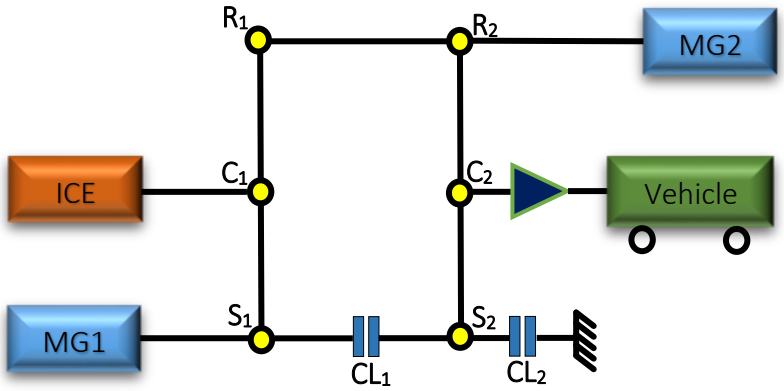


**Figure 2.4:** *Schematic diagram of multi-mode hybrid electric vehicle*

As vehicle speed is increases more than 92km/hr, and when the peed of MG1 reaches zero, then CL1 is engaged and CL2 is disengaged and the vehicle switches to compound split mode which is its second mode of operation. In compound split mode the speed of MG2 is not directly proportional to vehicle speed unlike input split mode, and this feature provides the extended range of operation of MG2 as well as vehicle.

The utilisation of 3PGs in hybrid powertrain is also an area of research by many researchers. Zhunag et al.[24] studied the effect of 3 PG set in a hybrid powertrain. Number of configuration of using 3PG sets are 3024 and at a maximum of 45 clutches can be used, however out of these 45 clutches 7 can be grounded resulting in 38 clutches to be altered. In order to carry out their analysis, they have used PEAR+ methodology for calculating fuel consumption. They have analyzed the possible modes for PG seta and clutches, in order to achieve more efficiency with hybrid powertrain. Using GM-2 as bench mark, they have concluded that using three PG, reduces the need of 38 clutches to 14 clutches and fuel consumption can be reduced to 16.8-22.5mg. This is a considerable reducing in fuel consumption, however implementation of this arrangement in the powertrain is a major issue to be addressed. 3PG set may drastically increase the weight of the entire powertrain, which will result in maintaining the center of gravity (Balancing) of vehicle. Again, 3PG will contribute to frictional and mechanical losses. These issues has not been addressed in the design analysis.

Qin et al.[25] reported a case study to identify better designs for Hybrid tracked dozers, having 3 PG set, 3 motors and 1 internal combustion engine. They have used automated modelling approach derived by Zhang et al. [2], for mode generation. However, mode screening approach is different in their study as number of motors have been increased. Author concluded that best design candidate after screening achieves 11% better fuel economy for a typical cycle. Integrated performance of straight driving and turning has also been improved using their reported algorithm. Integration of their

algorithm has not been made to HEV (cars), this could potentially be an alternative for better fuel economy for HEVs.

Studies show that optimal mode selection reduces fuel consumption in HEVs [26–29]. Up to 12 different topologies are possible in a 1-PG powertrain. By incorporating six clutches, eight modes per topology can be realised. However, 1152 topologies with two modes each are possible for 2-PG powertrains by using only two clutches. Evidently, there is a need for a systematic screening and analysis of modes to identify optimal topology to minimise fuel consumption. The latter is controlled not only by the mode selection but also by the Energy Management Strategy (EMS).

Furthermore, it is shown that increasing the number of PGs also improves fuel consumption of a power-split powertrain. For example, the authors in [30] reported a 4% improvement of energy consumption by increasing the number of PGs from 1 to 2. Benefiting from the reduction in total fuel consumption, Toyota and General Motors launched hybrid powertrains with two PGs for their Prius [6] and Chevrolet Volt [7] models. Later, the authors in [24] showed that a further increase in the number of PGs from 2 to 3 reduces the total energy consumption by 1.1% due to introducing new modes of operation which improve consumption of the city driving and highway cruising. However, the more number of modes, the more complex EMS is required to optimally distribute torque demand between drivetrains, as well as engage and disengage clutches [29, 27, 31]. Moreover, EMS must consider higher mechanical losses, resulting in reduced overall efficiency of the powertrain, due to frequent engagement and disengagement of the clutches.

The above mentioned studies investigated performance of the commercial hybrid electric vehicles with one, two and three PG(s) (which are respectively called 1PG, 2PG and 3PG topologies throughout the rest of this paper) and not the explicit effect of increasing the number of PGs on energy consumption. The latter analysis requires evaluating performance of the topologies when the power components are identical and optimally operating. Hence, the comparison relies on development of an optimal decision making algorithm, i.e. EMS, for each topology to choose the best mode, configuration and torque distribution over driving cycle and minimise the energy consumption, and hence $CO_2$ emission.

Due to the availability of multiple modes, the mode shift optimisation becomes necessary for the optimal operation and jerk-less driving experience within an electrified vehicle. A powertrain with dual motors with EMS consisting polynomial trajectories of speed can significantly reduce vehicle jerk [32]. Also, multi-speed transmission and electric transmission with high efficiency region of electric motor reduces the jerk faced by the driver as well as improves the dynamic and economic performance of the vehicle [33–35]. Each mode of operation of a power-split powertrian represents a type of configurations. A configuration is a topology with a particular order of clutch engagements. A power-split hybrid topology with multiple clutches can generate numerous configurations, where several of the generated configurations may belong to the same mode of operation. For example, a hybrid powertrain may operate at the fully electric mode where only the electric machines contribute to the torque of the wheels, whilst

this mode of operation can be realised with multiple configurations.

Out of many hybrid topologies, power-split powertrain that includes clutches is called a multi-mode topology, which provides better fuel economy than the traditional single-mode topologies due to the higher degrees of freedom (DoF) over a wider range of operating conditions [36]. Many recent studies proposed a wide variety of methods for studying power-split topologies [37–39, 29, 40–58]. Cammalleri et al. [59] proposed a parametric model which is an analysis tool to analyse the working of power-split transmissions with any number of planetary gearing and operating modes. The primary reason of power-split topology to be investigated is its functionality of decoupling the engine speed from the vehicle output speed (similar to series topology) as well as it enables engine to feed both the electric drive and the wheels (similar to parallel) topology [60–63, 36].

Increasing the number of PGs also appears to reduce energy consumption of a power-split powertrain. For example, Rajput et al. [30] reported a 4% decrease in energy consumption by increasing the number of PGs from one to two. Benefiting from the reduction in total fuel consumption, Toyota and General Motors launched hybrid powertrains with two PGs for their Prius [6] and Chevrolet Volt [7] models, respectively. Later, Zhuang et al. [24] showed that increasing from two to three PGs further reduces the total energy consumption by 1.1% due to the introduction of new modes of operation. However, the higher the number of modes, the more frequent the engagements and disengagements of clutches, the more complex the required EMS to optimally distribute torque demand between drivetrains, and the higher the mechanical losses [29, 27, 31].

The aforementioned studies investigated the fuel economy of commercial hybrid electric vehicles (HEVs) with one, two, and three PGs –referred to as 1PG, 2PG, and 3PG topologies from here forth– and not the explicit effect of increasing the number of PGs on energy consumption. The analysis of the latter requires evaluating the performance of the topologies when the power components are identical and optimally operating. Therefore, the comparison relies on the development of an optimal EMS for each topology to choose the best mode, configuration, and torque distribution over the driving cycle to minimise energy consumption.

## 2.2 Energy Management Strategies for Hybrid Powertrain

Literature also shows that engine and equivalent fuel consumption can be reduced by optimising the EMS. There are different types of energy management strategies used in HEVs, such as rule-based [64, 65], instantaneous optimisation-based [66–68, 9, 69], learning-based EMS [70] and predictive EMS [71, 72]. A gap in these strategies is that they do not incorporate mode selection because it leads to a challenging mixed-integer nonlinear optimisation problem. Moreover, these strategies have sequential mode selection and torque distribution, which does not guarantee optimal torque distribution

among powertrain components. To address these issues, we propose a simultaneous torque distribution and mode selection strategy. The proposed strategy is classified under instantaneous optimisation-based EMS.

Rule based EMS are significantly easy to develop and implement in a real vehicle drive but very high precision is required to calibrate the parameters/operating points to guarantee the performance with in a satisfactory range for any real time drive cycle. However the rules are not very scalable and cannot be used for any powertrain architectures and component sizes i.e. component sizing cannot be done using Rule based EMS strategies. Local optimization methods, for example, ECMS, A-PMP, A-ECMS have become more popular than DP over the years as these are the methods which can also be used to find global optimal with some modifications. By performing the offline optimization when the drive cycle is known, these methods give global optimum (using forward-looking vehicle simulator). Moreover, they are also being used to design adaptive optimal strategies (A-ECMS, A-PMS) to achieve near optimal performance for an unknown drive cycle.

Authors [5] presented a foundation which presents many opportunities to extend the work to include various other objectives in the optimal control cost function. For example, taking in to account engine exhaust emissions, battery aging, mechanical losses in gear box etc. The work can be further extended to include use of weather system, traffic information, and navigation system in order to provide more accuracy in the prediction of vehicle trajectory.

Musardo et al. [73] developed a real time novel EMS strategy known as Adaptive Equivalent Consumption Minimization Strategy (A-ECMS). This is a real time energy management for HEV which is obtained by adding an additional on-the-fly algorithm to the conventional ECMS. On-the-fly algorithm is used to estimate the equivalence factor (battery energy consumption conversion to fuel consumption) according to driving conditions. The main idea of A-ECMS is to periodically refresh the control parameter according to instantaneous vehicle load, so that fuel consumption is minimized and battery state of charge is maintained.

Donateo et al. [74] has proposed a novel control strategy for a series hybrid vehicle. Authors have used multi-objective approach due to many goals taken in to account. The Multi criteria decision-making (MCDM) techniques used in this paper are Hurwicz algorithm, Savage algorithm and GA optimization. Authors reported that Savage and Hurwicz can be used without a priori knowledge but have been proved to be unsatisfactory in their final result. GA technique was found to be very effective in satisfying all the performance and efficiency criteria for offline optimization.

Zhang et al. [69] proposed an extension to A-ECMS [75] which they have named IA-ECMS. Authors claims that IA-ECMS provides better performance as compared to conventional A-ECMS. The work can be summarized as: First, a novel method to realize equivalent factor for instantaneous adjustment according to predicted information of future driving condition has been calculated. Secondly, floating car data-based method is used to predict information of future driving condition. Simulation results proves that IA-ECMS can improves fuel economy while taking road conditions also in

to account.

Gupta [66] presented a model based hybrid algorithm for energy management in parallel HEV. The main objective of author is to develop a hybrid algorithm which can provide optimal solution for fuel consumption for both online and offline conditions. The proposed algorithm is divided in to two parts. First part select the mode of operation in parallel HEV operation using IF THEN ELSE rule. IF THEN ELSE rule is again used to optimize fuel consumption by selecting the engine to work in high efficiency zone. In second part fuel consumption is optimized using ECMS algorithm. The main advantage of this algorithm is that it does not need prior knowledge of drive cycle and can work both online and offline. Author claims that IF THEN ELSE + ECMS algorithm reduces the fuel consumption by 3% as compared to conventional ECMS in a US 06 drive cycle and 1.7% in EPA highway drive cycle. Author has considered vehicle velocity has input for proving then mode selection using IF THEN ELSE rule, however vehicle velocity as an input is not the most appropriate parameter for mode selection. Vehicle velocity at wheels is subjective to, traction force, rolling resistance and air drag, therefore optimum mode can be selected appropriately by using vehicle output shaft velocity.

There is an extensive list of previously developed EMS for hybrid powertrains including rule-based strategies [64], those which solve online optimisation problems [76, 77, 66, 68, 67], equivalent consumption minimization strategy (ECMS)-based algorithms [78–80], Pontryagin's minimum principle-based strategies [81], learning-based EMSs [70, 82–84], predictive EMSs [85], and Hierarchical EMSs [86]. These EMS strategies are either only suitable for single-mode topologies or providing a sub-optimal solution by decoupling the mode selection and torque distribution actions. This leads to a sub-optimal solution which is not suitable for the purpose of this work.

Utilising two motors in a hybrid powertrain has proved to the energy consumption [87–93]. The two-motor hybrid system realises both the environmental friendliness of zero-emission and provides higher mileage. Mild hybrid vehicles such as Daimler-Chrysler ESX3, Ford P2000, and Honda Insight consist of only one electric motor in their powertrain. The downfalls of having only one motor are - no self charging of battery, less power during the launch of vehicle, only one EV mode, and lower DoF for the powertrain components. The mild hybrid vehicles use an integrated motor generator (IMG) system. However, the full hybrid vehicle use a dual-machine approach. In the IMG system, the electric machine is attached to the end of the transmission such that the rotor is linked to the crankshaft. Since Motor is connected to the close proximity of engine, the overall powertrain temperature increases during operation. Hence, thermal cooling is a vital design consideration for the powertrains with one motor [94]. In the dual-machine strategy, one motor drives a separate axle or is integrated through one or more PGs. These PGs have a second electrical machine that acts primarily as a motor/generator and is interfaced with the engine and other electric motors during different modes of operation. Moreover, Research shows that dynamic performance of single motor full hybrid powertrain is 50% compare to Toyota Hybrid System (THS) [93]. Authors also claimed that using their design the times required to attain 100

km/h from 0 km/h is 6.69 s compared to THS which is 13.5 s.

Battery state of health (SoH) is also a important aspect of the lifetime performance of hybrid electric vehicles. Therefore, and energy management strategy using particle swarm optimization which considers battery SOH is proposed by Wang et. al [84]. Similarly [95] also showed that using a causal optimal control-based energy management strategy can significantly improve battery SOH. Studies have reported that frequent charging and discharging can have significant impact on battery aging [96]. Therefore, the equivalent cost of battery health must be an objective function for an EMS. As well as, when battery life reaches a certain extent, the performance of battery will change and can even cause failing of a pre-designed controller using a specific EMS [97, 98]. Integration of SOH as a state variable in the control problem, and two separate controllers, SOH controller and SoC controller, prove to be effective solution to enhance overall battery life [99, 95].

The energy consumption between ultracapacitor and battery has a direct relationship. Ultracapacitor provides benifits like - high power density, quick charge and discharge, and multiple cycles can compensate for lithium-ion battery shortages, which results in a longer battery life and improved power performance [100–102]. The EMS of the HEV is responsible for distributing and managing the output power of the ultracapacitor and battery. Therefore, the EMS should consider the battery degradation while meeting the demand power, as a result extending battery life and maximizing vehicle efficiency [103].

Battery capacity degradation models for lithium-ion batteries are classified into three categories: mechanism, equivalent model, and empirical models. The mechanism model is based on the physical and chemical characteristics of the battery, and uses it to understand the phenomenon of capacity decline within the battery and can be incorporated in EMS models. However, the second one which is the mechanism model is a complicated model and obtaining the electrochemical parameters involved in the model is difficult, therefore, it is generally used in battery research, rather than control problems [104]. The third model which is the empirical model has a wide range of applications owing to its simplicity and accuracy [105]. Studies [106, 107, 84, 108] have reported optimal battery SOH model using empirical models, thermal models, PSO, and deep reinforcement learning-based optimisation.

## 2.3 Research Gaps

Following are the gaps identified from the literature and are addressed in this work:

1. Literature did not show the effect of only increasing the number of PGs in a hybrid powertrain. The electrified powertrains in above investigations have different component sizes depending on whether they are within a one, two or three-PG architecture. This work shows systematic analysis of increasing the number of PGs in a hybrid powertrain having fixed component sizes.

2. The studies presented above consider sequential mode selection and torque distribution. The sequential mode selection and torque distribution do not guarantee optimal operation of powertrain components. Therefore, addressing this gap, this work proposes an optimal EMS for the multi-mode hybrid electric powertrains with different numbers of PGs. The developed EMS simultaneously selects modes as well as distributes torque of the components to minimise energy consumption over a driving cycle. The simultaneous selection of modes and torque distribution provides local optimal solution at each sampling time.

3. Literature did not use mix variable objective function for the EMS. This study uses different variables such as, SoC, mode selection, engine and equivalent fuel consumption in the objective function. The solution of the resulting EMS problem provides simultaneous mode selection adn torque distribution.

4. The powertrain component analysed in the literature have two motors, one having smaller capacity compared to other. The studies above have used this configuration for their work without the reason of having two motors of different capacities. This work presents the reasoning behind the use to one smaller and other bigger capacity motor.

# Chapter 3

# Hybrid Powertrain with Multiple Planetary Gears

Multi-mode hybrid powertrains use one or more planetary gears (PGs) to connect different powertrains like- engines, motors, and differential. Increasing the number of PG also increases the number of clutches resulting in different operating modes within a single powertrain topology. Topology in this work refers to how the powertrain's components (i.e., engine, motors, and output) are connected with the nodes of the planetary gears (PG). Liu et al. [5] presented an exhaustive search method to analyse all possible topologies for hybrid powertrains with multiple PGs. A 2-PG powertrain has more clutches than a 1-PG powertrain, achieving multi-mode operation by engaging or disengaging clutches. While Toyota Prius operates in one mode only, Zhang et al. [6] introduced four modes of operation using three clutches. Results show that this reduces fuel consumption from 115.3 g to 96.2 g. In turn, 2-PG-HEV designs incorporated by Toyota Prius and Chevrolet Volt are claimed to provide improved fuel economy compared to their 1-PG counterparts [7, 109] for the Federal Urban Drive Cycle (FUDS). In both cases, increasing the number of clutches increases the number of modes. Studies show that optimal mode selection reduces fuel consumption in HEVs [27, 26, 28, 29]. The literature shows that torque distribution and mode selection are a sequential process. However, this work presents an EMS which simultaneously selects modes and distributes torque.

This chapter discusses the different components used in this work. Also a discussion on deriving different modes from a given number of PGs and clutches is also presented. Finally this chapter elaborates the formulation, solution, and results of the proposed EMS.

## 3.1 Models of Powertrain Components

### 3.1.1 Planetary Gear

One or more PG(s) are in the core of the power-split hybrid powertrains. As shown in Figure 3.1, a PG consists of three gears, called as sun (S), ring (R), carrier (C) gears. Also, the radii of ring gear and sun gear are represented as $R_r$ and $S_s$, respectively. A PG, however, has two degrees of freedom because the angular velocities of these three gears are related as follows:

$$\omega_S S_s + \omega_R R_r = \omega_C (R_r + S_s) \tag{3.1}$$

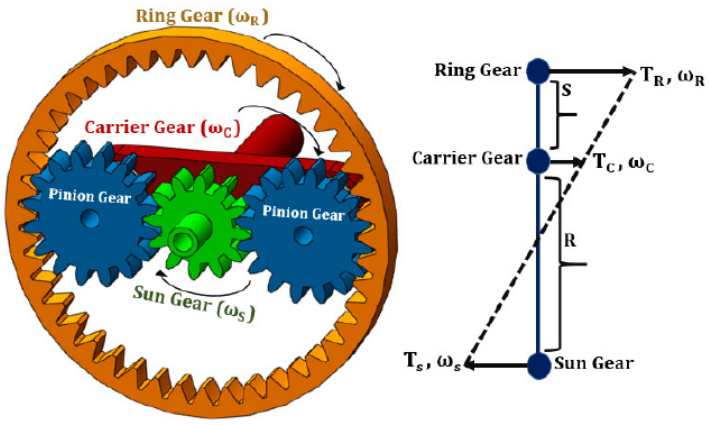


**Figure 3.1:** *3-D representation of a planetary gearbox and its lever analogy [30]*

In this work five different hybrid powertrains are investigated. Figure 3.2 illustrates a Lever diagram of each of the five hybrid topologies in this study. Table 3.2 also summarises the clutch engagements of the modes of operation these topologies can generate. Figure 3.2a shows the 1PG-1 topology that can realise three modes of operation with different clutch engagements. 2PG-1 and 2PG-2 topologies are shown in Figure 3.2b and Figure 3.2c, and realise up-to 5 modes. The 3PG-1 and 3PG-2 topologies are shown in Figure 3.2d and Figure 3.2e which can generate up to seven distinct modes of operation. Table 3.1 summarises the size of components and other parameters of the nominal car that hosts the five transmission.

Table 3.2 shows clutch engagements of different modes of operation. However, due to different number of clutches, the number of available modes for each topology are different. For example, mode 1, mode 3, and mode 4 are available for all five topologies, but mode 7 only exists in 3PG-2 topology. Furthermore, mode 8 which is the series mode is only available in 1PG-1 and 2PG-1 topologies. Modes 6, 7, and 9 which are fixed gear modes are only available in 3PGs topologies.

Each mode of operation is modelled by a binary value indicating whether the mode is selected or not. For example, $m_1$, as a binary variable, can be either 0 (not selected)

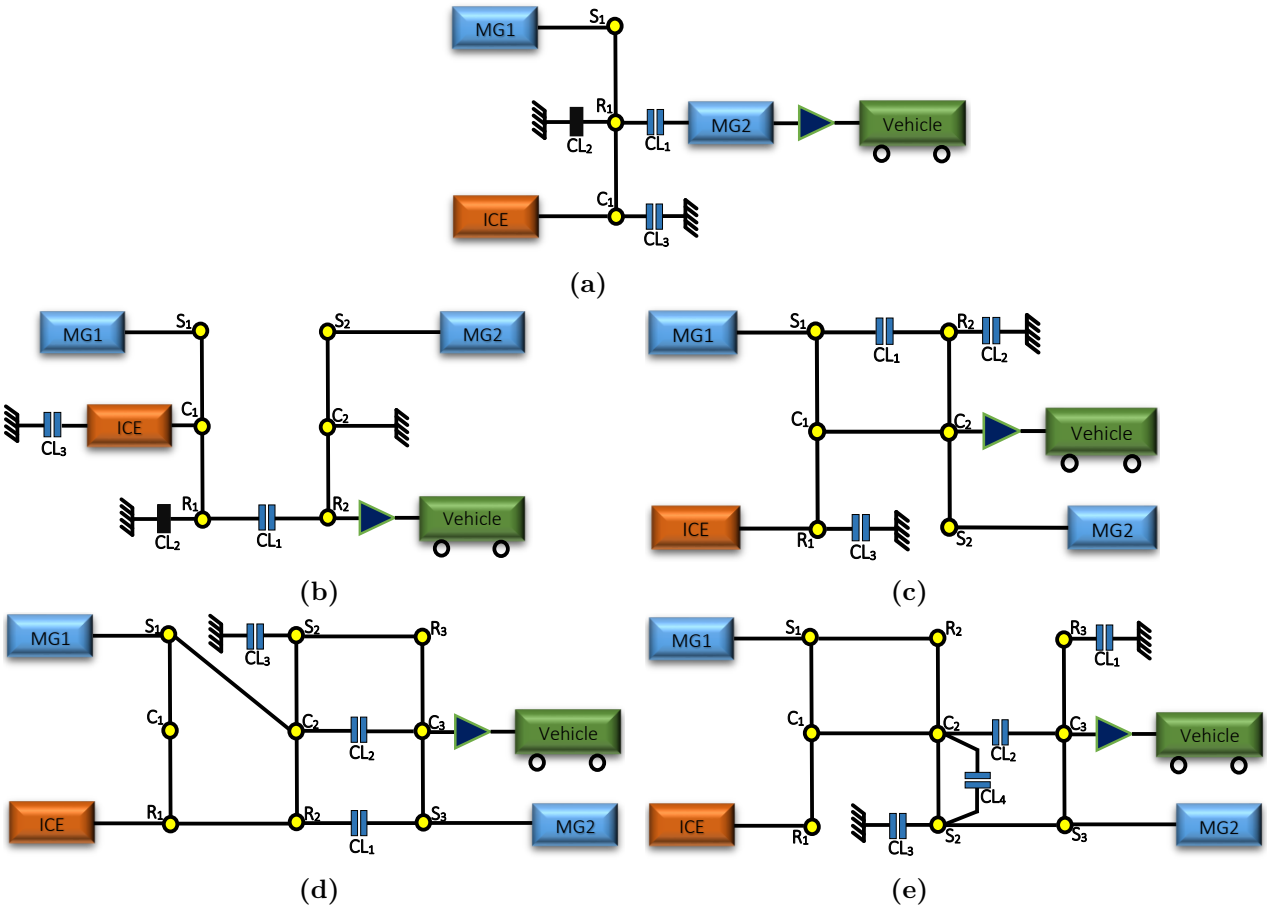


**Figure 3.2:** *Different types of topologies used in this study (**a**) 1PG topology, (**b**) 2PG-1 topology, (**c**) 2PG-2 topology, (**d**) 3PG-1 topology, (**e**) 3PG-2 topology. The solid black box represents the engaged clutch, while the two thick blue lines represent disengaged clutches.*

**Table 3.1:** *Sizes of the powertrain components.*

| Component Name | Parameters |
|---|---|
| Engine | 50 kW at 4500 rpm, 105 Nm at 2000 rpm, 33% bsfc at 2050 rpm |
| Motor Generator 2 | 60 kW, ±200 Nm, ±13,000 rpm |
| Motor Generator 1 | 42 kW, ±200 Nm, ±30,000 rpm |
| NCM - Battery Pack Capacity | 27 kWh (28 Modules) |
| 1PG topology, PG1 ($R_1$:$S_1$) | 2.6 |
| 2PG topologies, PG2 ($R_1$:$S_1$) | 2.6 |
| 2PG topologies, PG2 ($R_2$:$S_2$) | 2.63 |
| 3PG topologies, PG3 ($R_i$:$S_i$) | 2 ($i \in \{1,2,3\}$) |
| Differential Gear Ratio | 3.95 |
| Vehicle mass | 1450 kg |
| Tyre Radius | 0.33 m |

**Table 3.2:** *Clutch engagements of all the topologies in Figure 3.2 for realising different modes. N.A. shows that the specific mode is not available for the topology. $CL_i$+$CL_j$ and $CL_i$ represents that i, j clutches are engaged to generate the mode, where i,j $\in$ $\{1,2,3,4\}$. Remaining clutches are disengaged.*

| Modes \ Topologies | 1PG-1 | 2PG-1 | 2PG-2 | 3PG-1 | 3PG-2 |
|---|---|---|---|---|---|
| Mode 1 (2EV) | $CL_1$+$CL_3$ | $CL_1$+$CL_3$ | $CL_1$+$CL_3$ | $CL_3$ | $CL_1$ |
| Mode 2 (F.G. (1MG)) | N.A. | N.A. | $CL_1$+$CL_2$ | $CL_1$+$CL_2$ | $CL_1$+$CL_2$ |
| Mode 3 (Input-split) | $CL_1$ | $CL_1$ | $CL_2$ | $CL_1$ | $CL_1$ |
| Mode 4 (1EV) | $CL_2$+$CL_3$ | $CL_2$+$CL_3$ | $CL_2$+$CL_3$ | $CL_2$ | $CL_1$ |
| Mode 5 (Compound-split) | N.A. | N.A. | $CL_1$ | $CL_1$+$CL_3$ | $CL_2$ |
| Mode 6 (F.G. (2MG)) | N.A. | N.A. | N.A. | $CL_2$+$CL_3$ | $CL_1$+$CL_4$ |
| Mode 7 (F.G. with EVT) | N.A. | N.A. | N.A. | N.A. | $CL_2$+$CL_4$ |
| Mode 8 (Series) | $CL_3$ | $CL_3$ | N.A. | N.A. | N.A. |
| Mode 9 (F.G. (2DoF)) | N.A. | N.A. | N.A. | $CL_1$+$CL_2$+$CL_3$ | N.A. |

or 1 (selected). Obviously, at each moment of operation of the powertrain only one of the modes can be selected. Explanation of modes given in the table is described below.

- Mode 1 represents 2EV mode. In this mode, the clutches are engaged such that, both MG1 and MG2 provide the torque required. The DoF is one because only MG1 can choose optimal speed, speed of MG2 is directly proportional to vehicle speed. Engine do not operate in this mode.

- Mode 2 is a fixed gear mode with 1MG. In this mode, the clutches are engaged such that, both MG2 and engine provide the torque required. The DoF is one because only engine can choose optimal speed with the help of MG1, while the

speed of MG2 is directly proportional to vehicle speed. MG1 acts as speed controller for engine in this mode.

- Mode 3 is input-split mode. In this mode, the clutches are engaged such that, MG2 is coupled with vehicle output, while engine and MG1 are not disconnected with vehicle output. The DoF is one because only engine can choose optimal speed with the help of MG1. The speed of MG2 is directly proportional to vehicle speed. MG1 acts as speed controller for engine in this mode. In this mode MG that has fixed gear ratio with the vehicle output shaft can increase the torque which launching the vehicle. Since the ICE is decoupled from the vehicle output therefore ICE can be operated efficiently without being affected by vehicle output. These attributes make this mode type the most popular hybrid mode type nowadays: it is widely applied in all current Toyota hybrid vehicle fleets, Ford Fusion and some multi-mode hybrid vehicles such as the Silverado Hybrid and the second generation of Chevrolet Volt.

- Mode 4 represents 1EV mode. In this mode, the clutches are engaged such that, only MG2 provide the torque required. All other components of the powertrain are disconnected.

- Mode 5 is a compound split mode. In this mode, the clutches are engaged such that, both the MGs and engine provide the torque requested. The DoF is two because both engine and MG1 can choose optimal speed, while the speed of MG2 is directly proportional to vehicle speed.

- Mode 6 represents fixed gear with 2MG. This mode is similar to Mode 1 in operation, difference being the fixed gear ratio of both MGs and vehicle output.

- Mode 7 represents fixed gear with EVT (electronic variable transmission). In this mode, the vehicle is driven by engine and MG1. This powertrain arrangement is assisted with EVT so that engine speed can be controlled regardless of vehicle speed however it does not offer same flexibility in controlling engine torque. Engine torque cannot be arbitrary assigned when engine is operating at a certain speed. In addition, when the engine fuel is cut, its speed is no longer controllable.

- Mode 8 represents series mode. In this mode, the clutches are engaged such that, only MG2 provide the torque required. MG1 is used to charge the battery with the help of engine. Here, engine can operate in its bsfc region to reduce fuel consumption.

- Mode 9 is a fixed gear with 2DoF mode. In this mode engine is directly connected to vehicle output and Since both the MGs are decoupled from vehicle speed. Therefore, DoF becomes 2. This mode only exists in 3PG-1 topology.

### 3.1.2 Engine and Electric Motors

Electric motors and engine are the key components of a hybrid electric powertrain. In theory, thermodynamic based models like GT-Power and GT-Suite etc. are capable of fitting experimental data in to the model and can be used as an accurate simulation tool. However, both GT-Suite and GT-Power required very high computational demand. As well as they do not offer real-time simulation. Therefore, in this dissertation, we have used modes from dSPACE for both engine and electric motors.

The hybrid powertrain of this study uses a gasoline engine which is attached to different gears of the PGs depending on the topology. As shown in Figure 3.2, the engine is connected to the carrier gear of the first PG ($C_1$) in both 1PG-1 and 2PG-1 topologies, whereas it is connected to the ring gear of the first PG ($R_1$) in the remaining topologies. In order to make a fair comparison, all topologies use the same engine, which is represented as a map of its brake-thermal efficiency in terms of rotational speed and mechanical torque:

$$\eta_{bth} = \frac{\pi \tau_e}{\rho q Q_{HHV}}. \tag{3.2}$$

The fuel flow rate of the engine ($q_k$) is measured in $mm^3$/cycle and modelled as a polynomial of degree five (quintic function) in terms of the engine torque and angular velocity. The variable q used in Eq. 3.2 equation refers to mass flow rate of fuel per cycle which is modelled as a polynomial function of order 5 of engine torque ($T_e$) and engine speed ($\omega_e$):

$$\begin{aligned} q =& p00 + \\ & p10\omega_{e_k} + p01T_{e_k} + \\ & p20\omega_{e_k^2} + p11\omega_{e_k}T_{e_k} + p02T_{e_k^2} + \\ & p30\omega_{e_k^3} + p21\omega_{e_k^2}T_{e_k} + p12\omega_{e_k}T_{e_k^2} + p03T_{e_k^3} + \\ & p40\omega_{e_k^4} + p31\omega_{e_k^3}T_{e_k} + p22\omega_{e_k^2}T_{e_k^2} + p13\omega_{e_k}T_{e_k^3} + p04T_{e_k^4} + \\ & p50\omega_{e_k^5} + p41\omega_{e_k^4}T_{e_k} + p32\omega_{e_k^3}T_{e_k^2} + \\ & \qquad p23\omega_{e_k^2}T_{e_k^3} + p14\omega_{e_k}T_{e_k^4} + p05\omega_{e_k^5} \end{aligned} \tag{3.3}$$

where:

$$
\begin{aligned}
p00 &= 9.888 \times 10^{-1} \\
p10 &= 3.087 \times 10^{-4} \\
p02 &= 9.858 \times 10^{-3} \\
p30 &= 2.739 \times 10^{-11} \\
p21 &= 1.265 \times 10^{-8} \\
p12 &= 3.348 \times 10^{-7} \\
p13 &= 1.059 \times 10^{-11} \\
p04 &= 1.742 \times 10^{-6} \\
p50 &= 7.724 \times 10^{-19} \\
p41 &= 8.884 \times 10^{-18} \\
p32 &= 4.498 \times 10^{-15} \\
p23 &= 1.147 \times 10^{-13} \\
p14 &= -2.844 \times 10^{-12} \\
p05 &= -5.227 \times 10^{-9} \\
p01 &= -5.154 \times 10^{-2} \\
p20 &= -4.332 \times 10^{-8} \\
p11 &= -5.215 \times 10^{-5} \\
p03 &= -2.006 \times 10^{-4} \\
p40 &= -9.107 \times 10^{-15} \\
p31 &= -9.222 \times 10^{-13} \\
p22 &= -8.382 \times 10^{-11}
\end{aligned}
\tag{3.4}
$$

Figure 3.3 shows the engine brake specific fuel consumption (bsfc) curve used in this study. All five topolgies uses the same engine bsfc curve during operation.

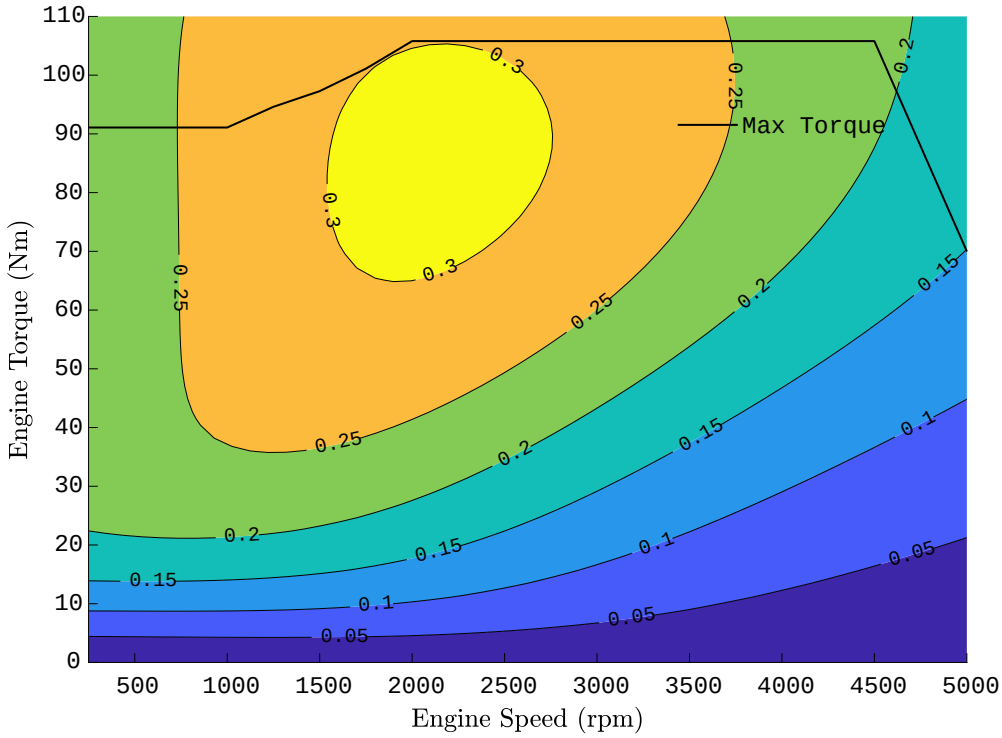


**Figure 3.3:** *BSFC map of engine [1]*

The hybrid powertrain in this study includes two electric motors which share the same torque characteristics but differ in their power and speed profiles. Motor-Generator 1 (MG1) operates as the engine speed controller in all modes, while it contributes towards the total torque request in $m_1$ and $m_6$ only. Motor-Generator 2 (MG2) is the only source of power in $m_4$, and the primary source of electric power in all other modes. MG2 is also used for regeneration in all topologies.

The electric motors in this study are modelled with their efficiency maps at different values of mechanical torque and rotational speed. The efficiency map of the electric motor $i \in \{1, 2\}$, which depends on the internal resistance and torque constant of the motor, is represented as in (3.5).

$$\eta_{\mathrm{mg}_i} = \left( \frac{1}{1 + \frac{\left(\tau_{\mathrm{mg}_i}/C_{\tau_{\mathrm{mg}_i}}\right)^2 R_{\mathrm{mg}_i}}{\tau_{\mathrm{mg}_i}\omega_{\mathrm{mg}_i}}} \right), \; i \in \{1, 2\} \tag{3.5}$$

The electric motors used in this study do not account the various losses. Due to which, the operation of motors is 100% efficient. It should be noted that, due to this virtue, the equivalent fuel consumption may be more optimal compared to real life situations.

The power consumed by both the electric motors is calculated using (3.6), where $T_{\mathrm{mg}}$ and $\omega_{\mathrm{mg}}$ are torque and rotational speed of the motors. If the sign of torque

and speed are same then MG is acting like a motor and the value of $\gamma$ becomes $-1$, otherwise MG is acting as a generator and the value of $\gamma$ becomes $+1$.

$$P_{\text{mg}} = T_{\text{mg}}\omega_{\text{mg}}\eta_{\text{mg}}^{\gamma}, \; i \in \{1, 2\} \tag{3.6}$$

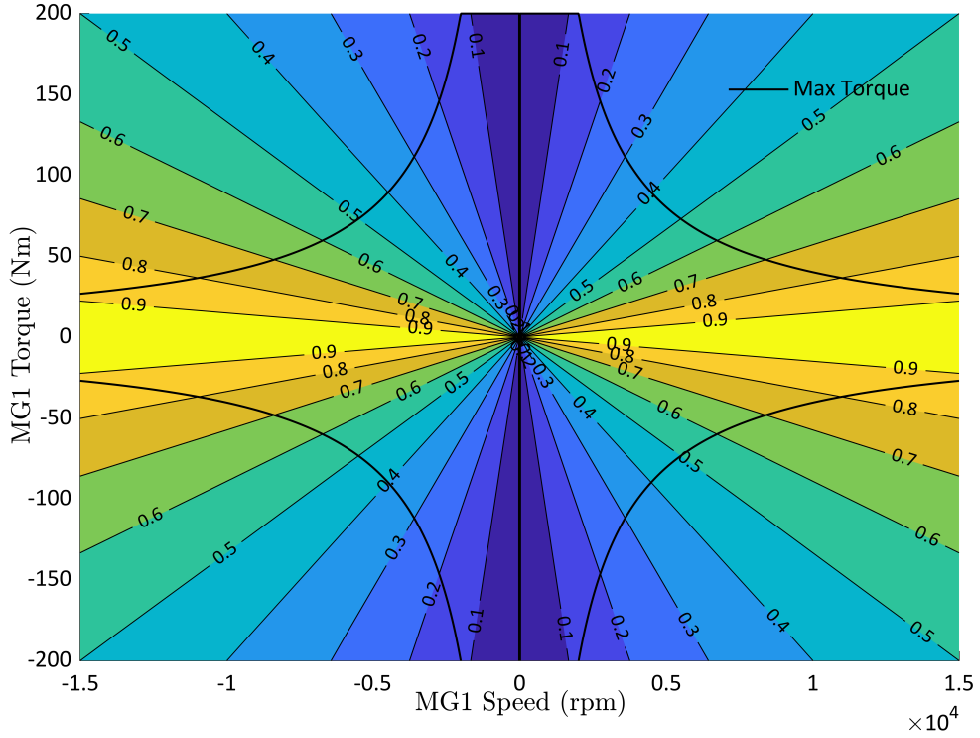


**Figure 3.4:** *The efficiency map of MG [1]*

Figure 3.4 shows the efficiency maps of both the electric motors used in this study. All five topolgies uses the same efficiency maps curve during operation.

The battery power is a hybrid algebraic function (i.e. a function of both continuous and discontinuous variables) of torque, angular velocity, and efficiency of MG1 and MG2:

$$P_{\text{batt}} = \tau_{\text{mg1}}\omega_{\text{mg1}}\eta_{mg1}^{\gamma_1} + \tau_{\text{mg2}}\omega_{\text{mg2}}\eta_{\text{mg2}}^{\gamma_2} \quad [6] \tag{3.7}$$

where $\gamma_1, \gamma_2 \in \{-1, 1\}$ are binary variables that, respectively, indicate whether MG1 and MG2 are in the motoring ($\gamma_i = -1$) or generating ($\gamma_i = 1$) mode of operation. Both the MG1 and MG2 are used for motoring in mode 1 whereas MG2 is the only source of electric traction in modes 2-8. Without loss of generality, it is assumed that only MG2 performs regeneration.

The state of charge (SoC) of batteries is a function of time, and of their charging and discharging power. This is modelled by the following ordinary differential equation

(ODE):

$$SoC_{k+1} = SoC_k - T_k \left( \frac{P_{\text{batt},k}}{3600 \cdot C_{\text{batt}}} \right) \tag{3.8}$$

where $P_{batt,k} > 0$ shows that the battery is being discharged. The sampling time of the driving cycles is normally one second (i.e. $T_k = 1$).

### 3.1.3 Modes Formulation for Multiple Modes

The hybrid powertrain consisting of one engine, two motors, and n number of planetary gears can generate multiple modes of operation due to the increased number of clutches. The connection between the powertrain components namely engine, motors, and differential and their connection to the nodes of sun, ring, and carrier gear of the PG is referred to as topology. The hybrid powertrain with 1PG can have up to 6 different topologies. The general formula to calculate maximum possible topologies and maximum number of clutches that can be used in a hybrid powertrain is as follows [27]:

$$n_{topologies} = C_{3n}^4 \tag{3.9}$$

$$n_{clutches} = C_{3n}^2 + 3n - 2n - 1 \tag{3.10}$$

where n is the number of PGs. In equation (3.10) first term represents total number of clutches that can be added between any two nodes of the PGs, second terms represents total number of grounding clutches, and the third term represents number of redundant clutched that can be eliminated from the system.

Furthermore, using all possible number of clutches for a 2 PG topology as presented in Figure 3.2b as a dynamic model in the form of $A\dot{\Omega} = T$ is derived in three steps as shown below.

*Step 1: Initialize the system matrix $A_o$*

Mode dynamics of a PG system can be represented as equation (3.11), where $T_o$ is the torque of components, $\dot{\Omega}_*$ is angular acceleration of components and $\dot{\Omega}_o$ is the generalised acceleration vector. $A_o$ is a $4_n \times 4_n$ matrix which is decomposed in to four parts: J is a $3_n \times 3_n$ diagonal matrix reflecting inertia of each node, where n is the number of PGs. The first four elements of the diagonal of J are the inertia of engine, MG1, MG2, and vehicle. After filling four places in the diagonal matrix of J, remaining places are filled with PG nodes which are not assigned to any powertrain component.

$$A\dot{\Omega}_o = \begin{bmatrix} J & D \\ D^T & 0 \end{bmatrix} \begin{bmatrix} \dot{\Omega}_* \\ F \end{bmatrix} = \begin{bmatrix} T \\ 0 \end{bmatrix} = T_o \tag{3.11}$$

The connections on the nodes of the planetary gear with the all four components determine the entries of the upper-right $3_n \times n$ constraint matrix D and its symmetric

$n \times 3_n$ matrix $D_T$ counterpart on the bottom-left. These two matrices of D and $D^T$ are associated with the internal force $F_i$ between the gear teeth, as well as the number of columns of D is equal to the number of PGs used. If a powertrain component is connected to a node of the PG, the corresponding "node coefficient" will be: $-R_i$, $-S_i$, and $R_i + S_i$ if the component and PG node connection is with the ring, sun, and carrier of the $i^th$ PG, respectively. All of the remaining entries of the D matrix will be zero. Therefore the corresponding $A_o$, $T_o$, and $\dot{\Omega}_o$ matrices are:

$$A_o = \begin{bmatrix} I_{out} + I_{R_2} & 0 & 0 & 0 & 0 & 0 & 0 & -R_2 \\ 0 & I_{C_1} + I_e & 0 & 0 & 0 & 0 & R_1 + S_1 & 0 \\ 0 & 0 & I_{S_1} + I_{mg1} & 0 & 0 & 0 & -S_1 & 0 \\ 0 & 0 & 0 & I_{S_2} + I_{mg2} & 0 & 0 & 0 & -S_2 \\ 0 & 0 & 0 & 0 & I_{R_1} & 0 & -R_1 & 0 \\ 0 & 0 & 0 & 0 & 0 & I_{C_2} & 0 & R_2 + S_2 \\ 0 & R_1 + S_1 & -S_1 & 0 & -R_1 & 0 & 0 & 0 \\ -R_2 & 0 & 0 & -S_2 & 0 & R_2 + S_2 & 0 & 0 \end{bmatrix} \tag{3.12}$$

$$T_o = \begin{bmatrix} T_{out} \\ T_e \\ T_{mg1} \\ T_{mg2} \\ 0 \\ 0 \\ 0 \\ 0 \end{bmatrix}, \dot{\Omega}_o = \begin{bmatrix} \dot{\omega_{out}} \\ \dot{\omega_e} \\ \dot{\omega_{mg1}} \\ \dot{\omega_{mg2}} \\ \dot{\omega_{R_1}} \\ \dot{\omega_{C_2}} \\ F_1 \\ F_2 \end{bmatrix} \tag{3.13}$$

*Step 2: Define transition matrices*

Transition matrices M and P are defined with respect to the clutch engagement. M is a identity matrix of $4_n \times 4_n$ dimension. When $u^{th}$ PG node is connected to $v^{th}$ and assuming $u < v$, equations (3.14) and (3.15) shows the execution of M. However, if the clutch is grounded then the $u^{th}$ node and $u^{th}$ row = [], where [] means this row is eliminated. After executing this step, M becomes a $(4_n - w) \times 4_n$ matrix, where w is the number of clutches engaged.

$$u^{th}row = u^{th}row + v^{th}row \tag{3.14}$$

$$v^{th}row = [] \tag{3.15}$$

The execution of P matrix is similar to that of M but with only row elimination. P is also an identity matrix of $4_n \times 4_n$ dimension. When $u^{th}$ PG node is connected to $v^{th}$ and assuming $u < v$ equation (3.14) is applied. Also, if the clutch is grounded then the $u^{th}$ node and $u^{th}$ row = [], where [] means this row is eliminated. After

executing this step, P becomes a $(4_n - w) \times 4_n$ matrix, where w is the number of clutches engaged. Using M and P matrices the dynamics of the system after clutch engagements is presented in equations (3.16) and (3.17).

$$A = MA_oM^T, T = MT_o, \dot{\Omega} = P\dot{\Omega_o} \tag{3.16}$$

$$A\dot{\Omega} = T \tag{3.17}$$

It is important to note that there are only three powertrain components (engine, MG1, and MG2), hence the degree of freedom of the system should be between one to three, so that the vehicle is drivable and controllable. Therefore, for each non-redundant clutch engagement, one degree of freedom will be reduced.

*Step 3: Dynamic equations for mode 1 (2EV)*

The dynamic matrix A for 2PG-1 topology during mode 1 with ($CL_1$+$CL_3$) engaged and $C_2$ grounded is generated through equation (3.16). The M, P, A, T, and $\dot{\Omega}$ matrices are shown in equations (3.18) and (3.19).

$$M = \begin{bmatrix} 1 & 1 & 0 & 0 & 1 & 0 & 0 & 0 \\ 0 & 0 & 1 & 0 & 0 & 0 & 0 & 0 \\ 0 & 0 & 0 & 1 & 0 & 0 & 0 & 0 \\ 0 & 0 & 0 & 0 & 0 & 0 & 1 & 0 \\ 0 & 0 & 0 & 0 & 0 & 0 & 0 & 1 \end{bmatrix} P = \begin{bmatrix} 1 & 0 & 0 & 0 & 0 & 0 & 0 & 0 \\ 0 & 0 & 1 & 0 & 0 & 0 & 0 & 0 \\ 0 & 0 & 0 & 1 & 0 & 0 & 0 & 0 \\ 0 & 0 & 0 & 0 & 0 & 0 & 1 & 0 \\ 0 & 0 & 0 & 0 & 0 & 0 & 0 & 1 \end{bmatrix} \tag{3.18}$$

$$A\dot{\Omega} = T = \begin{bmatrix} I_{out} + I_{R_1} & 0 & 0 & -R_1 & -R_2 \\ 0 & I_{mg1} & 0 & -S_1 & 0 \\ 0 & 0 & I_{mg2} & 0 & -S_2 \\ -R_1 & -S_1 & 0 & 0 & 0 \\ -R_2 & 0 & -S_2 & 0 & 0 \end{bmatrix} \times \begin{bmatrix} \dot{\omega}_{out} \\ \dot{\omega}_{mg1} \\ \dot{\omega}_{mg2} \\ F_1 \\ F_2 \end{bmatrix} = \begin{bmatrix} T_{req} \\ T_{mg1} \\ T_{mg2} \\ 0 \\ 0 \end{bmatrix} \tag{3.19}$$

Furthermore, upon solving equation (3.19) the torque equations for mode 1 are deduced. The angular velocities $\dot{\omega_{out}}$, $\dot{\omega_{mg1}}$, and $\dot{\omega_{mg2}}$ are steady state. The after multiplying the matrices, three equation are derived.

$$-R_1F_1 - R_2F_2 = T_{req} \tag{3.20}$$

$$-S_1F_1 = T_{mg1} \tag{3.21}$$

$$-S_2F_2 = T_{mg2} \tag{3.22}$$

Substituting the values of $F_1$ and $F_2$ in equation (3.20), the new equation will be:

$$T_{mg1} = \frac{S_1}{R_1}\left(T_{req} - \frac{R_2}{S_2}T_{mg2}\right) \tag{3.23}$$

The equation (3.23) shows the torque distribution between MG1 and MG2 to meet the torque requested by the vehicle. The torque for equations for different modes for all five topologies are presented as constraint equations in section 3.2.1.

### 3.1.4 1PG-1 modes formulation

1. Mode 1 (2EV)

$$\begin{bmatrix} \frac{mr_{tyre}^2}{K^2} + I_{mg2} & 0 & -R_1 \\ 0 & I_{mg1} & -S_1 \\ -R_1 & -S_1 & 0 \end{bmatrix} \begin{bmatrix} \dot{\omega}_{out} \\ \dot{\omega}_{mg1} \\ F_1 \end{bmatrix} = \begin{bmatrix} T_{mg2} - T_{req} \\ T_{mg1} \\ 0 \end{bmatrix} \tag{3.24}$$

2. Mode 8 (Series)

$$\begin{bmatrix} I_e & 0 & R_1 + S_1 \\ 0 & I_{mg1} & -S_1 \\ R_1 + S_1 & -S_1 & 0 \end{bmatrix} \begin{bmatrix} \dot{\omega}_e \\ \dot{\omega}_{mg1} \\ F_1 \end{bmatrix} = \begin{bmatrix} T_e \\ T_{mg1} \\ 0 \end{bmatrix} \tag{3.25}$$

$$\big(\frac{mr_{tyre}^2}{K^2} + I_{mg2}\big)\dot{\omega}_{out} = T_{mg2} - T_{req} \tag{3.26}$$

3. Mode 3 (Input Split mode).

$$\begin{bmatrix} I_e & 0 & 0 & R_1 + S_1 \\ 0 & \frac{mr_{tyre}^2}{K^2} + I_{mg2} & 0 & -R_1 \\ 0 & 0 & I_{mg1} & -S_1 \\ R_1 + S_1 & -R_1 & -S_1 & 0 \end{bmatrix} \begin{bmatrix} \dot{\omega}_e \\ \dot{\omega}_{out} \\ \dot{\omega}_{mg1} \\ F_1 \end{bmatrix} = \begin{bmatrix} T_e \\ T_{mg2} - T_{req} \\ T_{mg1} \\ 0 \end{bmatrix} \tag{3.27}$$

4. Mode 4 (1EV)

$$\big(\frac{mr_{tyre}^2}{K^2} + I_{mg2}\big)\dot{\omega}_{out} = T_{mg2} - T_{req} \tag{3.28}$$

### 3.1.5 2PG-1 modes formulation

1. Mode 1 (2EV)

$$\begin{bmatrix} I_{out} + I_{R_1} & 0 & 0 & R_1 & R_2 \\ 0 & I_{mg1} & 0 & S_1 & 0 \\ 0 & 0 & I_{mg2} & 0 & S_2 \\ R_1 & S_1 & 0 & 0 & 0 \\ R_2 & 0 & S_2 & 0 & 0 \end{bmatrix} \begin{bmatrix} \dot{\omega}_{out} \\ \dot{\omega}_{mg1} \\ \dot{\omega}_{mg2} \\ F_1 \\ F_2 \end{bmatrix} = \begin{bmatrix} T_{req} \\ T_{mg1} \\ T_{mg2} \\ 0 \\ 0 \end{bmatrix} \tag{3.29}$$

2. Mode 8 (Series)

$$\begin{bmatrix} I_e & 0 & R_1 + S_1 \\ 0 & I_{mg1} & S_1 \\ R_1 + S_1 & S_1 & 0 \end{bmatrix} \begin{bmatrix} \dot{\omega}_e \\ \dot{\omega}_{mg1} \\ F_1 \end{bmatrix} = \begin{bmatrix} T_e \\ T_{mg1} \\ 0 \end{bmatrix} \tag{3.30}$$

$$\begin{bmatrix} I_{out} & 0 & 0 & R_2 \\ 0 & I_{mg2} & 0 & S_2 \\ 0 & 0 & 0 & 0 \\ R_2 & S_2 & 0 & 0 \end{bmatrix} \begin{bmatrix} \dot{\omega}_{out} \\ \dot{\omega}_{mg2} \\ F_1 \\ F_2 \end{bmatrix} = \begin{bmatrix} T_{req} \\ T_{mg2} \\ 0 \\ 0 \end{bmatrix} \tag{3.31}$$

3. Mode 3 (Input Split)

$$\begin{bmatrix} I_{out}+I_{R_1} & 0 & 0 & 0 & R_1 & R_2 \\ 0 & I_e & 0 & 0 & R_1+S_1 & 0 \\ 0 & 0 & I_{mg1} & 0 & S_1 & 0 \\ 0 & 0 & 0 & I_{mg2} & 0 & S_2 \\ R_1 & R_1+S_1 & S_1 & 0 & 0 & 0 \\ R_2 & 0 & 0 & S_2 & 0 & 0 \end{bmatrix} \begin{bmatrix} \dot{\omega}_{out} \\ \dot{\omega}_e \\ \dot{\omega}_{mg1} \\ \dot{\omega}_{mg2} \\ F_1 \\ F_2 \end{bmatrix} = \begin{bmatrix} T_{req} \\ T_e \\ T_{mg1} \\ T_{mg2} \\ 0 \\ 0 \end{bmatrix} \tag{3.32}$$

4. Mode 4 (1EV)

$$\begin{bmatrix} I_{out} & 0 & 0 & R_2 \\ 0 & I_{mg2} & 0 & S_2 \\ 0 & 0 & 0 & 0 \\ R_2 & S_2 & 0 & 0 \end{bmatrix} \begin{bmatrix} \dot{\omega}_{out} \\ \dot{\omega}_{mg2} \\ F_1 \\ F_2 \end{bmatrix} = \begin{bmatrix} T_{req} \\ T_{mg2} \\ 0 \\ 0 \end{bmatrix} \tag{3.33}$$

### 3.1.6 2PG-2 modes formulation

1. Mode 1 (2EV)

$$\begin{bmatrix} I_{out}+I_{R_1} & 0 & 0 & R_1 & R_2 \\ 0 & I_{mg1} & 0 & S_1 & 0 \\ 0 & 0 & I_{mg2} & 0 & S_2 \\ R_1 & S_1 & 0 & 0 & 0 \\ R_2 & 0 & S_2 & 0 & 0 \end{bmatrix} \times \begin{bmatrix} \dot{\omega}_{out} \\ \dot{\omega}_{mg1} \\ \dot{\omega}_{mg2} \\ F_1 \\ F_2 \end{bmatrix} = \begin{bmatrix} T_{req} \\ T_{mg1} \\ T_{mg2} \\ 0 \\ 0 \end{bmatrix} \tag{3.34}$$

2. Mode 8 (Series)

$$\begin{bmatrix} I_e & 0 & R_1+S_1 \\ 0 & I_{mg1} & S_1 \\ R_1+S_1 & S_1 & 0 \end{bmatrix} \times \begin{bmatrix} \dot{\omega}_e \\ \dot{\omega}_{mg1} \\ F_1 \end{bmatrix} = \begin{bmatrix} T_e \\ T_{mg1} \\ 0 \end{bmatrix} \tag{3.35}$$

$$\begin{bmatrix} I_{out} & 0 & 0 & R_2 \\ 0 & I_{mg2} & 0 & S_2 \\ 0 & 0 & 0 & 0 \\ R_2 & S_2 & 0 & 0 \end{bmatrix} \times \begin{bmatrix} \dot{\omega}_{out} \\ \dot{\omega}_{mg2} \\ F_1 \\ F_2 \end{bmatrix} = \begin{bmatrix} T_{req} \\ T_{mg2} \\ 0 \\ 0 \end{bmatrix} \tag{3.36}$$

3. Mode 3 (Input Split)

$$\begin{bmatrix} I_{out}+I_{R_1} & 0 & 0 & 0 & R_1 & R_2 \\ 0 & I_e & 0 & 0 & R_1+S_1 & 0 \\ 0 & 0 & I_{mg1} & 0 & S_1 & 0 \\ 0 & 0 & 0 & I_{mg2} & 0 & S_2 \\ R_1 & R_1+S_1 & S_1 & 0 & 0 & 0 \\ R_2 & 0 & 0 & S_2 & 0 & 0 \end{bmatrix} \begin{bmatrix} \dot{\omega}_{out} \\ \dot{\omega}_e \\ \dot{\omega}_{mg1} \\ \dot{\omega}_{mg2} \\ F_1 \\ F_2 \end{bmatrix} = \tag{3.37}$$

$$\begin{bmatrix} T_{req} \\ T_e \\ T_{mg1} \\ T_{mg2} \\ 0 \\ 0 \end{bmatrix} \tag{3.38}$$

4. Mode 4 (1EV)

$$\begin{bmatrix} I_{out} & 0 & 0 & R_2 \\ 0 & I_{mg2} & 0 & S_2 \\ 0 & 0 & 0 & 0 \\ R_2 & S_2 & 0 & 0 \end{bmatrix} \times \begin{bmatrix} \dot{\omega}_{out} \\ \dot{\omega}_{mg2} \\ F_1 \\ F_2 \end{bmatrix} = \begin{bmatrix} T_{req} \\ T_{mg2} \\ 0 \\ 0 \end{bmatrix} \tag{3.39}$$

5. Mode 5 (Compound Split)

$$\begin{bmatrix} I_{out}+I_{R_1} & 0 & 0 & R_1 & R_2 \\ 0 & I_e+I_{mg1} & 0 & R_1+S_1 & S_1 \\ 0 & 0 & I_{mg2} & 0 & S_2 \\ R_1 & R_1+S_1 & 0 & 0 & 0 \\ R_2 & S_1 & S_2 & 0 & 0 \end{bmatrix} \begin{bmatrix} \dot{\omega}_{out} \\ \dot{\omega}_e+\dot{\omega}_{mg1} \\ \dot{\omega}_{mg2} \\ F_1 \\ F_2 \end{bmatrix} = \tag{3.40}$$

$$\begin{bmatrix} T_{req} \\ T_e+T_{mg1} \\ T_{mg2} \\ 0 \\ 0 \end{bmatrix} \tag{3.41}$$

### 3.1.7 3PG-1 modes formulation

1. Mode 1 (2EV)

$$\begin{bmatrix} I_{S_1}+I_{mg1} & 0 & 0 & 0 & 0 & -S_1 & R_2+S_2 & 0 \\ 0 & I_{S_1}+I_e & 0 & 0 & 0 & -R_1 & -R_2 & 0 \\ 0 & 0 & 0 & I_{mg2} & 0 & 0 & 0 & -S_3 \\ 0 & 0 & 0 & 0 & I_{out} & 0 & 0 & R_3+S_3 \\ -S_1 & -R_1 & 0 & 0 & 0 & 0 & 0 & 0 \\ R_2+S_2 & -R_2 & 0 & 0 & 0 & 0 & 0 & 0 \\ 0 & 0 & -S_3 & R_3+S_3 & 0 & 0 & 0 & 0 \end{bmatrix} \tag{3.42}$$

$$\begin{bmatrix} \dot{\omega}_{mg1} \\ \dot{\omega}_e \\ \dot{\omega}_{mg2} \\ \dot{\omega}_{out} \\ F_1 \\ F_2 \\ F_3 \end{bmatrix} = \begin{bmatrix} T_{mg1} \\ 0 \\ T_{mg2} \\ T_{req} \\ 0 \\ 0 \\ 0 \end{bmatrix} \tag{3.43}$$

2. Mode 2 (Parallel with fixed gear & 1MG)

$$\begin{bmatrix} I_{S_1}+I_{mg1}+I_{out} & 0 & 0 & 0 & 0 & -S_1 & R_2+S_2 & R_3+S_3 \\ 0 & I_{R_1}+I_e+I_{mg2} & 0 & 0 & 0 & -R_1 & -R_2 & -S_3 \\ 0 & 0 & I_{S_2}+I_{R_3} & 0 & 0 & 0 & -S_1 & -R_3 \\ -S_1 & -R_1 & -S_1 & 0 & 0 & 0 & 0 & 0 \\ R_2+S_2 & -R_2 & 0 & 0 & 0 & 0 & 0 & 0 \\ R_3+S_3 & -S_3 & 0 & -R_3 & 0 & 0 & 0 & 0 \end{bmatrix} \tag{3.44}$$

$$\begin{bmatrix} \dot{\omega}_{mg1}+\dot{\omega}_{out} \\ \dot{\omega}_e+\dot{\omega}_{mg2} \\ \dot{\omega}_{S_2}+\dot{\omega}_{R_3} \\ F_1 \\ F_2 \\ F_3 \end{bmatrix} = \begin{bmatrix} T_{mg1}+T_{out} \\ T_e+T_{mg2} \\ 0 \\ 0 \\ 0 \\ 0 \end{bmatrix} \tag{3.45}$$

3. Mode 3 (Input Split Mode)

$$\begin{bmatrix} I_{S_1}+I_{mg1} & 0 & 0 & 0 & 0 & -S_1 & R_2+S_2 & 0 \\ 0 & I_e+I_{mg2} & 0 & 0 & 0 & -R_1 & -R_2 & -S_3 \\ 0 & 0 & I_{R_1+S_1} & 0 & 0 & R_1+S_1 & 0 & 0 \\ 0 & 0 & 0 & I_{S_2} & 0 & 0 & -S_2 & -R_3 \\ 0 & 0 & 0 & 0 & 0 & I_{out} & 0 & R_3+S_3 \\ -S_1 & -R_1 & R_1+S_1 & 0 & 0 & 0 & 0 & 0 \\ R_2+S_2 & -R_2 & 0 & -S_2 & 0 & 0 & 0 & 0 \\ 0 & 0 & -S_3 & -R_3 & R_3+S_3 & 0 & 0 & 0 \end{bmatrix} \tag{3.46}$$

$$\begin{bmatrix} \dot{\omega}_{mg1} \\ \dot{\omega}_e \\ \dot{\omega}_{c1} \\ \dot{\omega}_{s2} \\ \dot{\omega}_{req} \\ F_1 \\ F_2 \\ F_3 \end{bmatrix} = \begin{bmatrix} T_{mg1} \\ T_e+T_{mg2} \\ 0 \\ 0 \\ T_{req} \\ 0 \\ 0 \\ 0 \end{bmatrix} \tag{3.47}$$

4. Mode 4 (1EV)

$$\begin{bmatrix} I_{S_1}+I_{mg1} & 0 & 0 & 0 & 0 & -S_1 & 0 & 0 \\ 0 & I_e+I_{mg2} & 0 & 0 & 0 & -R_1 & -R_2 & 0 \\ 0 & 0 & I_{R_1+S_1} & 0 & 0 & R_1+S_1 & 0 & 0 \\ 0 & 0 & 0 & I_{out}+I_{R_2+S_2} & 0 & 0 & R_2+S_2 & R_3+S_3 \\ 0 & 0 & 0 & 0 & I_{mg2} & 0 & 0 & -S_3 \\ -S_1 & -R_1 & R_1+S_1 & 0 & R_3+S_3 & 0 & 0 & 0 \\ 0 & -R_2 & 0 & R_2+S_2 & 0 & 0 & 0 & 0 \\ 0 & 0 & 0 & C_3 & -S_3 & 0 & 0 & 0 \end{bmatrix} \tag{3.48}$$

$$\begin{bmatrix} \dot{\omega}_{mg1} \\ \dot{\omega}_e \\ \dot{\omega}_{c1} \\ \dot{\omega}_{out} \\ \dot{\omega}_{mg2} \\ F_1 \\ F_2 \\ F_3 \end{bmatrix} = \begin{bmatrix} 0 \\ 0 \\ 0 \\ T_{req} \\ T_{mg2} \\ 0 \\ 0 \\ 0 \end{bmatrix} \tag{3.49}$$

5. Mode 5 (Compound split)

$$\begin{bmatrix} I_{S_1}+I_{mg1}+I_{R_2+S_2} & 0 & 0 & 0 & 0 & -S_1 & R_2+S_2 & 0 \\ 0 & I_e+I_{mg2} & 0 & 0 & 0 & -R_1 & -R_2 & -S_3 \\ 0 & 0 & I_{R_1+S_1} & 0 & 0 & R_1+S_1 & 0 & 0 \\ 0 & 0 & 0 & I_{out} & 0 & 0 & 0 & R_3+S_3 \\ -S_1 & -R_1 & R_1+S_1 & 0 & R_3+S_3 & 0 & 0 & 0 \\ 0 & R_2+S_2 & -R_2 & 0 & 0 & 0 & 0 & 0 \\ 0 & -S_3 & 0 & R_3+S_3 & 0 & 0 & 0 & 0 \end{bmatrix} \tag{3.50}$$

$$\begin{bmatrix} \dot{\omega}_{mg1} \\ \dot{\omega}_e+\dot{\omega}_{mg2} \\ \dot{\omega}_{c1} \\ \dot{\omega}_{out} \\ F_1 \\ F_2 \\ F_3 \end{bmatrix} = \begin{bmatrix} T_{mg1} \\ T_e+T_{mg2} \\ 0 \\ T_{out} \\ 0 \\ 0 \\ 0 \end{bmatrix} \tag{3.51}$$

6. Mode 6 (Parallel with fixed gear & 2MG)

$$\begin{bmatrix} I_{S_1}+I_{mg1}+I_{R_2+S_2}+I_{out} & 0 & 0 & -S_1 & R_2+S_2 & R_3+S_3 \\ 0 & I_{R_1}+I_e & 0 & -R_1 & -R_2 & 0 \\ 0 & 0 & I_{mg2} & 0 & 0 & -S_3 \\ -S_1 & R_2+S_2 & R_3+S_3 & 0 & 0 & 0 \\ 0 & -R_1 & -R_2 & 0 & 0 & 0 \\ 0 & 0 & -S_3 & 0 & 0 & 0 \end{bmatrix} \tag{3.52}$$

$$\begin{bmatrix} \dot{\omega}_{mg1}+\dot{\omega}_{out} \\ \dot{\omega}_e \\ \dot{\omega}_{mg2} \\ F_1 \\ F_2 \\ F_3 \end{bmatrix} = \begin{bmatrix} T_{mg1}+T_{out} \\ T_e \\ T_{mg2} \\ 0 \\ 0 \\ 0 \end{bmatrix} \tag{3.53}$$

7. Mode 9 (Parallel with fixed gear)

$$\begin{bmatrix} I_{S_1}+I_{mg1}+I_{R_2+S_2}+I_{out} & 0 & 0 & -S_1 & R_2+S_2 & R_3+S_3 \\ 0 & I_{R_1}+I_eI_{mg2}+ & 0 & -R_1 & -R_2 & S_3 \\ 0 & 0 & I_{R_1+S_1} & 0 & 0 & R_1+S_1 \\ -R_1 & -R_2 & S_3 & 0 & 0 & 0 \\ 0 & C_2 & -R_2 & 0 & 0 & 0 \\ R_1+S_1 & 0 & 0 & R_3+S_3 & 0 & 0 \end{bmatrix} \tag{3.54}$$

$$\begin{bmatrix} \dot{\omega}_{mg1}+\dot{\omega}_{out} \\ \dot{\omega}_e+\dot{\omega}_{mg2} \\ \dot{\omega}_{c1} \\ F_1 \\ F_2 \\ F_3 \end{bmatrix} = \begin{bmatrix} T_{mg1}+T_{out} \\ T_e+T_{mg2} \\ 0 \\ 0 \\ 0 \\ 0 \end{bmatrix} \tag{3.55}$$

### 3.1.8 3PG-2 modes formulation

1. Mode 1, 3, 4 (1EV, Input split, 2EV)

$$\begin{bmatrix} I_{S_1}+I_{R_2}+I_{mg1} & 0 & 0 & 0 & 0 & -S_1 & -R_2 & 0 \\ 0 & I_e & 0 & 0 & 0 & -R_1 & 0 & 0 \\ 0 & 0 & I_{R_1+S_1}+I_{R_2+S_2} & 0 & 0 & R_1+S_1 & R_2+S_2 & 0 \\ 0 & 0 & 0 & I_{mg2} & 0 & 0 & -S_2 & -S_3 \\ 0 & 0 & 0 & 0 & I_{R_3+S_3}+I_{out} & 0 & 0 & R_3+S_3 \\ -S_1 & -R_1 & R_1+S_1 & 0 & 0 & 0 & 0 & 0 \\ -R_2 & 0 & R_2+S_2 & -S_2 & 0 & 0 & 0 & 0 \\ 0 & 0 & 0 & -S_3 & R_3+S_3 & 0 & 0 & 0 \end{bmatrix} \tag{3.56}$$

$$\begin{bmatrix} \dot{\omega}_{mg1} \\ \dot{\omega}_e \\ \dot{\omega}_{c1}+\dot{\omega}_{c2} \\ \dot{\omega}_{mg2} \\ \dot{\omega}_{out} \\ F_1 \\ F_2 \\ F_3 \end{bmatrix} = \begin{bmatrix} T_{mg1} \\ T_e \\ 0 \\ T_{mg2} \\ T_{req} \\ 0 \\ 0 \\ 0 \end{bmatrix} \tag{3.57}$$

2. Mode 2 (Parallel with fixed gear & 1MG)

$$\begin{bmatrix} I_{S_1}+I_{R_2}+I_{mg1} & 0 & 0 & 0 & -S_1 & -R_2 & 0 \\ 0 & I_e & 0 & 0 & -R_1 & 0 & 0 \\ 0 & 0 & I_{R_1+S_1}+I_{R_2+S_2}+I_{R_3+S_3}+I_{out} & 0 & R_1+S_1 & R_2+S_2 & R_3+S_3 \\ 0 & 0 & 0 & I_{mg2} & 0 & 0 & -S_3 \\ -S_1 & -R_2 & R_1+S_1 & 0 & 0 & 0 & 0 \\ -R_1 & R_2+S_2 & -S_3 & 0 & 0 & 0 & 0 \\ R_1+S_1 & -S_2 & R_3+S_3 & 0 & 0 & 0 & 0 \end{bmatrix} \tag{3.58}$$

$$\begin{bmatrix} \dot{\omega}_{mg1} \\ \dot{\omega}_e \\ \dot{\omega}_{out} \\ \dot{\omega}_{mg2} \\ F_1 \\ F_2 \\ F_3 \end{bmatrix} = \begin{bmatrix} T_{mg1} \\ T_e \\ T_{req} \\ T_{mg2} \\ 0 \\ 0 \\ 0 \end{bmatrix} \tag{3.59}$$

3. Mode 5 (Compound split)

$$\begin{bmatrix} I_{S_1}+I_{R_2}+I_{mg1} & 0 & 0 & 0 & 0 & -S_1 & -R_2 & 0 \\ 0 & I_e & 0 & 0 & 0 & -R_1 & 0 & 0 \\ 0 & 0 & I_{R_1+S_1}+I_{R_2+S_2}+I_{R_3+S_3}+I_{out} & 0 & 0 & R_1+S_1 & R_2+S_2 & R_3+S_3 \\ 0 & 0 & 0 & I_{mg2} & 0 & 0 & -S_2 & -S_3 \\ 0 & 0 & 0 & 0 & I_{R_3} & 0 & 0 & -R_3 \\ -S_1 & -R_2 & -S_3 & 0 & 0 & 0 & 0 & 0 \\ -R_1 & R_2+S_2 & -R_3 & 0 & 0 & 0 & 0 & 0 \\ R_1+S_1 & -S_2 & R_3+S_3 & 0 & 0 & 0 & 0 & 0 \end{bmatrix} \tag{3.60}$$

$$\begin{bmatrix} \dot{\omega}_{mg1} \\ \dot{\omega}_e \\ \dot{\omega}_{out} \\ \dot{\omega}_{mg2} \\ \dot{\omega}_{R_3} \\ F_1 \\ F_2 \\ F_3 \end{bmatrix} = \begin{bmatrix} T_{mg1} \\ T_e \\ T_{req} \\ T_{mg2} \\ 0 \\ 0 \\ 0 \\ 0 \end{bmatrix} \tag{3.61}$$

4. Mode 6 (Parallel with fixed gear & 2MG)

$$\begin{bmatrix} I_{S_1}+I_{R_2}+I_{mg1} & 0 & 0 & 0 & 0 & -S_1 & -R_2 & 0 \\ 0 & I_e & 0 & 0 & 0 & -R_1 & 0 & 0 \\ 0 & 0 & I_{R_1+S_1}+I_{R_2+S_2}+I_{S_2}+I_{mg2} & 0 & R_1+S_1 & R_2+S_2 & -S_2 & -S_3 \\ 0 & 0 & 0 & 0 & I_{R_3+S_3}+I_{out} & 0 & 0 & R_3+S_3 \\ -S_1 & -R_1 & R_1+S_1 & R_2+S_2 & 0 & 0 & 0 & 0 \\ -R_2 & 0 & -S_2 & -S_2 & 0 & 0 & 0 & 0 \\ 0 & 0 & -S_3 & R_3+S_3 & 0 & 0 & 0 & 0 \end{bmatrix} \tag{3.62}$$

$$\begin{bmatrix} \dot{\omega}_{mg1} \\ \dot{\omega}_e \\ \dot{\omega}_{mg2} \\ \dot{\omega}_{out} \\ F_1 \\ F_2 \\ F_3 \end{bmatrix} = \begin{bmatrix} T_{mg1} \\ T_e \\ T_{mg2} \\ T_{req} \\ 0 \\ 0 \\ 0 \end{bmatrix} \tag{3.63}$$

5. Mode 7 (Parallel with fixed gear EVT)

$$\begin{bmatrix} I_{S_1}+I_{R_2}+I_{mg1} & 0 & 0 & 0 & -S_1 & -R_2 & 0 \\ 0 & I_e & 0 & 0 & -R_1 & 0 & 0 \\ 0 & I_{R_1+S_1}+I_{R_2+S_2}+I_{R_3+S_3}+I_{out} & 0 & 0 & R_1+S_1 & R_2+S_2 & R_3+S_3 \\ 0 & 0 & 0 & I_{mg2} & 0 & 0 & -S_3 \\ -S_1 & -R_2 & 0 & 0 & 0 & 0 & 0 \\ -R_1 & R_2+S_2 & -S_3 & 0 & 0 & 0 & 0 \\ R_1+S_1 & 0 & R_3+S_3 & 0 & 0 & 0 & 0 \end{bmatrix} \tag{3.64}$$

$$\begin{bmatrix} \dot{\omega}_{mg1} \\ \dot{\omega}_e \\ \dot{\omega}_{out} \\ \dot{\omega}_{mg2} \\ F_1 \\ F_2 \\ F_3 \end{bmatrix} = \begin{bmatrix} T_{mg1} \\ T_e \\ T_{req} \\ T_{mg2} \\ 0 \\ 0 \\ 0 \end{bmatrix} \tag{3.65}$$

### 3.1.9 Screening of Modes

All the modes realised by the maximum possible clutches and their engagement are not useful. The clutch engagement where vehicle is not powered by any powertrain component in a mode will be an infeasible mode. Modes for which dynamic equations are same, only one mode will be used and all others will be deemed as redundant modes. This section describes steps to identify between, infeasible, redundant, and useful modes.

*Step 1: Generating $A^*$ Matrix*

Inverting the A matrix provides us the dynamic equations that relate input to state variables. For a powertrain, where speed of each node of the PG is controlled is known as controllable powertrain system, and for a controllable powertrain system A matrix is always invertible. However, not all the elements of $A^{-1}$ are useful. The useful $A^{-1}$ matrix is shown below, and the final $A^*$ matrix is also presented. As example, generation of $A^*$ matrix for mode 1 as described in section above is elaborated.

$$\begin{bmatrix} \dot{\omega_{out}} \\ \dot{\omega_e} \\ \dot{\omega_{mg1}} \\ \dot{\omega_{mg2}} \end{bmatrix} = A^* \begin{bmatrix} T_{out} \\ T_e \\ T_{mg1} \\ T_{mg2} \end{bmatrix} \tag{3.66}$$

For constructing $A^*$ matrix, the columns and rows with free nodes (i.e. PGs nodes where no powertrains components are connected) in $A^{-1}$ matrix are eliminated, because they will have no impact on final state equation. There can arise two cases after this elimination.

1. If not powertrain component is grounded, then $A^*$ matrix will be obtained as described in the paragraph above. As shown from equation (3.19), the $A^*$ matrix presented in equation (3.66) is a $A^* = A^{-1}[1:4, 1:4]$ matrix representing first four elements of the first four rows.

2. If juxtaposition of elements occurs, the torque coefficients corresponding to juxtaposition components are duplication, then their corresponding row in $A^*$ matrix is set to zero.

The final $A^{-1}$ and $A^*$ matrices for mode 1 of 2PG-1 topology are given below:

$$A^{-1} = \begin{bmatrix} A_{11}^{inv} & A_{12}^{inv} & A_{13}^{inv} & A_{14}^{inv} & A_{15}^{inv} \\ A_{21}^{inv} & A_{22}^{inv} & A_{23}^{inv} & A_{24}^{inv} & A_{25}^{inv} \\ A_{31}^{inv} & A_{32}^{inv} & A_{33}^{inv} & A_{34}^{inv} & A_{35}^{inv} \\ A_{41}^{inv} & A_{42}^{inv} & A_{43}^{inv} & A_{44}^{inv} & A_{45}^{inv} \\ A_{51}^{inv} & A_{52}^{inv} & A_{53}^{inv} & A_{54}^{inv} & A_{55}^{inv} \end{bmatrix}, \begin{bmatrix} \dot{\omega}_{out} \\ \dot{\omega}_{mg1} \\ \dot{\omega}_{mg2} \\ F_1 \\ F_2 \end{bmatrix} = A^{-1} \begin{bmatrix} T_{req} \\ T_{mg1} \\ T_{mg2} \\ 0 \\ 0 \end{bmatrix} \tag{3.67}$$

$$A^{-1} = \begin{bmatrix} A_{11}^{inv} & A_{12}^{inv} & A_{12}^{inv} & A_{13}^{inv} \\ A_{21}^{inv} & A_{22}^{inv} & A_{22}^{inv} & A_{23}^{inv} \\ A_{21}^{inv} & A_{22}^{inv} & A_{22}^{inv} & A_{23}^{inv} \\ A_{31}^{inv} & A_{32}^{inv} & A_{32}^{inv} & A_{33}^{inv} \end{bmatrix} \tag{3.68}$$

*Step 2: Refinement of the $A^*$ Matrix*

In the $A^*$ matrix, if three out of four elements of any row are zero, then all elements of that row are set to zero, for checking the rank of the matrix in later step. As well as, if both first and the second element of third and fourth row of $A^*$ matrix are zero, then the entire third and fourth row is set to zero.

*Step 3: Define the Entries of $A^*$ Matrix*

In the $A^*$, the four rows are termed as $V_{veh}$, $V_{eng}$, $V_{mg1}$, $V_{mg2}$, respectively. The elements of $V_{veh}$ row vector are knows as $C_{veh}$, $C_{eng}$, $C_{mg1}$, $C_{mg2}$.

If the first row of the $A^*$ is zero, it implies that vehicle output is not connected to any PG node and hence this mode is infeasible. Additionally, from the modes having identical $A^*$ matrix only one mode is kept and other are made redundant.

### 3.1.10 Classification of Modes

There are 14 different types of modes possible in an electrified powertrain for any number of PGs with any number of clutches [6]. In this section 14 different modes of 2PG-1 topology will be discussed. Note that, the classification criteria of each mode type is mutually exclusive.

If the first row of the $A^*$ is zero, it implies that vehicle output is not connected to any PG node and hence this mode is infeasible. Additionally, from the modes having identical $A^*$ matrix only one mode is kept and other are made redundant. The degree

of freedom stands (DoF) for number of components with independent speeds. The DoF is determined by the auxiliary matrices shown in the steps below:

*Step 1: Determination of System DoF*

The DoF is similar to the rank of $A^*$ matrix which can not be more than three. Each row of $A^*$ matrix represents the relationship between rank of $A^*$ matrix, torque and acceleration of components. Therefore, reduction in the rank of the $A^*$ matrix means that acceleration of one or more than one components has a linear combination with remaining components.

*Step 2: Formulating the Auxiliary Matrices*

There are six other matrices which are needed for the rank analysis: $M_{ve} = [V_{veh};V_{eng}]$, $M_{vmg1} = [V_{veh};V_{mg1}]$, $M_{vmg2} = [V_{veh};V_{mg2}]$, $M_{emg1} = [V_{veh};V_{mg1}]$, $M_{emg2} = [V_{veh};V_{mg2}]$, and $M_{mg1mg2} = [V_{mg1};V_{mg2}]$. The ranks of these matrices is shown as $r_{ve}$, $r_{mg1}$, $r_{mg2}$, $r_{emg1}$, $r_{emg2}$, $r_{mg1mg2}$. These ranks are used for modes classification which is discussion in the section below.

### Mode 1: 2EV (2MGs, 0DoF)

Figure 3.5 shows the configuration of 2EV mode for 2PG-2 topology. The criteria of this mode is as follows:

$$DoF = 1, V_{eng} = 0, C_{mg1}C_{mg2} \neq 0$$

In this mode type, the engine is disabled and both the motors provides the torque requested by the vehicle. For this topology, the DoF is zero which means speed of both the motors is linearly dependent on vehicle speed. However, it is possible to achieve 1DoF for this mode for other topologies.

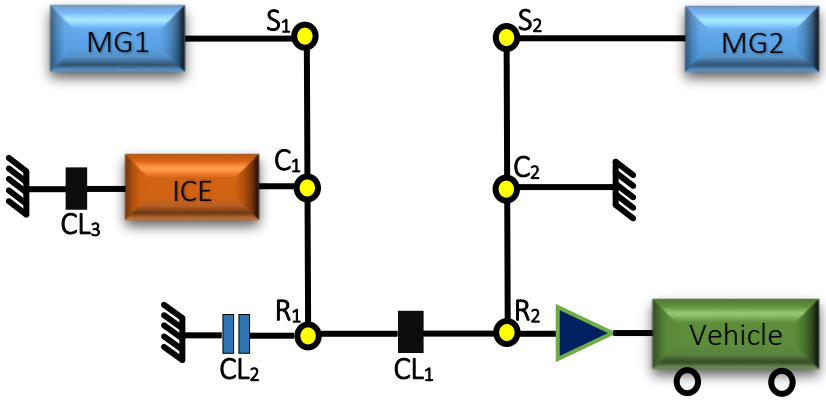


**Figure 3.5:** *Configuration of mode 1 i*

### Mode 2: Parallel with Fixed Gear (Engine + 1MG, 1DoF)

Figure 3.6 shows the configuration of mode 2 for 3PG-2 topology. The criteria of this mode is as follows:

$$DoF = 1, C_{eng} \neq 0, C_{mg1}C_{mg2} = 0, C_{mg1^2} + C_{mg2^2} \neq 0$$

In this mode, the speeds of all the components are proportional to each other. This mode provides the flexibility to choose engine torque with in its bsfc region. This mode is only available in 3PG topologies and provides benefit over other topologies during engine operation. There are two more fixed gear modes which are discussed later, they also provide the benefit of improved fuel economy.

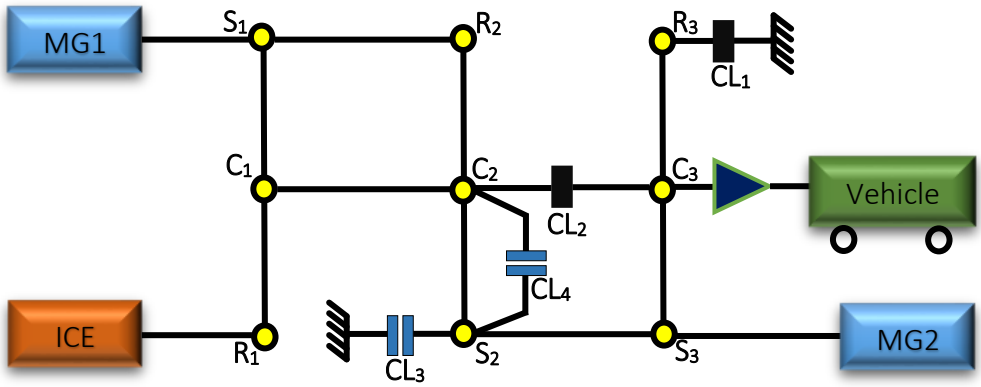


**Figure 3.6:** *Configuration of mode 2*

### Mode 3: Input Split (2 DoF)

Figure 3.7 shows the configuration of input split mode realised in 2PG-1 topology. The criteria of this mode is as follows:

$$DoF = 1, r_{vmg2vmg2} = 2, C_{eng}C_{mg1}C_{mg2} \neq 0$$

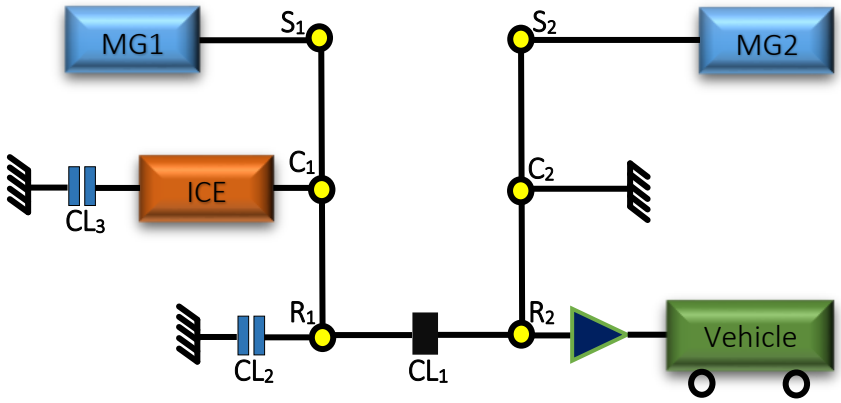


**Figure 3.7:** *Configuration of mode 3*

The input-split mode can have either 1 or 2 DoF. For the configuration shown here the DoF is 1. All the components are connected to output shaft mechanically via 2PGs. In this mode, the speed of engine is controlled by MG1 and the speed of MG2 is directly proportional to vehicle speed. Also, the torque of engine can be chosen from the optimal bsfc region.

### Mode 4: 1EV (1MG, 0DoF)

Figure 3.8 shows the configuration of 1EV mode realised in 2PG-1 topology. The criteria of this mode is as follows:

$$DoF = 1, V_{eng} = 0, C_{mg1}C_{mg2} = 0, C_{mg1^2} + C_{mg2^2} \neq 0$$

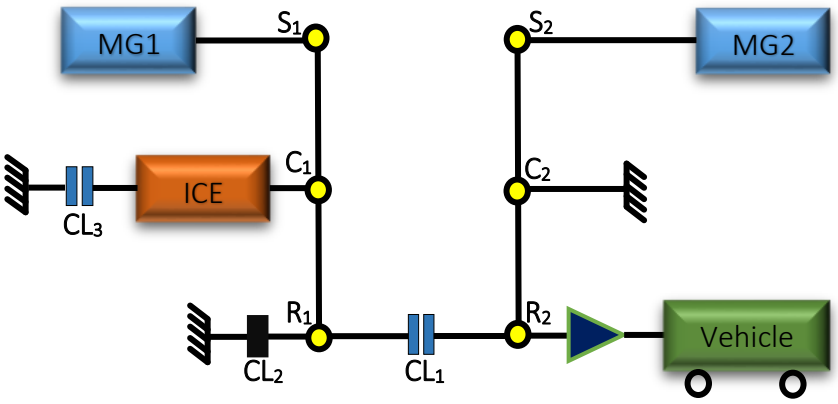


**Figure 3.8:** *Configuration of mode 4*

In this mode vehicle is propelled by only MG2. Both MG1 and engine are disconnected from the output shaft.

### Mode 5: Compound Split (2DoF)

Figure 3.9 shows the configuration of mode 5 realised in 2PG-2 topology. The criteria of this mode is as follows:

$$DoF = 2, r_{vmg1} = 2, r_{vmg2} = 2, r_{ve} = 2, r_{emg1} = 2, r_{emg2} = 2, r_{mg1mg2} = 2, C_{eng}C_{mg1}C_{mg2} \neq 0$$

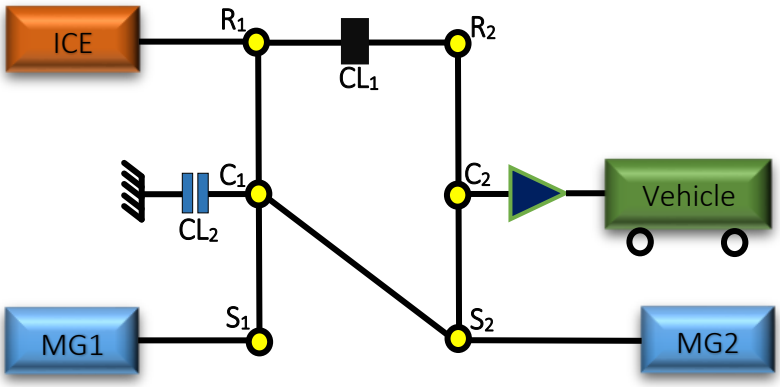


**Figure 3.9:** *Configuration of mode 5*

The Dof of this mode is 2. The speed of vehicle, engine, and both of the MGs are not coupled with each other. This mode is useful for producing very high speed at the output shaft.

### Mode 6: Parallel with Fixed Gear (Engine + 2MGs, 2 DoF)

Figure 3.10 shows the configuration of mode 6 realised in 3PG-2 topology. The criteria of this mode is as follows:

$$DoF = 2, C_{eng} \neq 0, C_{mg1}C_{mg2} \neq 0, r_{ve} = 1$$

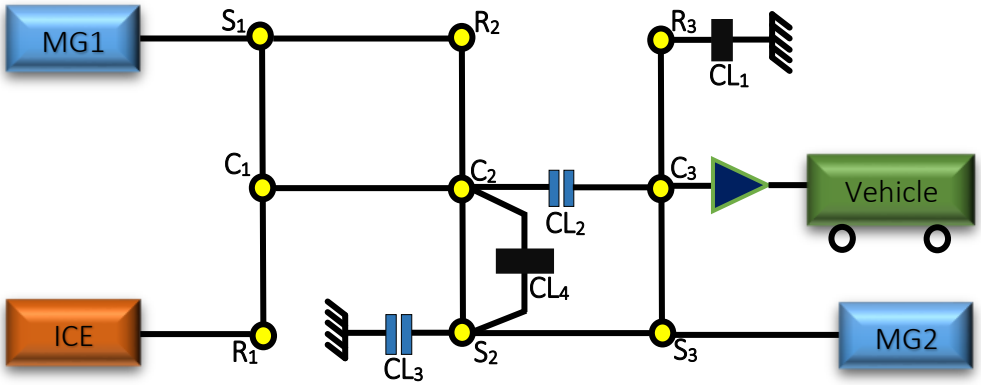


**Figure 3.10:** *Configuration of mode 6*

In this mode, the speed of engine is directly related to the speed of vehicle. The speed of MG1 and MG2 can be manipulated to achieve high electrical drive efficiency. This high efficiency motor operation leads to reduced equivalent fuel consumption.

### Mode 7: Parallel with EVT (Engine + 1MG, 1 DoF)

Figure 3.11 shows the configuration of mode 6 realised in 2PG-2 topology. The criteria of this mode is as follows:

$$DoF = 2, C_{eng} \neq 0, C_{mg1}C_{mg2} = 0, C_{mg1^2} + C_{mg2^2} \neq 0$$

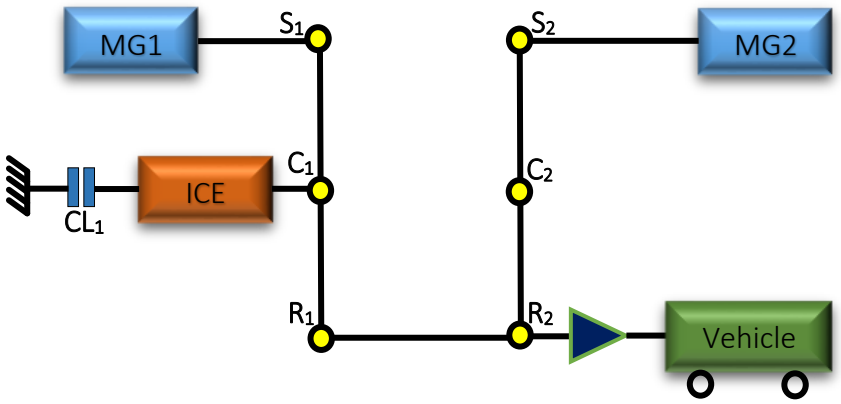


**Figure 3.11:** *Configuration of mode 7*

This mode is similar to input split without the MG coupled with the vehicle output shaft. The vehicle is propelled by engine and MG2 but in this mode only the speed of engine can be manipulated, restricting torque in the optimal bsfc region is not possible.

### Mode 8: Series Mode (1DoF)

Figure 3.12 shows the configuration of series mode realised in 2PG-1 topology. The criteria of this mode is as follows:

$$DoF = 1, C_{eng} = 0, V_{eng} \neq 0, C_{mg1}C_{mg2} = 0$$

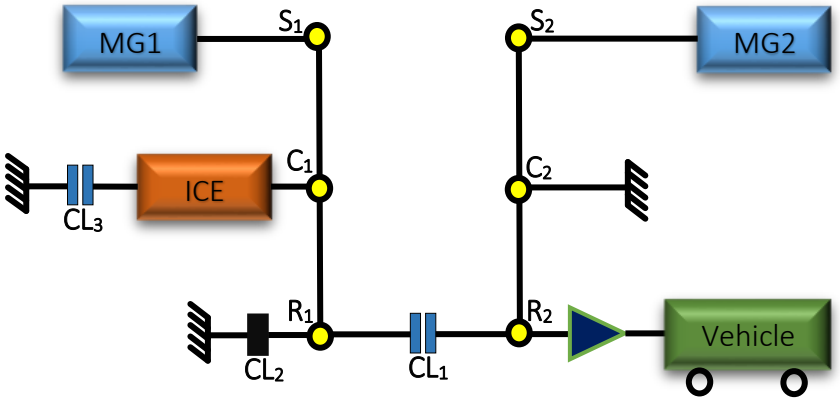


**Figure 3.12:** *Configuration of mode 8*

The series mode can have DoF either 1 or 2. However in the given configuration of the 2PG-1 topology only speed of engine is independent, hence the DoF is 1. In this mode, engine can run at this optimal bsfc zone and recharge the battery using MG1, while MG2 provides the torque requested by the vehicle.

### Mode 9: Parallel with Fixed Gear (Engine + 2MGs, 1DoF)

Figure 3.13 shows the configuration of mode 9 realised in 3PG-1 topology. The criteria of this mode is as follows:

$$DoF = 2, C_{eng} \neq 0, C_{mg1}C_{mg2} \neq 0,$$

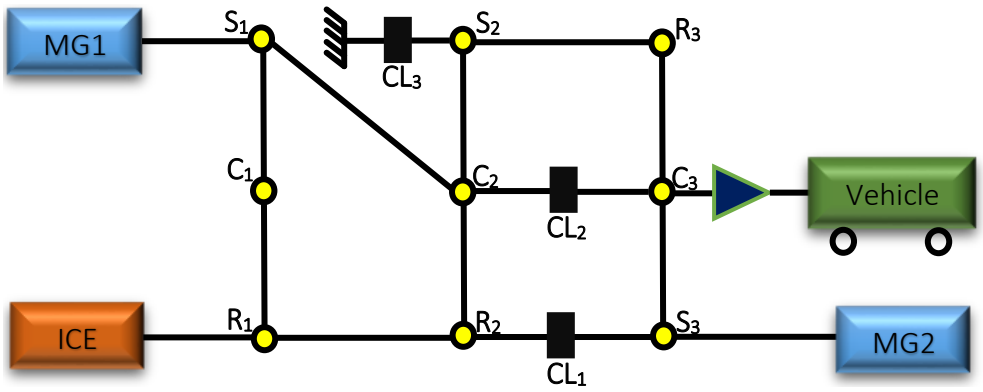


**Figure 3.13:** *Configuration of mode 9*

This mode is similar to mode 7 with both the MGs providing the torque request. The vehicle is propelled by engine,MG2, and MG1 but in this mode only the speed of engine can be manipulated, restricting torque in the optimal bsfc region is not possible.

### Mode 10: Parallel with EVT (Engine + 2MGs in series)

Figure 3.14 shows the configuration of mode 9 realised in 2PG-2 topology. The criteria of this mode is as follows:

$$DoF = 2, C_{eng} \neq 0, C_{mg1mg2} \neq 0, r_{mg1mg2} = 1$$

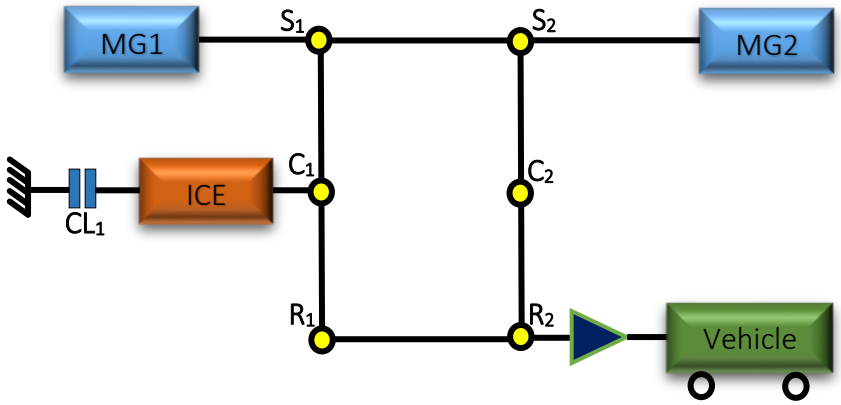


**Figure 3.14:** *Configuration of mode 10*

In the mode, the EVT function of the vehicle is realised by connecting MG1, MG2, engine, and output shaft in series. In this mode, when the engine fuel is stopped, the components' speeds will be uncontrollable. Therefore. this mode is only theoretically feasible and no such vehicle is commercialised using this mode.

### Mode 11: EV (2MGs, 2DoF)

Figure 3.15 shows the configuration of mode 11 realised in 2PG-2 topology. The criteria of this mode is as follows:

$$DoF = 2, V_{eng} = 0$$

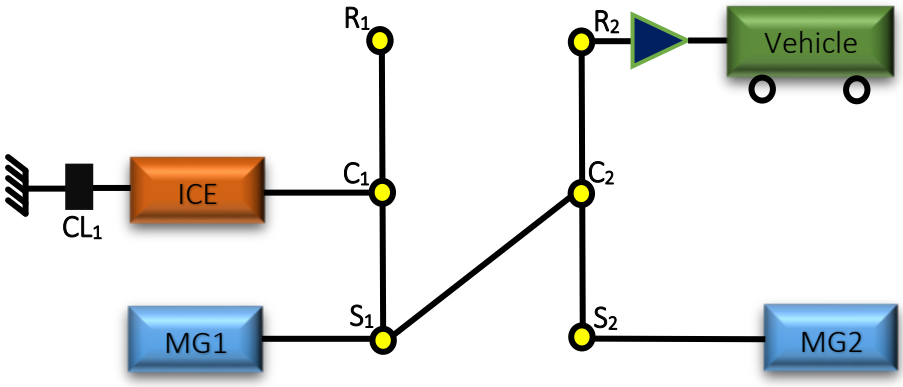


**Figure 3.15:** *Configuration of mode 11*

In this mode type, the engine is disabled and both the motors provides the torque requested by the vehicle. This mode is similar to mode 1 but with 2 DoF.

### Mode 12: Output Split (2 DoF)

Figure 3.16 shows the configuration of mode 12 realised in 2PG-2 topology. The criteria of this mode is as follows:

$$DoF = 2, r_{emg1} r_{emg2} = 2, C_{eng} C_{mg1} C_{mg2} \neq 0$$

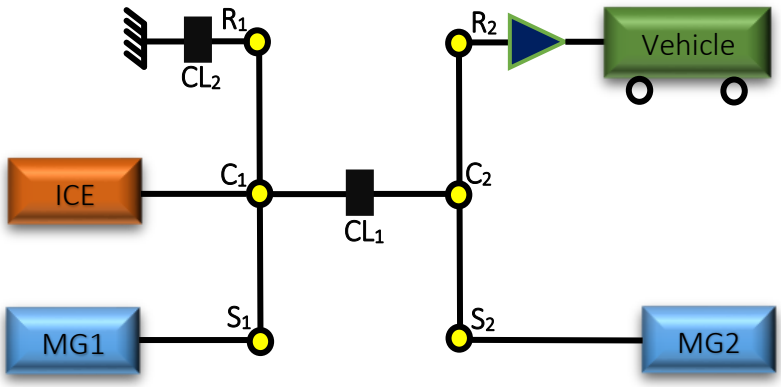


**Figure 3.16:** *Configuration of mode 12*

In an output split mode, the DoF is 2 and all the powertrain component are connected to output shaft via the mechanical connection of 2PGs. This mode is similar to input split mode. The main difference between input split and output split mode is engine torque is connected to MG2 torque and can not be chosen from optimal bsfc zone, as used in input split mode.

### Mode 13: Compound Split (3DoF)

Figure 3.17 shows the configuration of mode 12 realised in 2PG-2 topology. The criteria of this mode is as follows:

$$DoF = 3$$

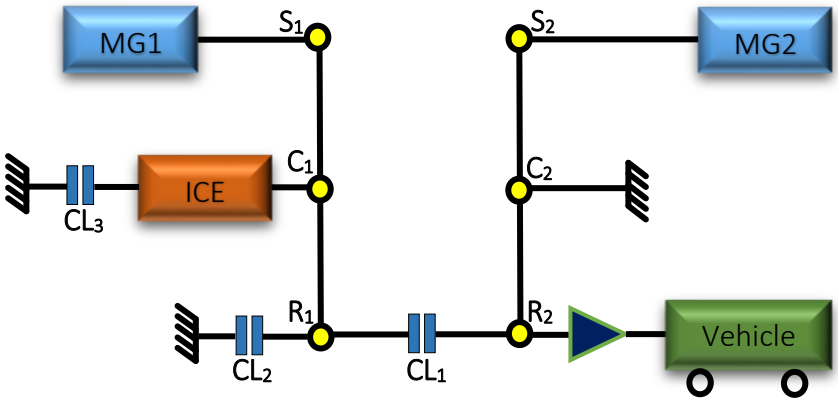


**Figure 3.17:** *Configuration of mode 13*

In this mode, all the powertrain components are independent of vehicle speed. Since the number of independent component and and component of powertrain both are 3, no flexibility on torque will be allowed. Due to this reason, this mode also becomes a theoretical mode.

### Mode 14: Engine Only (0DoF)

Figure 3.18 shows the configuration of mode 14 realised in 2PG-2 topology. The criteria of this mode is as follows:

$$DoF = 1, C_{eng} \neq 0, C_{mg1^2} + C_{mg2^2} \neq 0$$

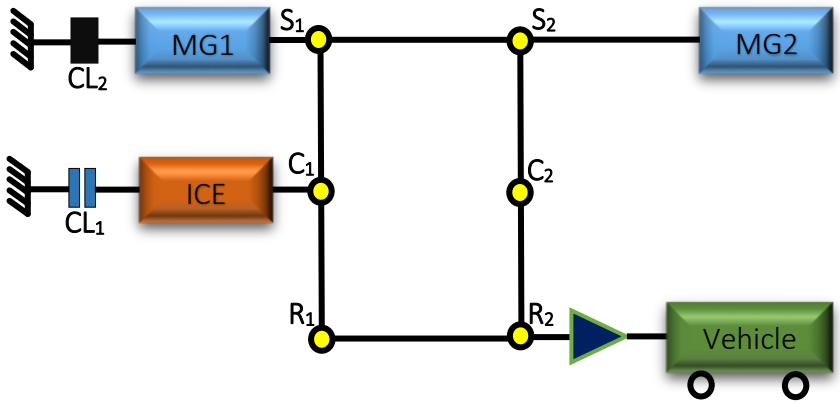


**Figure 3.18:** *Configuration of mode 14*

Both the MGs are disables in this mode and vehicle torque request is provided by engine only. This mode is used when battery SoC is below 40% and electric power is completely cut-off.

## 3.2 Energy Management Strategy Problem Formulation and Solution

In this study, the performances of drivetrains with 1PG, 2PGs, and 3PGs topologies are compared. For a meaningful comparison between topologies, they must be operating at their optimal performance. Since modes have an impact on the performance of powertrain components, it is crucial that the EMS selects modes and torque distribution simultaneously. Therefore, the energy management strategy (EMS) proposed in this work considers both mode selection and torque distribution simultaneously. The EMS proposed mitigates the drawbacks of existing EMS where mode selection and torque distribution are sequential.

Developing an EMS with mode selection is a difficult optimisation problem because of mixed-integer variables and discontinuity in mode selection within a continuous drive cycle. In addition, the torque distribution is different for every mode, adding non-convexity to the system. Complementarity is used to formulate mode selection to address discontinuity within the modes.

### 3.2.1 Energy Management Strategy Problem Formulation

The energy management strategy is a multistage problem discretised with a sampling time of 1 s for the US06 drive cycle. The objectives of the EMS are to minimise total fuel consumption, mode shifting and deviation of battery SoC. The problem is turned into a single-objective optimisation problem by means of a convex combination of these objectives. For an unbiased study, energy consumption of the hybrid powertrain with different number of PGs must be compared when the powertrain operates optimally over the driving cycle, Therefore, this work proposes an EMS that performs both the mode selection and torque distribution simultaneously to utilise the powertrain optimally for driving over a given cycle. EMS with simultaneous modes selection and torque distribution is a complex mixed-integer optimisation problem due to the existence of discontinuity caused by changing mode of operation (i.e. due to engaging and disengaging the clutches and switching the operation of the electric motors between motoring and generating). This fact along with nonlinearity of components and existence of algebraic constraints make EMS a mixed-integer nonlinear optimal control problem (OCP) with differential and algebraic equations (DAEs) as follows:

$$\mathbf{u}^*(.) = \arg\min_{\mathbf{u}(.)} \sum_{k=0}^{N} J(\mathbf{x}_k, \mathbf{z}_k, \mathbf{u}_k; \theta_k) \tag{3.69a}$$

$$\text{s.t. :} \quad (3.75)\text{–}(3.79)$$

$$0 <= m_{p,k} \perp m_{q,k} >= 0, \quad \forall p \neq q \in \{1..9\} \tag{3.69b}$$

$$\sum_{p=1}^{9} m_{p,k} = 1 \tag{3.69c}$$

$$F_i\big(\mathbf{x}_k, \mathbf{z}_k, \mathbf{u}_k; \theta_k\big) = 0 \tag{3.69d}$$

$$\underline{\mathbf{u}} \leq \mathbf{u}_k \leq \overline{\mathbf{u}} \tag{3.69e}$$

$$\underline{\mathbf{x}} \leq \mathbf{x}_k \leq \overline{\mathbf{x}} \tag{3.69f}$$

$$\underline{\mathbf{z}} \leq \mathbf{z}_k \leq \overline{\mathbf{z}} \tag{3.69g}$$

$$i \in \{\text{1PG-1}, \text{2PG-1}, \text{2PG-2}, \text{3PG-2}, \text{3PG-1}\} \tag{3.69h}$$

where the decision variables are the engine torque, MG2 torque, angular velocity of MG1, modes and $\alpha$, and hence $\mathbf{u} = [\tau_e, \tau_{mg2}, \omega_{mg1}, m_1, m_2, m_3, m_4, m_5, m_6, m_7, \alpha]^T$. Binary variable $\alpha$ represents the states of the electric motors and $\alpha = 0$ during regeneration and $\alpha = 1$ during motoring. The battery SoC is a differential state variable: $\mathbf{x} = [SoC]$. The algebraic variables of the problem are the torque of MG1, angular velocity of MG2 and angular velocity of engine, and hence $\mathbf{z} = [\tau_{mg1}, \omega_{mg2}, \omega_e]^T$. The parameters used in this problem are the torque demand $\tau_{req}$ and longitudinal speed of vehicle $V_{vehicle}$, and hence $\theta = [\tau_{req}, V_{vehicle}]$. $N$ is the prediction horizon which equals to the length of driving cycle in seconds divided by the sampling time $T_s$. The rest of the problem (3.69) is explained as below.

The objectives of the EMS are to minimise energy consumption and penalties due to mode shifting and deviation of the battery SoC from its initial value $\mathrm{SoC}_0$. The problem is turned into a single-objective optimisation problem by a convex combination of these objectives as follows:

$$J = \sum_{k=0}^{N} \Big\{ \beta_m \dot{m} + \beta_s \dot{s}_k + \beta_{soc} (\mathrm{SoC}_0 - \mathrm{SoC}_k)^2 \Big\} \tag{3.70}$$

where $[\beta_m, \beta_s, \beta_{soc}] = [0.5, 0.1, 0.4]$ are the convex combination coefficients and $\dot{m}_{t_k}$ is the rate of energy consumption:

$$\dot{m}_{t,k} = \dot{m}_{\mathrm{e},k} + \dot{m}_{\mathrm{eqv},k} \tag{3.71}$$

and:

$$\dot{m}_{\mathrm{e},k} = \frac{q \rho \omega_{\mathrm{e},k}}{120} \tag{3.72}$$

$$\dot{m}_{\mathrm{eqv},k} = \begin{cases} \frac{\tau_{\mathrm{mg2},k}\omega_{\mathrm{mg2},k}}{\eta_{mg2,k}\eta_{\mathrm{char}}/\eta_{\mathrm{dischar}}}\frac{1}{0.35\mathrm{Q}_{\mathrm{HHV}}}m_{i,k}\alpha_k & \text{if } m \in \{2,3,...,9\}; \\ \frac{\eta_{\mathrm{char}}}{\eta_{\mathrm{dischar}}}\frac{1}{0.35\mathrm{Q}_{\mathrm{HHV}}}m_{1,k}\alpha_k\left(\frac{\tau_{\mathrm{mg2},k}\omega_{\mathrm{mg2},k}}{\eta_{\mathrm{mg2},k}}+\right. & \\ \left.\frac{\tau_{\mathrm{mg1},k}\omega_{\mathrm{mg1},k}}{\eta_{\mathrm{mg1},k}}\right) & \text{otherwise.} \end{cases} \tag{3.73}$$

Minimising $\dot{s}_k$ in (3.74) leads to minimising the number of mode shifts. Frequent mode shifts in the hybrid powertrain will lead to excessive mechanical losses due to repeated engagement and disengagement of clutches.

$$\dot{s}_k = \frac{1}{2}\delta\gamma\left(I_{\mathrm{e}}\left[\omega_{\mathrm{e},k} - \omega_{\mathrm{e},k-1}\right]^2 + I_{\mathrm{mg1}}\left[\omega_{\mathrm{mg1},k} - \omega_{\mathrm{mg1},k-1}\right]^2\right) \tag{3.74}$$

where $\gamma$ is a weighting factor fixed to 0.02 [110]. The mode change factor $\delta = 0$ when the next and current modes are the same, whilst $\delta = 1$ otherwise. where $\gamma$ is a weighting factor fixed to 0.02 [110]. The mode change factor is $\delta$ and $\delta = 0$ when the next and current modes are the same, whilst $\delta = 1$ otherwise. Mode shift penalty reduces the number of mode shifts. Frequent mode shift in the hybrid powertrain will lead to excessive mechanical losses due to repeated engagement and disengagement of clutches.

Equations (3.69b) and (3.69c) represent the multi-mode operation of the powertrain. The discontinuities due to the gearbox and electric motor operations are modelled by complementarity constraints (3.69b), where the operator $\perp$ indicates that at least one of the bounds is active (i.e., at each time $k$ either $m_{j,k}$ or $m_{l,k}$ is zero). At each sample $k$, only one of the modes $m_i, \forall i \in \{1..8\}$, is active which is modelled as Equation (3.69c).

The constraints in Equations (3.75)-(3.79) and Equations (3.69b-3.69c) show the distribution of torque at every mode for 1PG-1, 2PG-1, 2PG-2, 3PG-1, and 3PG-2 topologies respectively.

## 1PG-1

$$T_{mg2_k} = \left(\frac{-T_{mg1_k} R_1}{S_1}\alpha_k + \frac{T_{req_k}}{D_{GR}}\right) m_{1,k} \tag{3.75a}$$

$$T_{mg1_k} = -S_1\left(\frac{T_{e_k}}{R_1 + S_1}\right) m_{2,k}, T_{e_k} m_{8,k} \tag{3.75b}$$

$$\omega_{mg1_k} = \frac{R_1}{S_1}\omega_{mg2_k} m_{1,k}\alpha_k \tag{3.75c}$$

$$T_{mg2_k} = \frac{T_{req_k}}{D_{GR}} m_{2,4,k} \tag{3.75d}$$

$$T_{mg2_k} = -R_1\left(\frac{T_{e_k}}{R_1 + S_1}\alpha_k + \frac{T_{req_k}}{D_{GR}}\right) m_{3,k} \tag{3.75e}$$

$$\omega_{mg2_k} = D_{GR}\frac{V_{veh_k}}{r_{tyre}} m_{1,2,3,4,k} \tag{3.75f}$$

$$\omega_{e_k} = \left(\frac{\omega_{mg1_k}}{1 + \frac{R_1}{S_1}} + \frac{\omega_{mg2_k}}{1 + \frac{S_1}{R_1}}\right) m_{3,k}\alpha_k \tag{3.75g}$$

$$\omega_{e_k} = \left(\frac{\omega_{mg1_k}}{1 + \frac{R_1}{S_1}}\right) m_{2,k} \tag{3.75h}$$

$$\omega_{mg1_k} = \omega_{e_k}\left(S_1 + \frac{R_1}{S_1}\right) m_{8,k} \tag{3.75i}$$

## 2PG-1

$$T_{mg1_k} = \frac{S_1}{R_1}\Big( - \frac{R_2}{S_2} T_{mg2_k}\alpha_k + \frac{T_{req_k}}{D_{GR}}\Big) m_{1,k} \tag{3.76a}$$

$$T_{mg1_k} = -S_1\Big(\frac{T_{e_k}}{R_1 + S_1}\Big) m_{2,k}, T_{e_k} m_{8,k} \tag{3.76b}$$

$$\omega_{mg1_k} = \Big(\frac{S_2}{S_1}\Big)\omega_{mg2_k} m_{1,k}\alpha_k \tag{3.76c}$$

$$T_{mg2_k} = \frac{S_2}{R_2}\frac{T_{req_k}}{D_{GR}} m_{2,4,k} \tag{3.76d}$$

$$T_{mg2_k} = \frac{S_2}{R_2}\Big( - R_1 \frac{T_{e_k}}{R_1 + S_1}\alpha_k + \frac{T_{req_k}}{D_{GR}}\Big) m_{3,k} \tag{3.76e}$$

$$\omega_{mg2_k} = -\frac{R_2}{S_2}\frac{D_{GR}}{r_{tyre}} V_{veh_k} m_{1,2,3,4,k} \tag{3.76f}$$

$$\omega_{e_k} = \left(\frac{\omega_{mg1_k} S_1}{R_1 + S_1} - \frac{\omega_{mg2_k} S_2}{R_2 + S_2}\right) m_{3,k}\alpha_k \tag{3.76g}$$

$$\omega_{e_k} = \left(\frac{\omega_{mg1_k}}{1 + \frac{R_1}{S_1}}\right) m_{2,k} \tag{3.76h}$$

$$\omega_{mg1_k} = \omega_{e_k}\Big(S_1 + \frac{R_1}{S_1}\Big) m_{8,k} \tag{3.76i}$$

## 2PG-2

$$T_{mg2_k} = \frac{S_2}{R_2 + S_2}\Big( - T_{mg1_k}\frac{R_1 + S_1}{S_1}\alpha_k + \frac{T_{req_k}}{D_{GR}}\Big) m_{1,k} \tag{3.77a}$$

$$T_{mg2_k} = \frac{S_2}{R_2 + S_2}\Big( - T_{e_k}\frac{R_1 + S_1}{R_1}\alpha_k + \frac{T_{req_k}}{D_{GR}}\Big) m_{2,k} \tag{3.77b}$$

$$T_{mg2_k} = \frac{S_2}{R_2 + S_2}\Big( - T_{e_k}\alpha_k - T_{mg1_k}\alpha_k + \frac{T_{req_k}}{D_{GR}}\Big) m_{3,5,k} \tag{3.77c}$$

$$T_{mg2_k} = \frac{S_2}{R_2 + S_2}\frac{T_{req_k}}{D_{GR}} m_{4,k} \tag{3.77d}$$

$$\omega_{mg2_k} = \Big(\frac{R_2 + S_2}{S_2}\Big) D_{GR}\frac{V_{veh_k}}{r_{tyre}} m_{i,k}, i \in \{1,2,3,4\} \tag{3.77e}$$

$$\omega_{mg2_k} = \Big(\frac{R_2 + S_2}{S_2}\Big) D_{GR}\frac{V_{veh_k}}{r_{tyre}} - \frac{S_1}{S_2}\omega_{mg1_k} m_{5,k}\alpha_k \tag{3.77f}$$

$$\omega_{mg1_k} = \Big(\frac{R_1 + S_1}{S_1}\Big) D_{GR}\frac{V_{veh_k}}{r_{tyre}} m_{1,k}\alpha_k \tag{3.77g}$$

$$\omega_{e_k} = \Big(\frac{R_2 + S_2}{R_1}\Big) D_{GR}\frac{V_{veh_k}}{r_{tyre}} m_{2,k}\alpha_k \tag{3.77h}$$

$$\omega_{e_k} = \Big(\frac{R_2 + S_2}{R_1}\Big) D_{GR}\frac{V_{veh_k}}{r_{tyre}} + \frac{S_1}{R_1}\omega_{mg1_k} m_{3,5,k}\alpha_k \tag{3.77i}$$

## 3PG-1

$$T_{mg2_k} = \Big( - T_{mg1_k}\alpha_k + \frac{T_{req_k}}{D_{GR}} \frac{S_3}{(R_3 + S_3)} \Big) m_{1,k} \tag{3.78a}$$

$$T_{mg2_k} = \Big( - T_e\alpha_k + \frac{T_{req_k}}{D_{GR}} \frac{S_3}{(R_3 + S_3)} \Big) m_{2,3,6,k} \tag{3.78b}$$

$$T_{mg2_k} = \frac{T_{req_k}}{D_{GR}} \frac{S_3}{(R_3 + S_3)} m_{4,k} \tag{3.78c}$$

$$\omega_{mg2_k} = \Big( \frac{R_3 + S_3}{S_3} \Big) D_{GR} \frac{V_{veh_k}}{r_{tyre}} m_{1,2,4,6,k} \tag{3.78d}$$

$$\omega_{mg2_k} = D_{GR} \frac{V_{veh_k}}{r_{tyre}} \frac{R_1}{S_2} \omega_{mg1_k} m_{3,k} \tag{3.78e}$$

$$\omega_{mg1_k} = D_{GR} \frac{V_{veh_k}}{r_{tyre}} m_{1,6,k}, i \tag{3.78f}$$

$$\omega_{mg1_k} = \frac{R_2}{S_2} D_{GR} \frac{V_{veh_k}}{r_{tyre}} m_{2,k}, i \tag{3.78g}$$

$$\omega_{e_k} = \frac{R_2 + S_2}{R_2} \omega_{mg1_k} m_{6,k}, \alpha_k \tag{3.78h}$$

$$\omega_{e_k} = \frac{R_2}{S_2} \frac{R_2 + S_2}{R_2} \omega_{mg1_k} m_{2,k}, \alpha_k \tag{3.78i}$$

$$\omega_{e_k} = \omega_{mg2_k} m_{3,k} \alpha_k \tag{3.78j}$$

## 3PG-2

$$T_{mg2_k} = \Big( - T_{e_k} \frac{S_2}{R_2 R_1} \alpha_k + \frac{T_{req_k}}{D_{GR}} \frac{S_3}{(R_3 + 1)} \Big) m_{3,7,k} \tag{3.79a}$$

$$T_{mg2_k} = \Big( - T_{e_k} \alpha_k + \frac{T_{req_k}}{D_{GR}} \frac{S_3}{(R_3 + 1)} \Big) m_{2,k} \tag{3.79b}$$

$$T_{mg2_k} = \Big( - T_{e_k} \frac{S_2}{R_2 R_1} \alpha_k + \frac{T_{req_k}}{D_{GR}} \frac{S_3}{(R_3 + 1)} \Big) m_{6,k} \tag{3.79c}$$

$$\omega_{mg2_k} = \Big( \frac{R_3 + S_3}{S_3} \Big) D_{GR} \frac{V_{veh_k}}{r_{tyre}} m_{2,3,k} \tag{3.79d}$$

$$\omega_{e_k} = \frac{S_2}{R_2} \Big( D_{GR} \frac{V_{veh_k}}{r_{tyre}} \frac{R_3 + S_3}{S_3} + \omega_{mg1_k} \Big) m_{3,k} \alpha_k \tag{3.79e}$$

$$\omega_{e_k} = \frac{S_2}{R_1 R_2} \Big( D_{GR} \frac{V_{veh_k}}{r_{tyre}} \frac{R_3 + S_3}{S_3} + \omega_{mg2_k} \Big) m_{6,k} \alpha_k \tag{3.79f}$$

$$\omega_{e_k} = \Big( \frac{R_3}{R_3 + S_3} \omega_{mg2_k} - \frac{S_1}{R_1} \omega_{mg1_k} \Big) m_{2,k} \alpha_k \tag{3.79g}$$

$$\omega_{mg2_k} = \omega_{mg1_k} = \omega_{e_k} = D_{GR} \frac{V_{veh_k}}{r_{tyre}} m_{7,k} \alpha_k \tag{3.79h}$$

### 3.2.2 Energy Management Strategy Solution

The Energy Management Strategy (EMS) describes above is formulated using A Mathematical Programming Language (AMPL) [111]. AMPL was designed as a mathematical modeling language for linear programming, but later it is extended to formulate integer, mixed-integer linear, mixed-integer non-linear, and complementarity problems [112]. There are significant advantages of modeling optimization problems with AMPL due to its symbolic problem representation. This includes the possibility of automated analysis of model parts for linearity, convexity, automatic differentiation, extended error checking, and automatic generation of model code for lower-level languages. The success of AMPL can be seen by the extensive pool of mathematical optimization software packages available on NEOS Server for optimization [113**?** ]. This problem falls in the category of Mixed Integer Non-Linear Programming (MINLP) and is also non-convex. Due to mixed integers and non-convexity, it becomes difficult to get a locally optimal solution. The AMPL codes for all five topologies are given in appendix A.

To address these issues Knitro solver is used for solving the optimization problem. Knitro is a commercially used solver which is developed by Richard et al. [114]. The solver is designed for solving large-scale, smooth nonlinear programming problems, and it is also effective for the following special cases: unconstrained optimization, nonlinear systems of equations, least squares, and linear and quadratic programming. Various algorithmic options are available, including two interior methods and an active-set method. It also provides crossover techniques between algorithmic options as well as automatic selection of options and settings.

The Knitro solver used for solving the optimisation problem is accessed using NEOS server [115], which is an open source server. The NEOS server is supported by Morgridge Institute for Research [116] and Wisconsin Institute for Discovery [117]. The current NEOS team consists of Jeff Dischler, Michael Ferris, Ben Huebner, Jeff Linderoth, and Elizabeth Wong. The limitation is NEOS server is that simulation time is limited to 5 minutes. Therefore, to get the optimal solution for all data points, the problem is initialized every 5 minutes using the output of previous simulation results as in the input of the next simulation.

## 3.3 Energy Management Strategy Results and Discussion

### 3.3.1 Optimal EMS Results and Discussions

This section explains the results obtained by solving the Energy Management Strategy (EMS) problem using Knitro solver. The drive cycle chosen for this study is United States 06 (US06). Figure 3.19 summarises the simulation results for fuel consumption of all five topologies over US06 drive cycle. The US06 drive cycle is used in this work because this drive cycle has both aggressive and steady-state acceleration zones, and

the efficiency of different operating modes (with engine and without engine) can be analysed together. As shown in Figure 3.19a, during the time interval of 0-150 s and 500-600 s there is a frequent acceleration and deceleration, the torque demand will be very high during these time intervals and frequent tracking can also be observed. However, during the time interval of 160-500 s a constant acceleration can be seen, and high speed demand will be requested by the vehicle. Therefore, this drive cycle is ideal to investigate the optimal operation of the engine and the motors. Because the vehicle is requesting both high torque and high-speed demands.

Modes selection for all five topologies is shown in Figure 3.19b. Modes available for all the topologies are presented in Table 3.2. The modes are the decision variables of the EMS problem and optimally distributes torque demands amongst the power components whilst also controlling clutches. During the time intervals of 0-180 s and 500-600 s, higher fluctuation between mode selection is observed. The modes selected are mainly the ones that provide high torque, due to high torque demand by the vehicle. 1PG, 2PGs, and 3PG-1 topologies fluctuates between mode 3 (input-split), mode 4 (1EV mode), mode 5 (compound-split mode), and mode 6 (Parallel with fixed-gear mode). However, 3PG-2 topology only fluctuates between mode 3 (input split) and mode 7 (Parallel with fixed-gear mode). The reduction in mode fluctuation in 3PG-2 topology is due the fact that it can operate in mode 1 (2EV mode), mode 4 (1EV mode), and mode 3 (input-split) by only engaging clutch 1 ($CL_1$), while other topologies needs different clutch engagements to realise three different modes.

Total fuel consumption of the 2PG-1 topology as shown in Figure 3.19c is 5% less than the 1PG-1 topology. This improvement mostly happens during mode 3 (i.e., the input-split mode), where both the MG2 and engine contributes to the torque at wheels and MG1 has to restrain the speed of the engine within the optimal range to reduce brake specific fuel consumption (bsfc). The engine speed of 2PG-1 topology is close to its optimal value (which is 2050 rpm as in Table 3.1), whilst engine speed is high in 1PG-1 topology. This particularly happens during the time intervals of 0–180 s and 500–600 s. During this time interval, the speed of MG2 in 2PG-1 topology is higher compared to the speed of MG2 in 1PG-1 topology. Due to the higher rotational speed of MG2, the electric drive provides higher power in 2PG-1 topology and reduced the power demand from the engine. The electrical power in 1PG-1 topology is less due reduced speed of the electrical motors owing to the lower gear ratio between MG2 and the vehicle. Therefore, the engine provides higher power to meet the requested power demand. This higher power supplied by the engines becomes the source of higher engine fuel consumption in the 1PG-1 topology as presented in Figure 3.19d. Due to reduced power demand from the electric drive in 1PG-1 topology, the equivalent fuel consumption reduces as shown in Figure 3.19e. This reduction can be observed as highest battery state of charge for 1PG-1 topology at the end of drive cycle, and is illustrated in Figure 3.19f.

3PG-2 topology also benefits from the higher rotation of MGs to drop fuel consumption, however, increasing the number of PGs from two to three further reduces the total fuel consumption by an extra 1.6% as shown in Figure 3.19c . This is because

of the availability and selection of fixed-gear modes (i.e., mode 2, 6, and 7), as shown in Figure 3.19b. The fixed-gear modes reduce equivalent energy consumption because of omitting the need of MG1 to regulate the engine speed (and hence excluding corresponding losses). During the time intervals 80-100 s, 170-180 s and 295-345 s EMS of the 3PG-2 topology chooses fixed-gears modes (mode 2, 6, and 7), while other topologies with 1 and 2 PGs operate in 2EV mode (mode 1). This fixed gear modes selection is the reason for lowest equivalent fuel consumption in 3PG-2 topology. Moreover, during mode 7, which is only available in 3PG-2 topology, the speeds of all components are the same as vehicle speed with a gear ratio of one, the engine operates at low speeds and provides high torque, which reduces total engine fuel consumption. Therefore, due to fixed gear modes 2, 6, and 7 both engine and equivalent fuel consumption reduce in 3PG-2 topology, resulting in the lowest total fuel consumption among all the topologies.

3PG-1 topology also has fixed gear modes and shows the reduction in equivalent fuel consumption, but due to the reduced gear ratio between engine and MG1, the engine operation is not optimised, resulting in higher engine fuel consumption. It is also observed in 2PG-2 topology that, EMS chooses 1EV mode for the time interval of 420 - 500 due to which equivalent fuel consumption is lower compared to 2PG-1 and 1PG-1 topology.

As presented in Table 3.2, the maximum number of modes possible 1PG-1 and 2-PG-1 topology are 4, and for 2PG-2, 3PG-1, and 3PG-2 are 5, 7, and 8, respectively. As represented in Figure 3.19b, mode 8 and mode 9 are never chosen by the EMS of any of the topologies. The EMS did not choose mode 8 (series mode) because the initial battery state of charge (SoC) is set to be 80%, and mode 8 can only be selected when SoC is 40%. During the entire US06 drive cycle, SoC did not drop to 40% resulting in non-selection of mode 8. The EMS also did not select mode 9 (parallel with fixed-gear mode 1MG, 1DoF). During mode 9, MG1 and engine should provide the torque requested by the vehicle. The EMS and ASM models developed in this study use MG1 as a speed controller for the engine for the modes where engine is active. Therefore, the mode in which only MG1 is requested to provide vehicle torque with engine can not be selected.

Figure 3.21 shows the speeds and torques of the engine, MG1, and MG2 for all five topologies during US06 drive cycle. Engine speed is highest for 1PG-1 topology as shown in Figure 3.21a, and is lowest for 2PG-1 topology. However, engine provides higher torque in 1PG-1 topology compared to 2PG-1 topology as presented in Figure 3.21b. This high torque and low speed operation of engine is the primary source of highest engine fuel consumption in 1PG-1 topology. The high speed and low torque engine operation is also observed in 2PG-2 and 3PG-1 topology, due to which engine fuel consumption from these two topologies is also high. However, for 3PG-2 topology, engine behavior is similar to 2PG-1, but engine operates for higher time duration in 3PG-2 topology. Due to increase in engine run time, engine fuel consumption is also increased.

Speed of motor generator 1 (MG1) presented in Figure 3.21c is a decision variable

responsible to restrict engine speed in its optimal operation for all other modes except mode 1 (2EV mode). During mode 1, MG1 also provides torque requested along with MG2, as presented in Figure 3.21d. The speed of MG1 is a critical factor in determining the operation of engine. In 1PG-1 topology, the speed of MG1 is higher compared to all other topologies during mode 3, and is the primary reason for engine operation in low efficiency region. However, during mode 1, MG1 torque is high in 3PG-1 topology, which is reflected in increased equivalent fuel consumption.

Figure 3.21e and Figure 3.21f shows the resulting operating points of motor generator 2 (MG2), which has a significant impact on the total fuel consumption of the topologies as the main source of power in all the modes. The main difference between the operation of MG2 in the 1-PG, 2-PG, and 3-PG topologies is in the magnitude of rotation. The higher speed of MG2 allows it to provide higher power while keeping it in high efficiency regions. The high efficiency operation of MG2 reduces the equivalent fuel consumption.

## 3.4 Systematic Comparison between Hybrid Powertrains with One, Two, and Three Planetary Gears

This section provides a systematic comparison between the hybrid powertrains with one, two, and three planetary gears. Figure 3.19a shows the tracking performance of the developed powertrain with 1PG-1, 2PG-1, 2PG-2, 3PG-1, and 3PG-2 topologies. The speeds of the vehicle with 3PG topologies are the ones that deviate the most from the desired profile. This is due to the fact that 3PG topologies introduce more modes of operation and hence more clutch fluctuations, which increases the resulting tracking error of speed. More precisely, there are 7 modes in 3PG-1 and 6 modes in 3PG-2 topologies, compared to 4 modes in 1PG and 5 modes in 2PG topologies. The root mean square values of tracking error for 3PG-1 and 3PG-2 topologies are 14.23 m/s and 12.76 m/s, respectively. The corresponding tracking errors for the 1PG-1, 2PG-1, and 2PG-2 topologies are 8.22 m/s, 10.05 m/s, and 11.65 m/s, respectively.

The total fuel consumption which is the sum of the fuel consumption by the engine and the equivalent fuel consumption by the electric motors. To calculate the equivalent fuel consumption, engine operates at its optimal point after finishing the driving cycle to charge the battery through MG1. The equivalent fuel consumption is then the amount of burned fuel to recharge the battery to its initial SoC (80%).

Total fuel consumption as illustrated in Figure 3.19c of the 2PG-1 topology is 566 $g$ which is 5.0% less than 596 $g$ of the 1PG-1 topology. Moving from 2PG to 3PG can also improve the total fuel consumption by an extra 1.5% (i.e., 6.5% in total) as compared to 1PG topology. As shown in Table 3.3, the 2PG-2 and 3PG-1 also improve fuel consumption by, respectively, 1.3% and 2.8% as compared to 1PG topology. Fuel consumption by engine in all topologies with multiple PGs is lower than 1PG topology with the cost of small increase in equivalent fuel consumption. In other words, for a maximum of 1.6% deeper discharged battery, the topologies with multiple PGs consume up to 67 $g$ less fuel. As shown in Figure 3.19d, direct fuel consumption by engine is similar for all the topologies during the time interval of 200-500 s, whilst it is much less for 2PG-1 and 3PG-2 (particularly 2PG-1) during the time intervals of 0–180 s and 500–600 s. Equivalent fuel consumption of 1PG and 2PG-1, on the other hand, are similar and more than 3PG-2 during the time interval of 200–500 s, which is similar to the trend of SoC of battery in Figure 3.19f.

**Table 3.3:** *Summary of the EMS results of over US06 drive cycle.*

| Description | 1PG-1 | 2PG-1 | 2PG-2 | 3PG-1 | 3PG-2 |
|---|---|---|---|---|---|
| Total Fuel Consumption | 596 g | 566 g | 588 g | 579 g | 557 g |
| Engine Fuel Consumption | 101 g | 33.8 g | 50 g | 71 g | 54.2 g |
| Equivalent Fuel Consumption | 495 g | 532.2 g | 538 g | 508 g | 502.8 g |
| Battery SoC at the end of cycle | 70.2% | 68.6% | 68.3% | 69.1% | 69.3% |

The main reasons for improvement in fuel consumption by the 2PG and 3PG topologies lies in two facts that i) the speed of electric motors are higher with multiple PG topologies leading to less power demand from engine, and ii) fixed-gear ration topologies save the electric power losses required to regulate the engine speed. These facts are explained in more details throughout the rest of this section.

From Table 3.2, 1PG-1 and 2-PG-1 topologies can generate up to 4 modes, whilst the number of modes supported by 2PG-2, 3PG-1, and 3PG-2 are, respectively, 5, 7, and 8.

As in Figure 3.19b, EMS of never choose mode 8 and mode 9 for any of the topologies. EMS does not choose mode 8 (series mode) because the initial state of charge (SoC) of battery is 80%, and mode 8 can only be selected when SoC is 40% or less. However, during the entire US06 drive cycle, SoC did not drop to 40%. EMS also does not select mode 9 because of the fact that the developed EMS and simulation models in this study use MG1 as a speed controller for the engine if engine is active. Hence, mode 9, where MG1 and engine should simultaneously provide torque to the wheels, is infeasible.

Figure 3.19b shows that EMS chooses mode $\in \{1, 3, 4\}$ for 1PG and 2PG-1 topologies and mode $\in \{1, 2, 3, 4, 6, 7\}$ for 3PG-2 during the time intervals of 0–180 s and 500–600 s. From Table 3.3, mode 1 and 4 are EV modes where, respectively, both MGs and only one MG contributing torque to the wheels. In input-split mode 3, on the other hand, all the drivetrains contribute to the wheel torque, whilst the speed of engine is regulated by the speed of MG1. Modes 2, 6 and 7 represent parallel topologies with a fixed ratio between the speed of engine and the speed of vehicle, however, unlike mode 4, mode 2 utilises only one of the MGs.

Unlike in 1PG topology, speed of MG2 in all modes (except mode 7 for 3PG-2) of 2PG-1 and 3PG-2 are larger than the speed of final drive with a coefficient of, respectively, $\frac{R_2}{S_2} > 1$ and $1 + \frac{R_3}{S_3} > 1$ (For more details, refer to Appendix A). For example, given the gear ratio of Table 3.1, the speed of MG2 in 2PG-1 over US06 is illustrated in Figure 3.22a that is up to 2.6 times higher than the speed of MG2 in 1PG-1 topology. Moreover, as shown in Figure 3.22b, engine in 2PG-1 and 3PG-2 rotates closer to its optimal speed (which is 2050 rpm as in 3.1) because of higher speed of MG2 (for more details, refer to Appendix A), whilst it is too high in 1PG-1 topology. Figure 3.22c shows that there is not a major difference in operation of MG1

between different topologies.

The higher speed of MG2 enables it to operate at high power with higher efficiency due to the shape of efficiency map in Figure 3.22a. Hence, EMS utilises MG2 of 2PG and 3PG topologies at higher power and efficiency than the MG2 of 1PG topology, as shown in Figure 3.25a and 3.25b. This will also reduce the required power from engine, as in Figure 3.25c, and hence direct fuel consumption by engine. This is shown in Figure 3.22b where compares the brake specific fuel consumption (bsfc) of engine of the 2PG-1 and 3PG-2 topologies against 1PG topology. This is with the cost of degrading efficiency of MG1 for a similar delivered power, as in Figure 3.25f. However, MG1 does not contribute to the wheel torques during the time intervals of 0–180 s and 500–600 s, and hence such reduction of efficiency causes an insignificant drawback.

As discussed before and shown in, Figure 3.23, increasing the number of PGs from two to three further reduces the total fuel consumption by an extra 1.5%. This is partially because the speed of MG2 in 3PG-2 topology can be even larger than 2PG-1 (see Figure 3.22a) meaning that MG2 can provide more power with the high efficiency than 2PG-1. However, the main reason for this extra improvement is the availability and selection of the fixed-gear modes (i.e., mode 2 and 6), as shown in Figure 3.19b. The fixed-gear modes reduce equivalent energy consumption because of omitting the need of MG1 to regulate the engine speed (and hence excluding corresponding losses) [118]. During the time intervals 80-100 s, 170-180 s and 295-345 s EMS of the 3PG-2 topology chooses these fixed-gears modes, while other topologies with 1 and 2 PGs, which do not support fixed-gear modes, operate in 2EV mode (mode 1). Moreover, during mode 7, which is only available in 3PG-2 topology, the speeds of all components are the same and proportional to the vehicle speed (See Appendix A). EMS uses this mode whenever there is a demand for high torque at low vehicle speed to reduce direct fuel consumption.

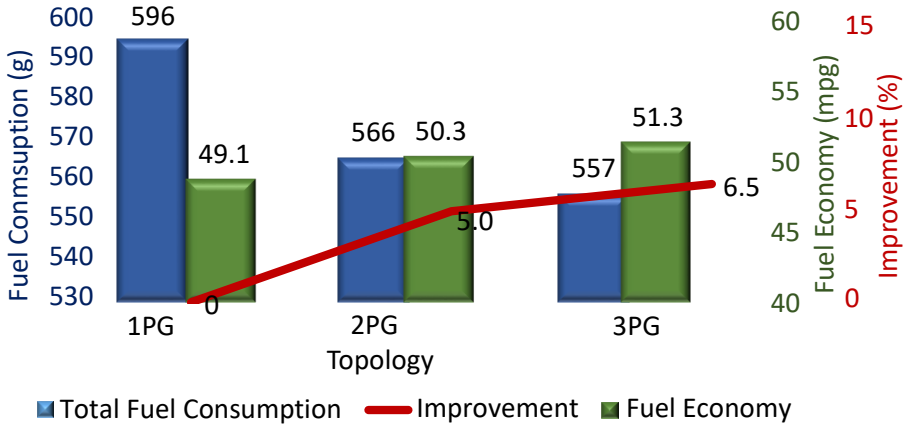


**Figure 3.23:** *Comparison of total fuel consumption, fuel economy, and reduction in percentage of fuel consumption for topologies with different numbers of PGs over US06 drive cycle.*

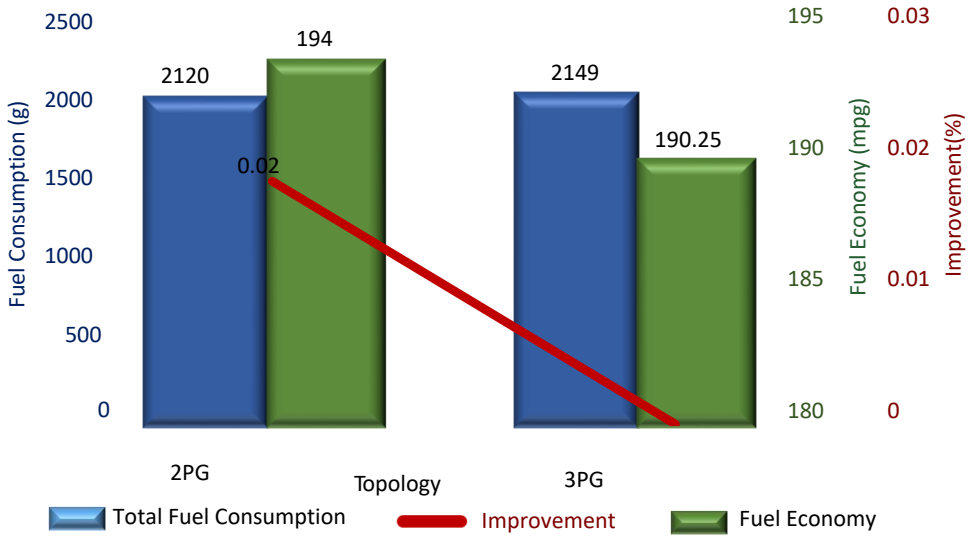


**Figure 3.24:** *Comparison of total fuel consumption, fuel economy, and reduction in the percentage of fuel consumption for 2PG and 3PG topologies, when the drive cycle is repeated 3-times.*

However, the fuel economy of 3PG topology reduces by 0.02% compared to 2PG topology as shown in Figure 3.24, when the US06 drive cycle is repeated 3-times as illustrated in Figure 3.20a. Total fuel consumption is decreased in 2PG topology when driven three times on the same drive cycle. 2PG topology saves 29 g of the total fuel consumption compared to 3PG topology, as shown in Figure 3.20b. The primary reason for this behavior by 3PG is due to higher engine fuel consumption, as illustrated in Figure 3.20c. During the start and end of drive cycles, the 3PG topology chooses fixed gear modes (modes - 2, 6, and 7), resulting in increased engine fuel consumption. However, Figure 3.20d and Figure 3.20e, shows that the use of electric motors is rather less in 3PG topology. The final SoC of 3PG topology is 5% higher than 2PG, equating to the difference in equivalent fuel consumption. Further investigation by repeating the drive cycle is only carried out for 2PG and 3PG topologies because the difference between total fuel consumption between 1PG and others is relatively high. As well as, the vehicles the real-world have also discontinued their 1PG powertrains.

## 3.5 Concluding Remarks

The contributions of this section are as follows:

- Evaluation of the impact of the number of PGs on the energy consumption of HEVs. It is shown that increasing the number of PGs from one to two and from two to three reduces the energy consumption by 5% and 1.5%, respectively.
- Optimal EMS for the multi-mode hybrid electric powertrains with different numbers of PGs. The developed EMS simultaneously controls the clutches of the

gearbox as well as energy flows of components to minimise energy consumption over a driving cycle.

- The energy consumption increases by 0.02% in three PG topology as compared to two PG, when both the topologies are repeated three times on US06 drive cycle.
- Design rules are introduced for HEVs with multiple PGs:
    1. Electric motors with higher speed give flexibility to improve the engine efficiency and therefore reduce energy consumption. This can happen by both the 2PG and 3PG topologies.
    2. Engine can operate within the optimum range of its rotational speed using the fixed-gear modes and without involvement of electric motors. This is possible in 3PG topologies and reduces the electric losses and hence the energy consumption.

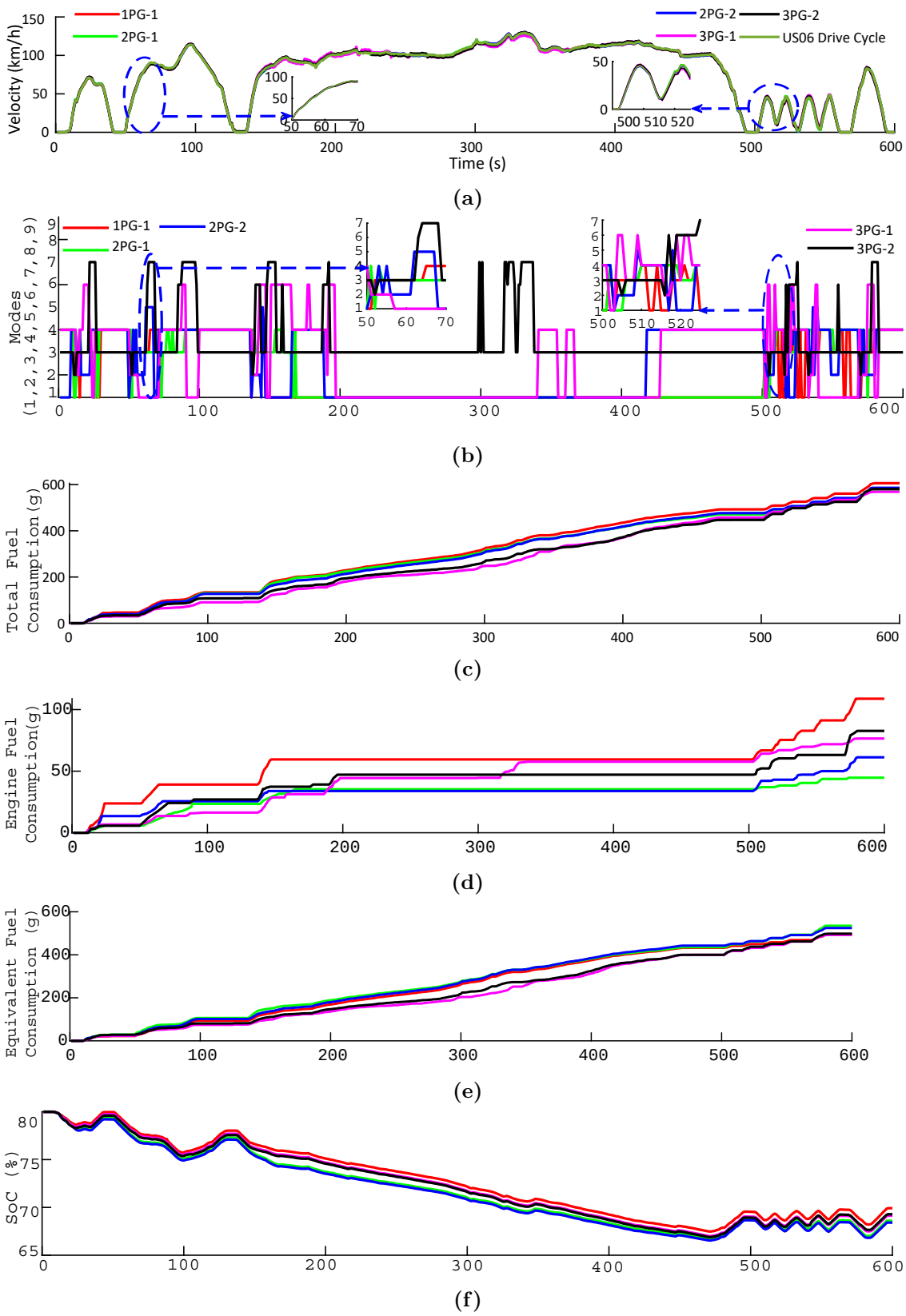


**Figure 3.19:** *Fuel consumption over US06 drive cycle for all topologies (a) US06 drive cycle, (b) Modes (c) Total fuel consumption, (d) Engine fuel consumption, (e) Equivalent fuel consumption, (f) Battery state of charge.*

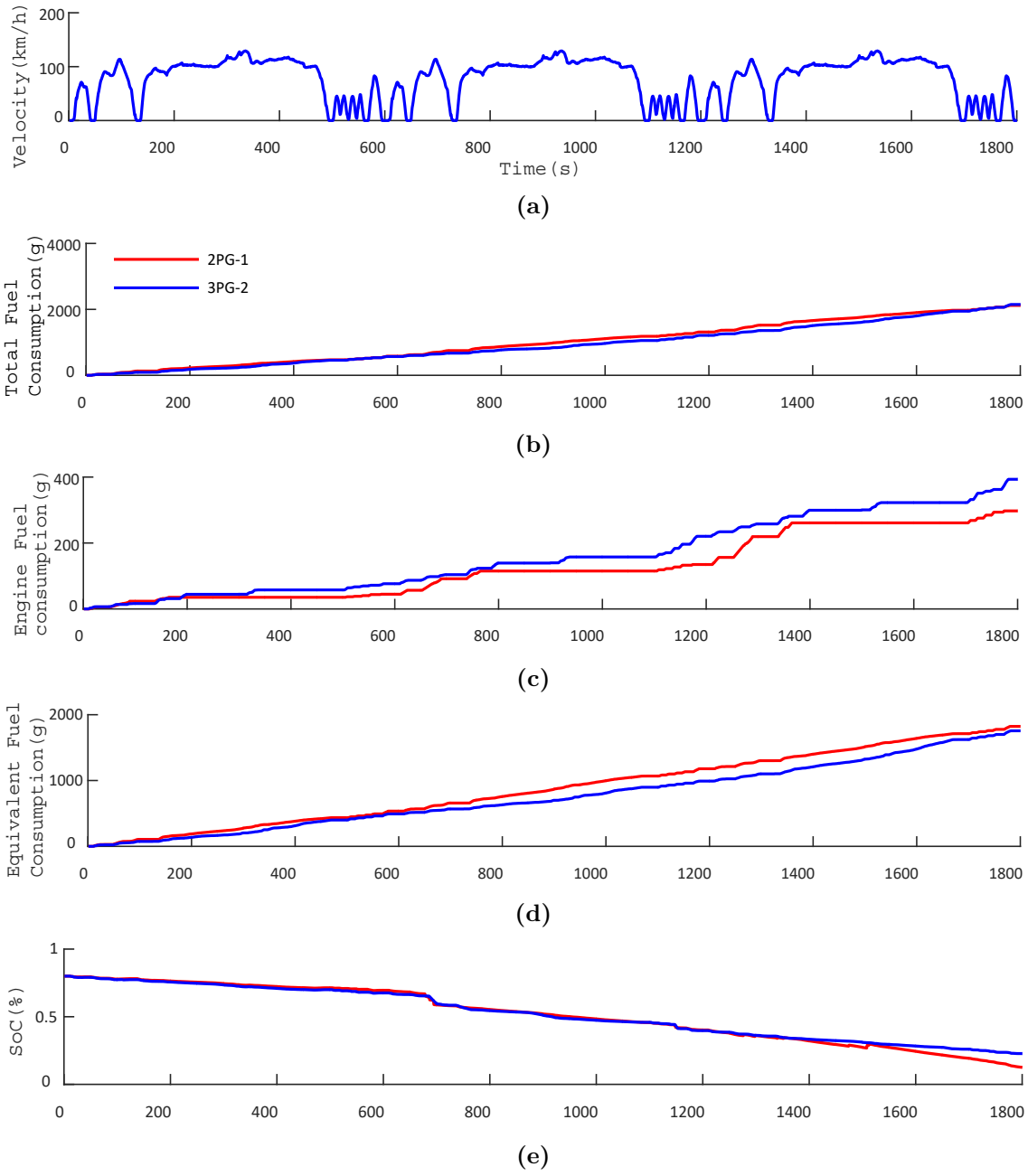


**Figure 3.20:** *Fuel consumption over US06 drive cycle for 2PG-1 and 3PG-2 topologies till SoC is below 20% (a) US06 drive cycle, (b) Total fuel consumption, (c) Engine fuel consumption, (d) Equivalent fuel consumption, (e) Battery state of charge.*

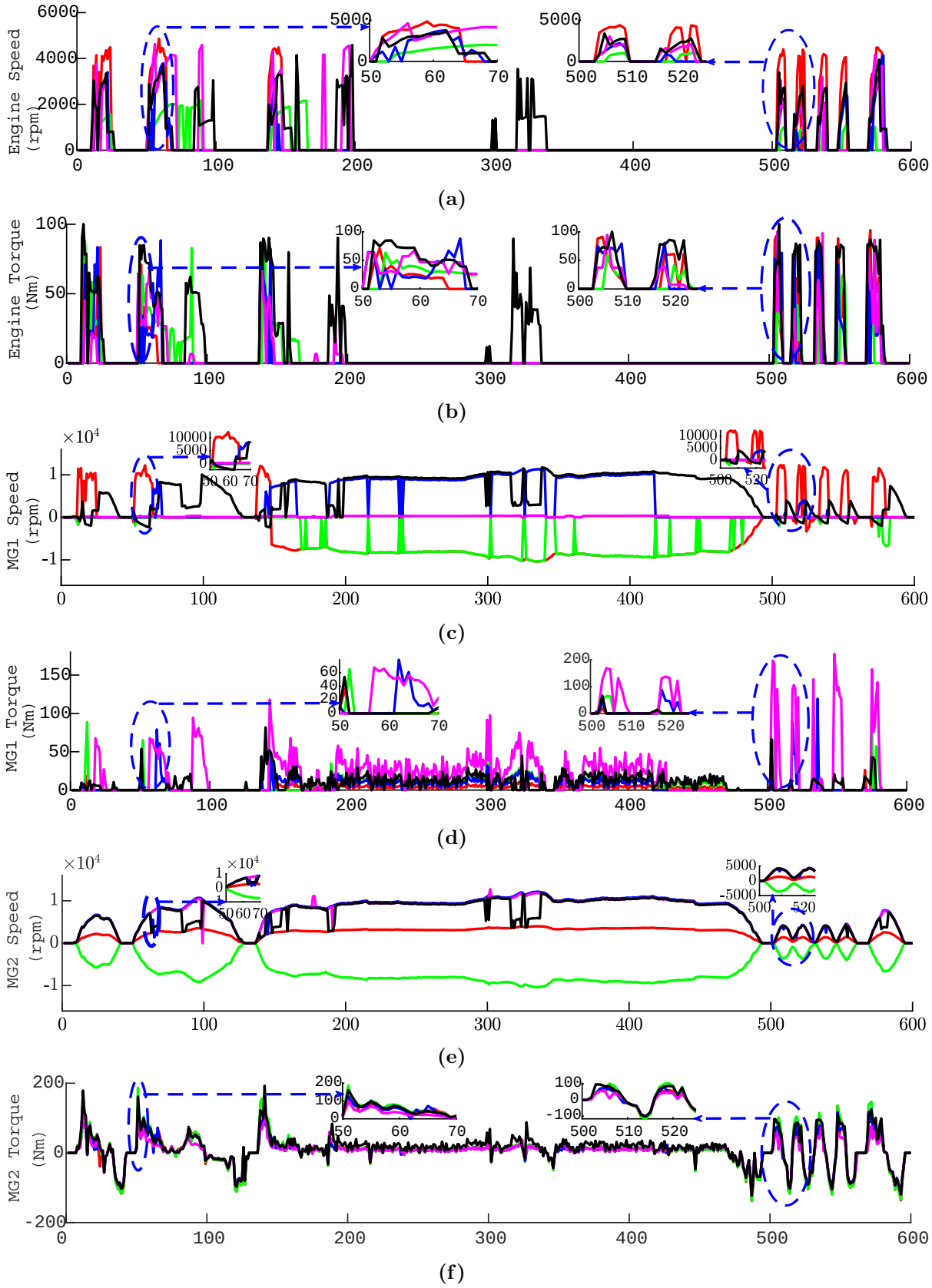


**Figure 3.21:** *Results of the real-time simulation of all five topologies including (a) Engine speed, (b) Engine torque, (c) MG1 speed, (d) MG1 torque, (e) MG2 speed, (f) MG1 torque.*

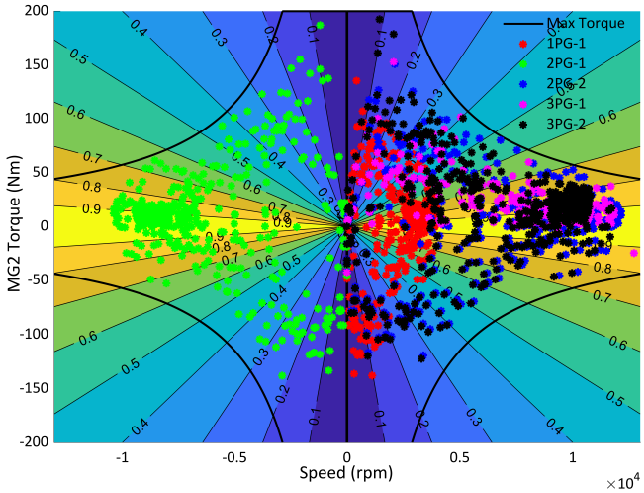


**(a)**

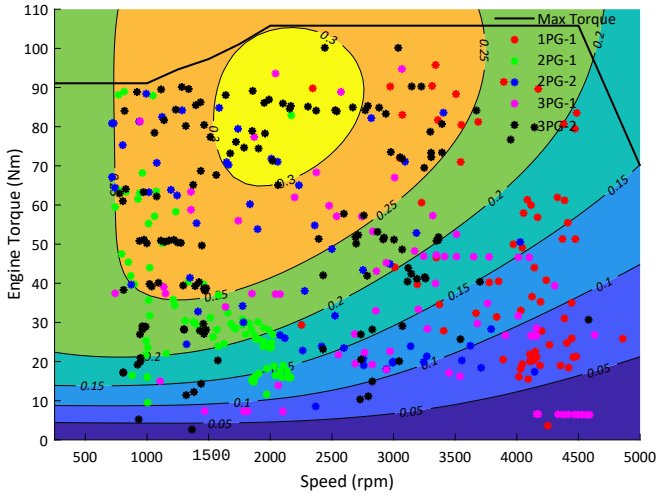


**(b)**

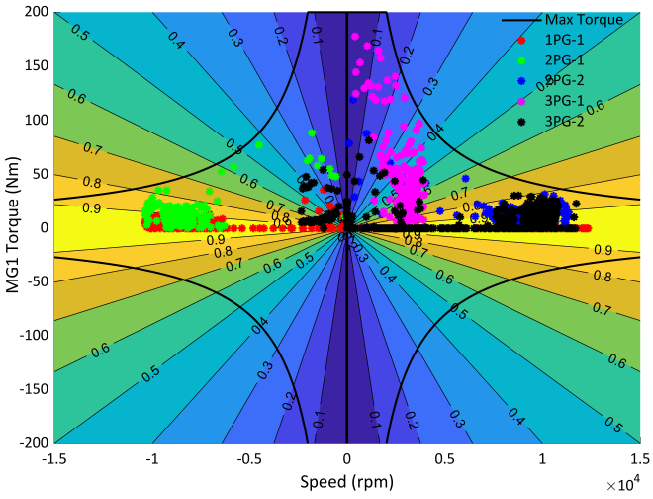


**(c)**

**Figure 3.22:** *Operating points of all five topologies (**a**)Engine, (**b**)MG1, (**c**)MG2.*

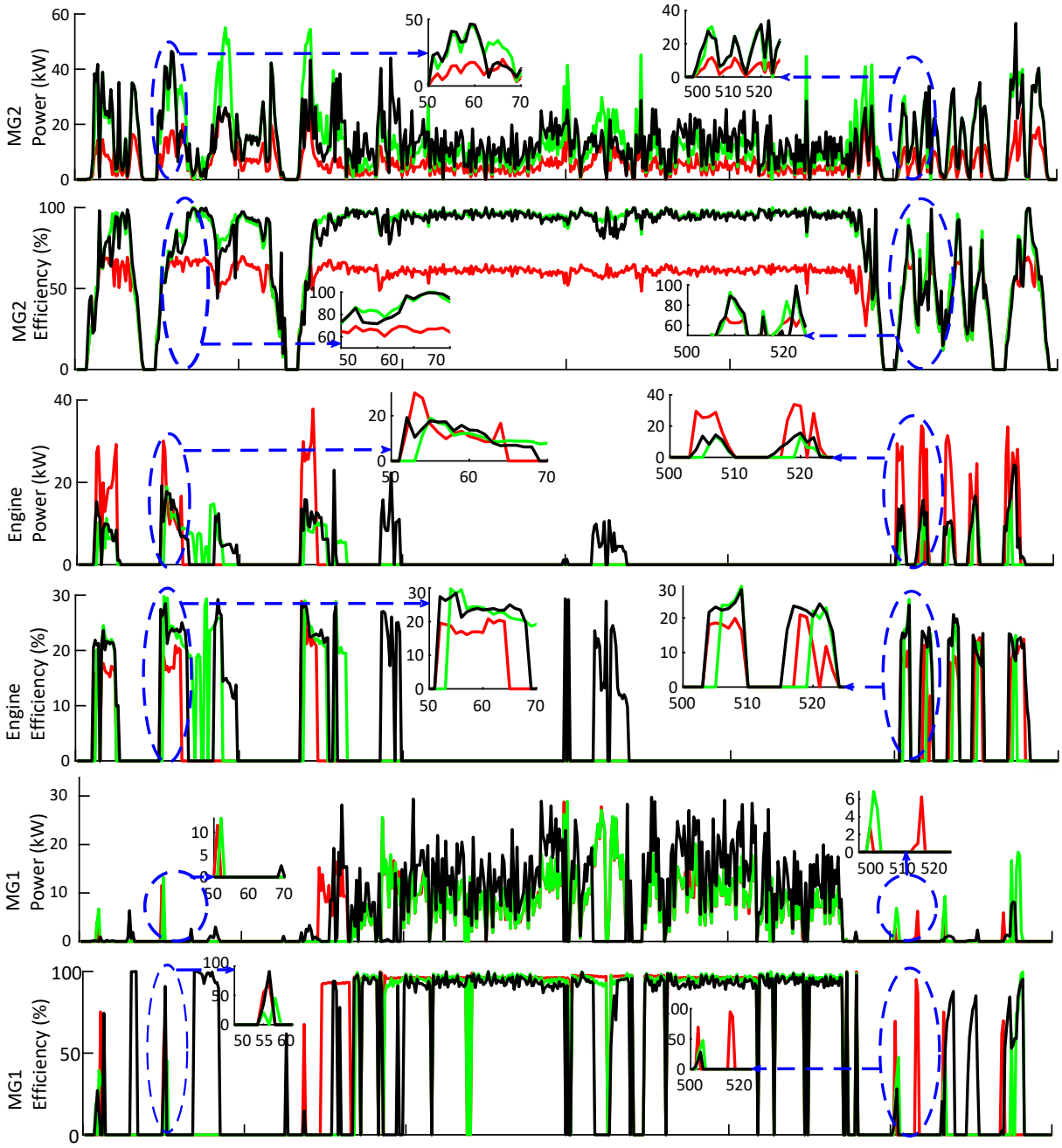


(f)

**Figure 3.25:** *Results of the real-time simulation of all five topologies including (a) MG2 power, (b) MG2 efficiency, (c) Engine power, (d) Engine efficiency, (e) MG1 power, (f) MG1 efficiency.*

# Chapter 4

# Software-in-the-Loop Test Platform

This work uses the automotive simulation models (ASM), provided by dSAPCE, to develop the real-time simulation models of the five studied hybrid topologies. The models, as shown in Figure 4.1, consist of vehicle dynamics, an internal combustion engine, planetary gearbox including clutches, final drive, two motor-generators labeled as MG1 and MG2, batteries and electronics, inner controllers and the EMS as developed in Chapter 3. The developed models are simulated over the United States 06 (US06) drive cycle with 80% initial battery state of charge and the sampling time of 1 ms.

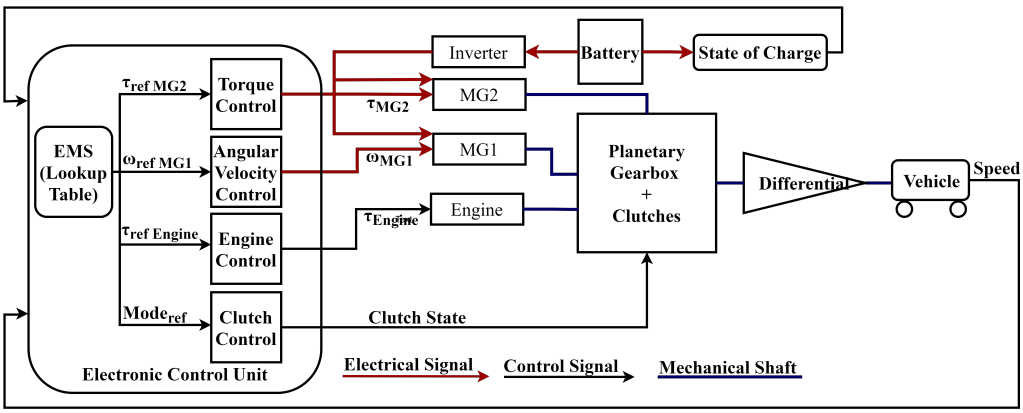


**Figure 4.1:** *A generic layout of the developed real-time simulation models using dSPACE ASM library for the different powertrain topologies.*

There are two main differences among all the topologies. First, the number of PGs in the planetary gearbox block varies from one to three depending on the chosen topology. Second, there is a specific EMS to each topology, which is solved offline and stored as a lookup table in the ECU. The ECU also contains inner controllers for the torques of MG2 and engine, the angular velocity of MG1 and the gearbox clutches. The main idea of implementing the ASM models is to check if the results are still valid if a higher fidelity and more representative plant models are used. As shown in Figure 4.1, it is a feedback loop which contains entire vehicle dynamics.

## 4.1 Modelling of Hybrid Powertrains

Five simulation in loop (SIL) hybrid powertrain models are developed using ASM library of dSPACE in this study. Figure 4.2 shows the high level components of the model. The six different component blocks namely soft ECU, engine, electric components, drivetrain, vehicle dynamics, and environment are there in every model. The major difference between the blocks of all five topologies lies among soft ECU and drive train.

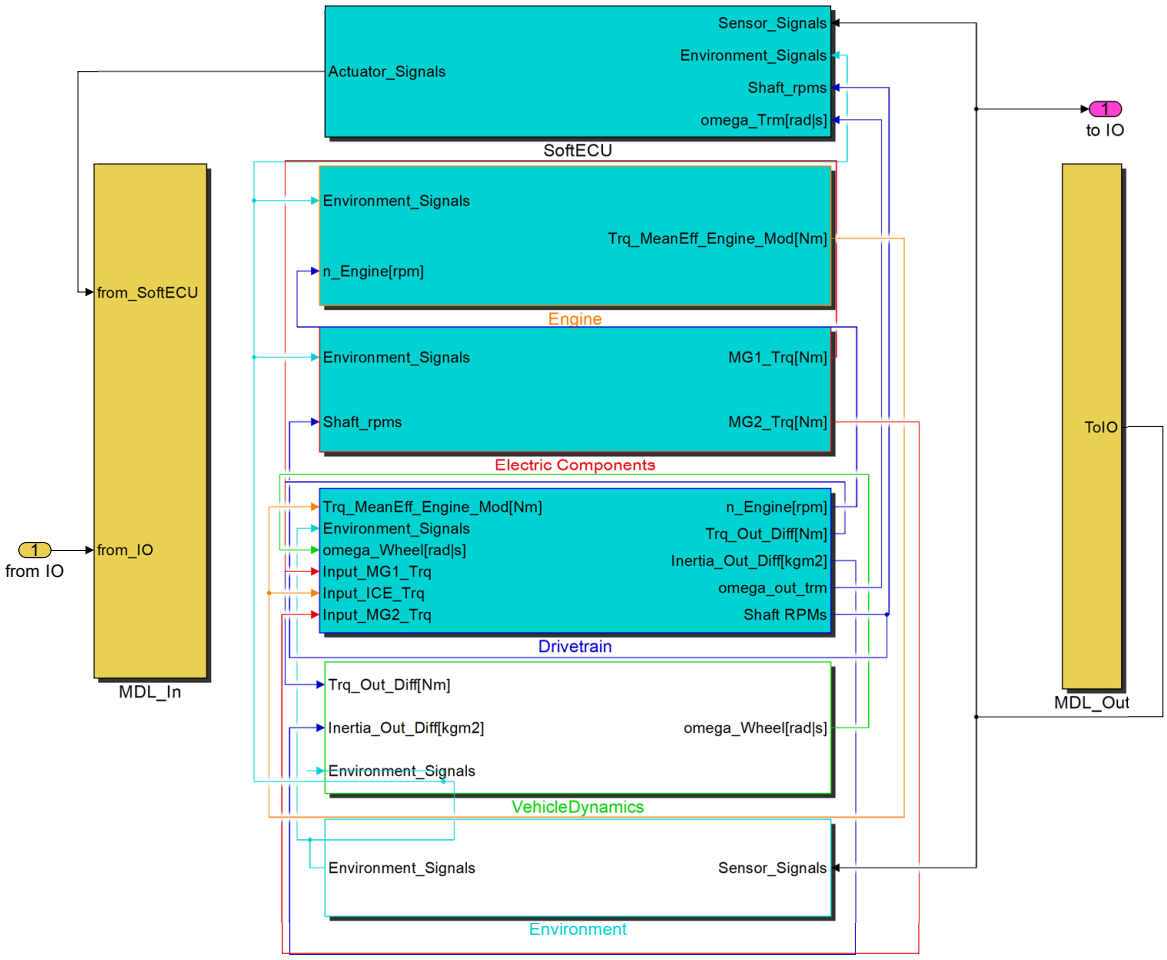


**Figure 4.2:** *First layer layout of developed SIL model*

### 4.1.1 Soft ECU Model

Soft ECU which is different in all five topologies has six component blocks as shown in Figure 4.3 and only torque controller, speed controller, and clutch controller are the models which are different within each topology. MG2 and engine together form torque controller. MG1 is used as speed controller to restrict engine speed in optimal bsfc zone during different modes. The clutch controller controls clutch engagement and

disengagement for any chooses mode.

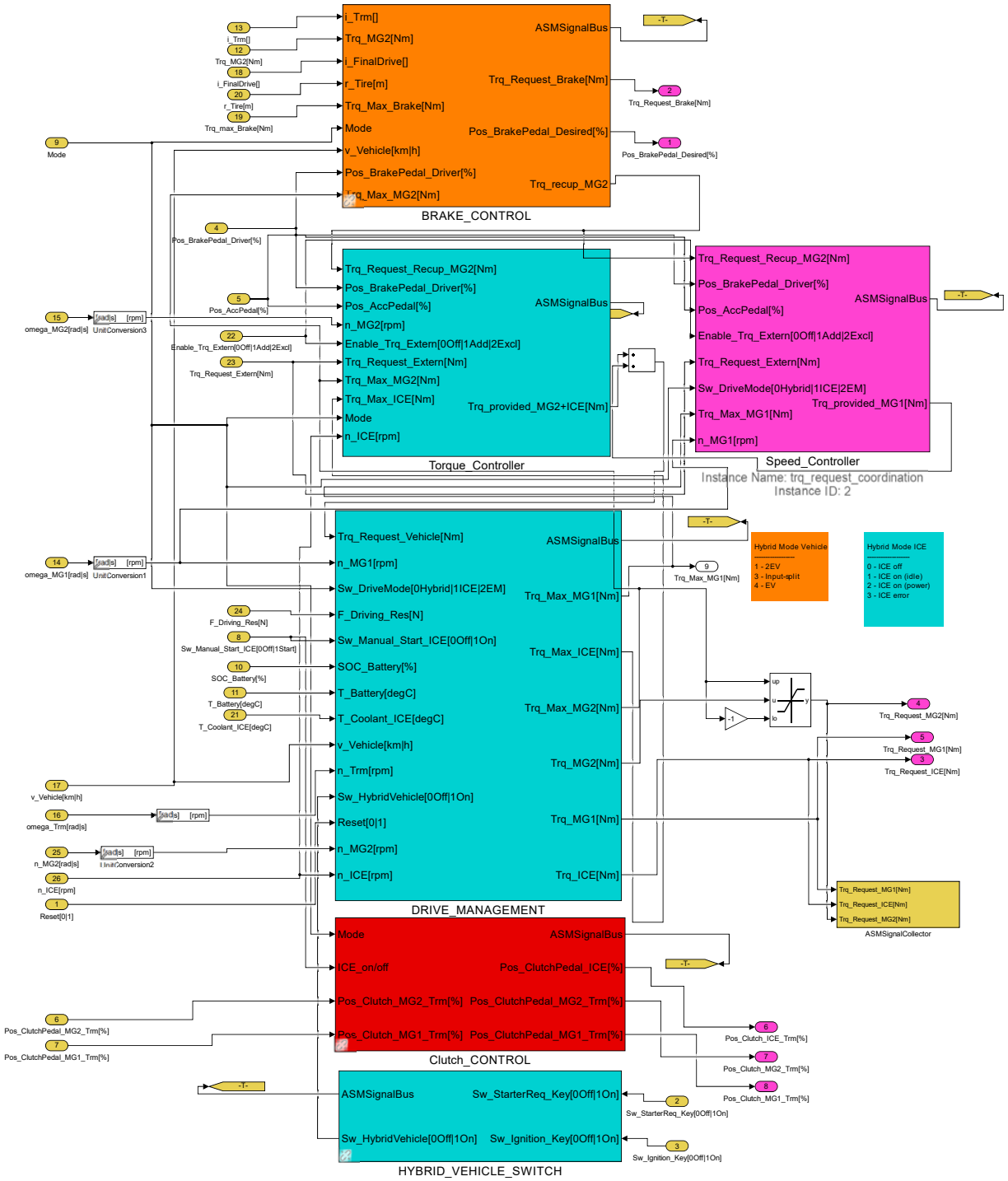


**Figure 4.3:** *Soft ECU with torque, speed, and clutch controller. Torque and speed controllers uses optimal EMS as lookup table.*

The soft ECU reads accelerator pedal position (APP) and vehicle speed and will

execute relevant mode for the asked vehicle speed at a certain time. As presented in Figure 4.3, the logic of soft ECU contains optimal operating points of engine and MG2 torque, MG1 speed, and modes derived from solving the EMS problem (as discussed in Chapter 3) and use them as look up table respective component blocks. For example, the lookup table containing optimal engine and MG2 torque is stored in torque controller, the lookup table containing optimal MG1 speed is stored in speed controller, and the lookup table containing optimal mode selection is stored in clutch control model. Some data points of EMS as lookup table for all five topologies are presented in Appendix B.

### 4.1.2 Engine Model

The engine model simulates a 50 kW engine which provides maximum torque of 105 Nm at 2000 rpm, maximum power at 4500 rpm, and has 33% brake specific fuel consumption (bsfc) at 2050 rpm. To reduce the complexity of the system and for energy consumption modeling only torque, speed, and fuel consumption are required and modeled.

Engine receives torque request from the torque controller and the speed of engine is provided as the input. These inputs will be used with static maps derived from engine data to determine fuel consumed and provide engine torque. The engine model also provides system limitations of the engine, such as maximum and minimum torque and speed limits. The output of engine model are engine torque, engine speed and fuel consumption.

### 4.1.3 Drivetrain Model

The input of drivetrain model are the output from torque, speed, and mode controller becomes input for drivetrain and engine component block models. As shown in Figure 4.4, all the signals from soft ECU are collected and provided as input to the sub block of drivetrain named as PG1 and $TEST\_BENCH$. The component block PG1 contains the planetary gear as simulink model.

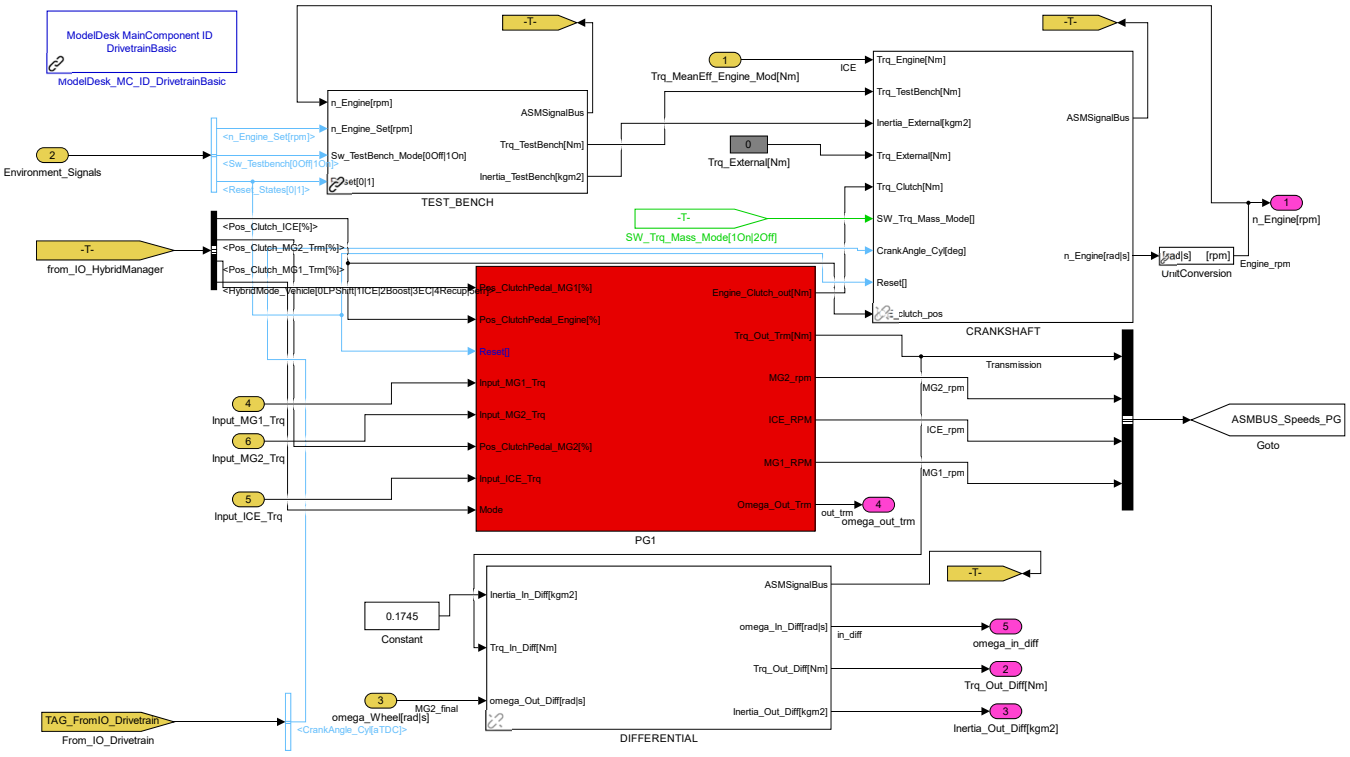


**Figure 4.4:** *Drivetrain model containing planetary gear, engine shaft, MG1 shaft, MG2 shaft, and differential shaft.*

The simulink model of 1PG-1 topology is shown in Figure 4.5. This model consists of one compound planetary gear named as planetary gear 1 consisting of ring, sun and carrier gears. Sensors for ring, sun, and carrier gears, inertia blocks providing a constant inertia to the gears. The sensors receives input from torque source and provides this torque as input to the planetary gear. Since all the signals provided to the PG1 component block are simulink signals, and torque source can only read a physical signal, therefore a simulink to physical signal (simulink-PS converter) is also added between input signal and ideal torque source. The input signal (Input_C1_ICE) has the value of torque to be delivered by ICE at the any sampling time. Since ICE is connected at carrier gear in this topology, therefore the input signal, simulink-PS converter, ideal torque source and inertia are also connected at carrier gear.

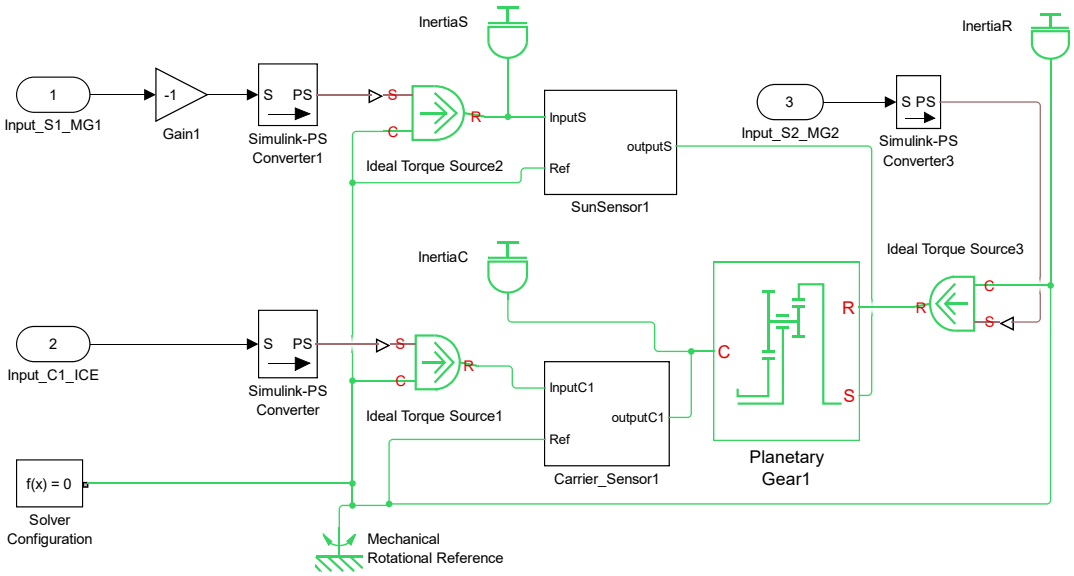


**Figure 4.5:** *Simulink model of 1PG-1 topology, showing one planetary gear.*

The output of this model are the angular velocities and torques from engine, MG1, MG2, and vehicle. These output becomes input to the respective component model i.e. engine and electric components. However, the output from vehicle which is connected at ring gear in 1PG-1 topology also acts as input to MG2 and differential component block situated at one layer higher to the PG1 block.

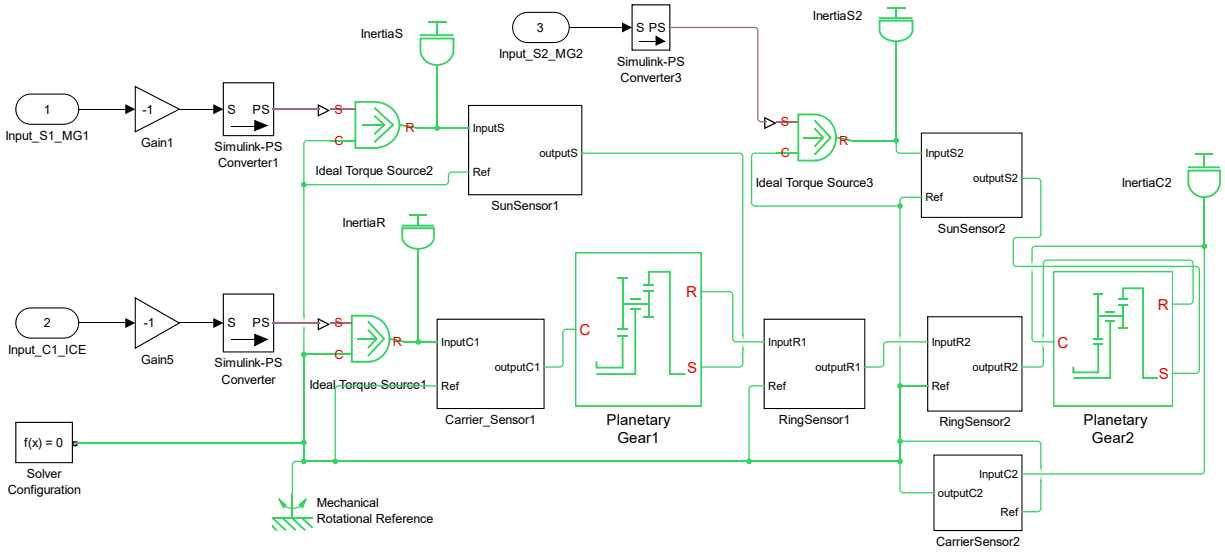


**Figure 4.6:** *Simulink model of 2PG-1 topology, showing two planetary gears and their connections.*

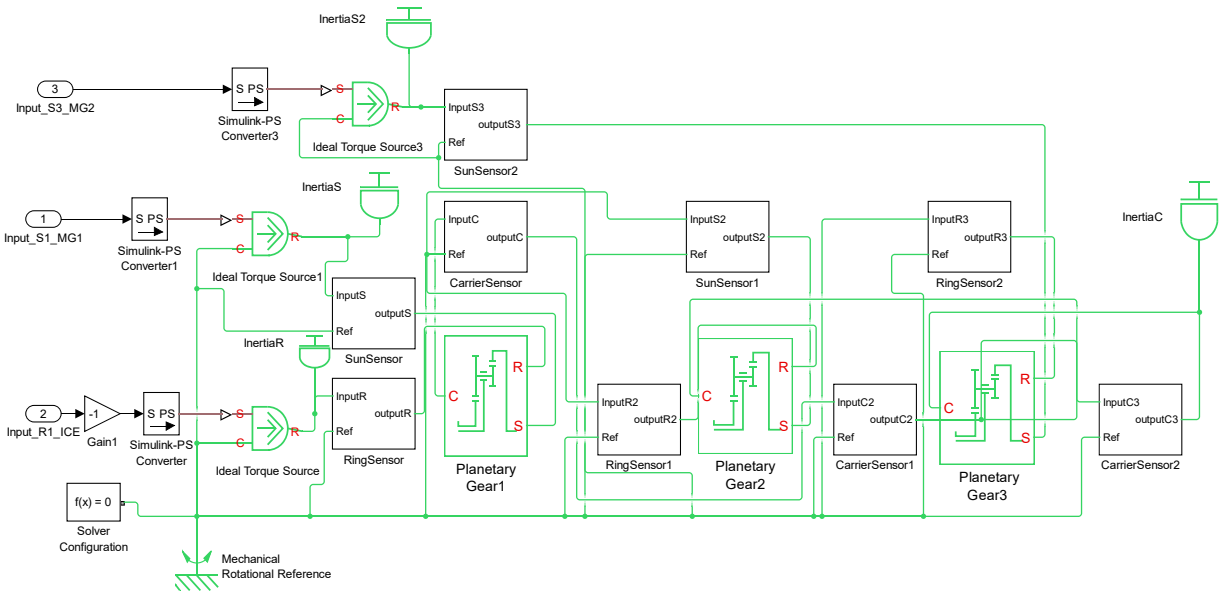


**Figure 4.7:** *Simulink model of 3PG-2 topology, showing three planetary gears and their connections.*

Similarly, Figure 4.6 and Figure 4.7 shows the simulink models of the planetary gears of 2PG-1 and 3PG-2 topologies containing two and three planetary gears, respectively. The connection between engine, MG1, MG2, and planetary gears is based on their topologies. The output of each component is based on the combined gear ratios of its connection with the PGs. Therefore, increasing the number of PGs reduces engine, MG1, and MG2 torque demand at the component level but the torque demand from the vehicle is still satisfied.

### 4.1.4 Electric Components Model

Minimising the deviation of battery state of charge (SoC) from initial to final state is also one of the objective of this study. The minimisation function is included in the EMS formulation and is implemented in the soft ECU as lookup table. Figure 4.8 shows the layout of electric components. Electric components consists of two electric motors and a battery multi cell. The battery multi cell is made up of Nickel-Metal Hydride (NiMH) battery cell and has 28 modules in its pack.

The battery multi cell receives the current as input from the motors and delivers voltage as output. In order to reduce the complexity of the battery model parameters like - ambient temperature, initial battery SoC, battery SOH, coefficient of conduction for cooling etc are kept constant. The operation of electric motors is the key factor for the operation of battery system.

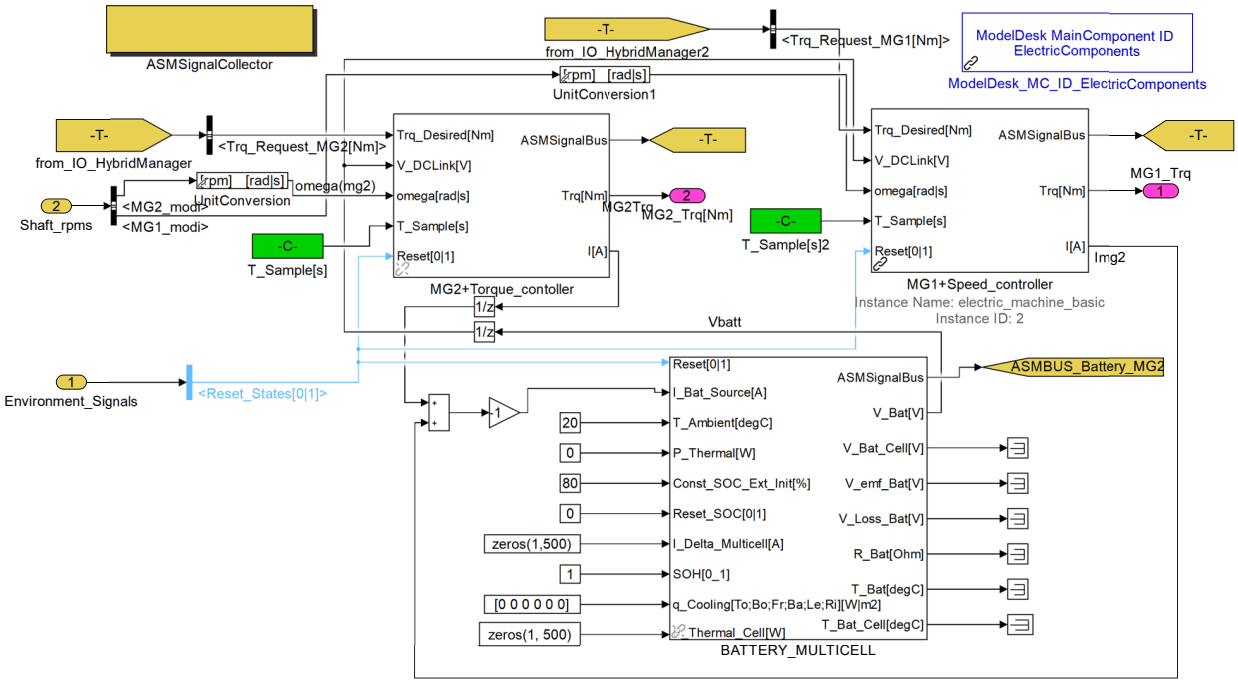


**Figure 4.8:** *Simulink model of electric components which are identical in all five topologies.*

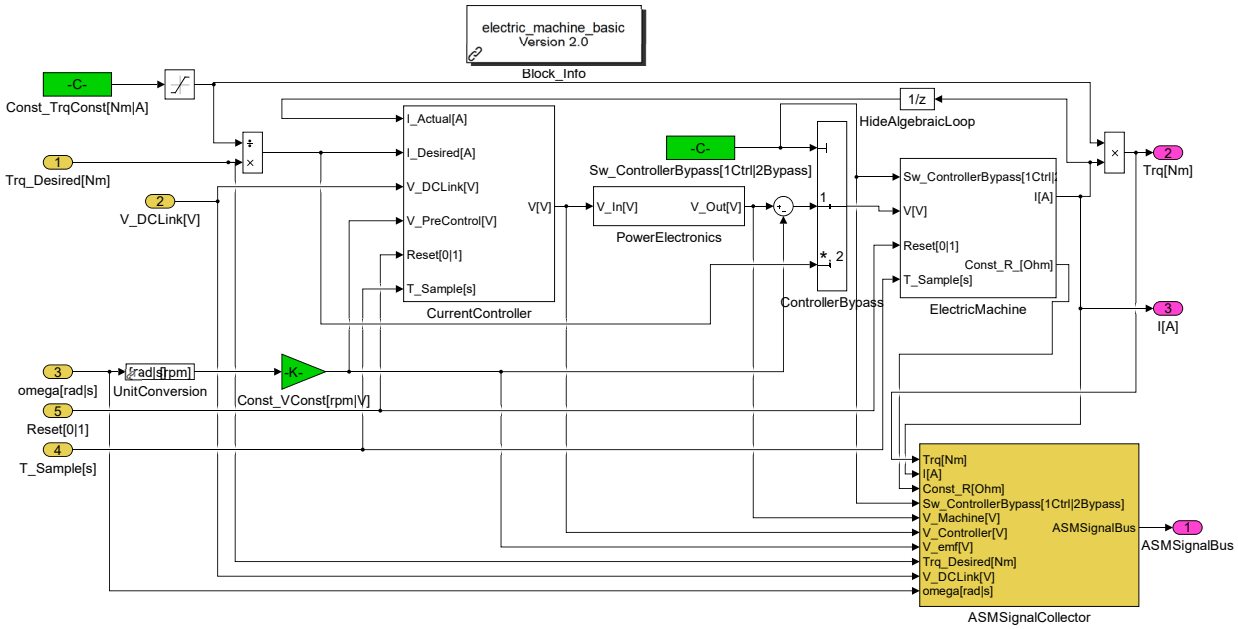


**Figure 4.9:** *Simulink model of electric motor which is identical in all five topologies.*

Figure 4.9 shows the model of Motor generator 1 (MG1) which is identical to the model of MG2, but the values of coefficients of speed to voltage and torque to current

converters are different. In this model the conversion of torque requested and angular velocity in to current and torque provided by the motor generator 2 (MG2) occurs. The main requirement of the electric model is to take torque request as input and provide power produced by the motor and the current drawn as output. The MG1 and MG2 models also provide the constraints of maximum and minimum torque and speeds for both the motors. This current drawn from the motors are the inputs to battery multi cell model. The models of MG1 and MG2 do not contain any actuator or sensor dynamics. They are simply a combination of efficiency maps taken from the library of dSPACE.

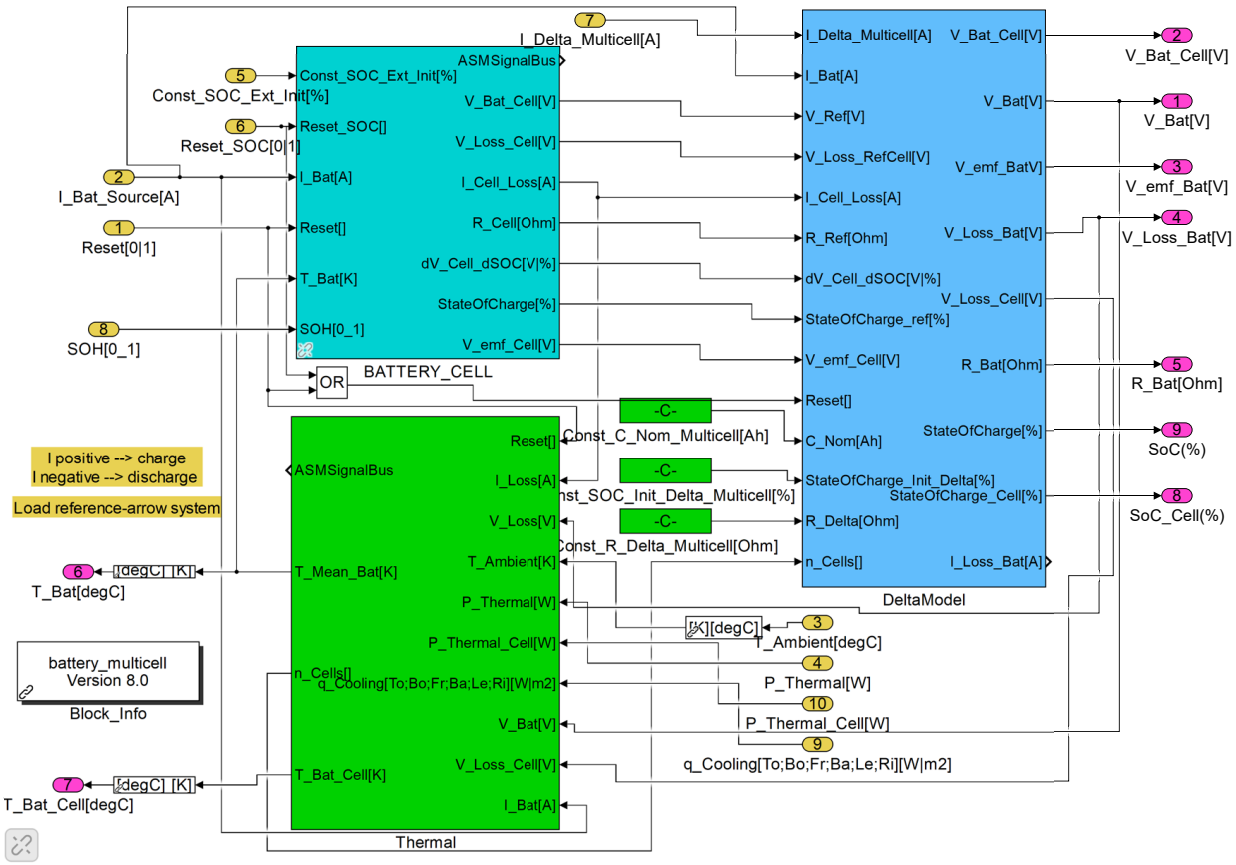


**Figure 4.10:** *Simulink model of battery delta model where battery SoC is calculated.*

The output of thermal and battery cell models acts as input for delta model as shown in Figure 4.10. Delta model is the model where the overall SoC of the battery pack is calculated. This delta model uses coulomb counting method to calculate battery SoC of the pack from the individual battery cells. Equation 4.1 shows the coulomb counting used method to calculate battery SoC.

$$SoC = SoC_o - \frac{1}{6.5}\int I_{cell}dt \tag{4.1}$$

where $SoC_o$ is the initial battery SoC, 6.5Ah is the nominal cell capacity, $I_{cell}$ is the current drawn per cell in amps, and dt is the time step in milliseconds. However, it should be noted that battery pack used in this work has the limitation of maximum operating temperature of 40degC and minimum operating temperature of 20degC.

### 4.1.5 Vehicle Dynamics Model

The main purpose of vehicle dynamics model is to convert torque produced by the powertrain components into the force at the wheels. The vehicle dynamics block is shown as the second last block in Figure 4.2. It is also required to determine the vehicle speed and road load resistance acting on the entire vehicle. The vehicle experiences the types of loads namely aerodynamic drag, rolling resistance by tire, and load due to road grade. The dissipative forces due to these three loads are given by Equation 4.2.

$$F_{load} = Mgcos\theta C_r + Mgsin\theta + (\frac{1}{2}\rho_a A_f C_d(\frac{V_{veh}}{3.6})^2) \tag{4.2}$$

The first term of the equation accounts for the road load resistance which is responsible to decelerate the vehicle. The second term shows the losses due to road grade where $\theta$ is the angle of inclination. The third term of the equation represents the aerodynamic losses due to the drag forces.

The overall model is assumed to be quasi-static model and the dynamics only occur at vehicle level. Therefore, vehicle acceleration is the sum of dissipative and tractive forces. This vehicle acceleration is further integrated with respect to time to achieve the velocity of vehicle. Similarly vehicle position can be obtained by integrating the velocity with respect to time. Equation 4.3 and Equation 4.4 shows the vehicle velocity and position for a given time interval.

$$V_{veh} = \int_0^k \dot{V}_{veh} dt \tag{4.3}$$

$$X_{veh} = \int_0^k \dot{V}_{veh} dt \tag{4.4}$$

The results obtained from the model are also used to calculate the vehicle fuel economy (mpg) by the ratio of cumulative distance covered over US06 drive cycle in miles to the total fuel consumed in gallons.

## 4.2 Results and Discussion

This section presents simulation results for the developed models for all the topologies over the US06 drive cycle. Figure 4.11a illustrates the speed profile of the US06 drive cycle requested by model desk and provided by the models of 1PG-1, 2PG-1, 2PG-2,

3PG-1, and 3PG-2 topologies. 3PGs topologies show the maximum deviation from the actual drive cycle. The root mean square error values (rms) for 3PG-1 and 3PG-2 topologies are 14.23 m/s and 12.76 m/s. However, the error rms values for 1PG-1, 2PG-1, and 2PG-2 topologies are 8.22 m/s, 10.05 m/s, and 11.65 m/s, respectively. The higher error in 3PGs topologies is due to the increased number of PGs, which adds complexity to the drivetrain model. Moreover, there are 8 and 6 modes in 3PG-1 and 3PG-2 topologies, but only 3 and 5 modes in 1PG and 2PGs topologies. These increased number of modes increases clutch fluctuations, therefore error in speed tracking increases.

Figure 4.11b shows the torque tracking of the components for all five topologies. Torque tracking error is the amount of error of torque which is over or under met with respect to torque requested by the vehicle. The torque tracking error is for entire US06 drive cycle is 11.37 Nm, 13.17 Nm, 13.47 Nm, 16.04 Nm, and 15.23 Nm for 1PG-1, 2PG-1, 2PG-2, 3PG-1, and 3PG-2 topologies, respectively. . The reason for the torque tracking error is due to the speed tracking error observed in Figure 4.11aa. As discussed above, the complexity of the ASM model increases by increasing the number of PGs, resulting in higher tracking error for the model with a higher number of PGs.

The total fuel consumption is the sum of engine fuel and equivalent fuel consumption. Engine fuel is calculated by engine model for 0-600 s, and the accumulated engine fuel is presented. However, for equivalent fuel consumption calculation, the engine operates at optimal speed and provides constant torque to MG1. MG1 charges the battery from the final state of charge (SoC) to the initial battery SoC. Engine fuel consumption for charging the battery back to 80% SoC is the equivalent fuel consumption. Figure 4.11c shows the engine fuel consumption by all five topologies. The engine fuel consumption is illustrated between the 0-600 s is the lowest for 2PG-1 topology and highest for 1PG-1 topology. The trend of engine fuel consumption is same as the results of simplified simulation model used for EMS formulation, as discussed in section 3.4.

The total fuel consumption of the 1PG-1 topology is 585 $g$ whereas that of the 2PG-1 topology is 558 $g$ (i.e. 4.6% lower). Moving from 2PG to 3PG can reduce the total fuel consumption by a further 1.8% (i.e. 6.4% lower than that of the 1PG topology). As shown in Table 4.1, the 2PG-2 and 3PG-1 topologies also reduce fuel consumption with respect to the 1PG-1 topology by 1.9% and 2.9%, respectively. Engine fuel consumption by every topology with multiple PGs is lower than that consumed by the 1PG topology at the expense of a small increase in the equivalent fuel consumption. In other words, for a maximum of 1.8% deeper discharged battery, the topologies with multiple PGs consume up to 62 $g$ less engine fuel.

As shown in Figure 4.11c shows the evolution of the total fuel consumption of the 2PG-1 and 3PG-2 topologies over the US06 drive cycle as compared to 1PG-1 topology. The fuel consumed by the engine is independent of the topology during the 200-500 s time interval, whilst it is much lower for the 2PG-1 and 3PG-2 topologies (especially the former) during the 0–180 s and 500–600 s time intervals. On the other hand, equivalent fuel consumption of 1PG-1 and 2PG-1 topologies are similar and higher than that of

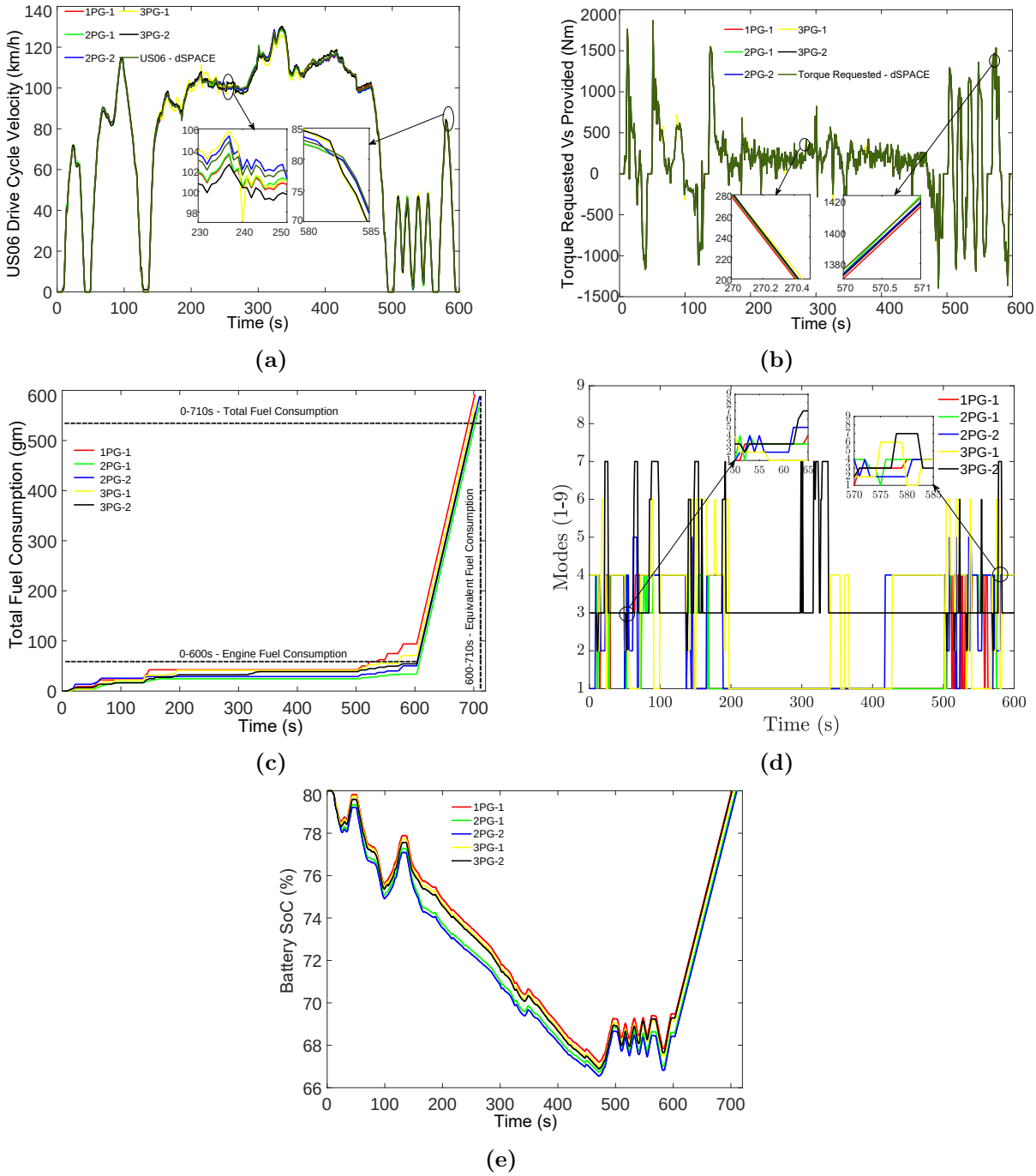


**Figure 4.11:** *Real-time SIL results of all five topologies for (**a**) US06 drive cycle, (**b**) Torque demand requested vs provided, (**c**) Total fuel consumption, (**d**), Modes selection (**f**) Battery state of charge.*

the 3PG-2 topology during the 200–500 s time interval. This is a similar trend to the one observed for the battery SoC in Figure 4.11e. The main reasons for the reduction

of fuel consumption of the 2PG and 3PG topologies are: i) the speed of electric motors is higher with multiple PG topologies, leading to lower power demand from the engine; and ii) fixed-gear ratio topologies save the electric power losses resulting from regulating the engine speed.

**Table 4.1:** *Summary of the real-time SIL results from dSPACE for US06 drive cycle.*

| **Description** | **1PG-1** | **2PG-1** | **2PG-2** | **3PG-1** | **3PG-2** |
|---|---|---|---|---|---|
| Total Fuel Consumption | 589 g | 562 g | 577.6 g | 571.4 g | 551.2 g |
| Engine Fuel Cons. | 92 g | 30 g | 53 g | 68 g | 50.5 g |
| Equivalent Fuel Cons. | 497 g | 532 g | 524.6 g | 503.5 g | 500.7 g |
| Battery SoC final | 70% | 68.2% | 69% | 69.4% | 69.7% |

Figure 4.11d shows that the EMS chooses mode $\in \{1, 3, 4\}$ for 1PG-1 and 2PG-1 topologies and mode $\in \{1, 2, 3, 4, 6, 7\}$ for 3PG-2 during the 0–180 s and 500–600 s time intervals. Modes 1 and 4 are EV modes (see Table 3.2), where the former uses both MGs and the latter only MG2 to provide torque to the wheels. Conversely, all drivetrains contribute to the wheel torque in input-split mode 3, with the engine speed being regulated by the speed of MG1. Modes 2, 6 and 7 represent parallel topologies with a fixed ratio between the engine speed and the vehicle speed. However, unlike mode 4, mode 2 utilises only one MG.

Figure 4.11e shows the final SoC of batteries are 70%, 68.2%, 69%, 69.4%, and 69.7% for 1PG-1, 2PG-1, 2PG-2, 3PG-1, and 3PG-2 topologies respectively, the equivalent fuel consumption values are also in similar order. In the real time simulation, the equivalent fuel consumption is calculated using charging the battery back to inital SoC using engine. Engine operates at its optimal bsfc and the torque provided by engine is used by MG1 to charge the battery. It must be noted that, in the real time models the equivalent fuel consumption is only calculated using chagring the battery via engine.

Figure 4.12a and Figure 4.12b shows the speed and torque provided by the engine shaft for all the topologies. The reference torque of engine is the optimal engine torque provided by the results of EMS proposed in this study. From 0-600 s engine provides the torque requested, while after 600 s engine operates at constant torque and speed to recharge the battery. It can be observed that that for 2PG-1 and 3PG-2 topologies, the engine does not deviate much from a constant speed, providing reduced fuel consumption for the same amount of torque requested compared to other topologies.

Figure 4.12c and Figure 4.12d presents the torque and speed provided by the MG1 shaft for all the five topologies. MG1 is used as a speed controller to restrict engine speed for all the modes except mode 1. From 0-600 s MG1 provides the speed and torque requested, while after 600 s MG1 operates at constant torque and speed relative to the engine and recharges the battery. MG1 provides high torque and low speed in 3PG-1 topology due to its direct connection with the vehicle. This low-efficiency operation of MG1 increases its energy consumption resulting in higher equivalent fuel consumption among 3PGs topologies. It should be noted that only MG1 and engine

operates even after the end of US06 drive cycle i.e. 600 s. This operation of MG1 and engine is to recharge the battery back to 80% state of charge, the fuel consumed by engine during this time is the equivalent fuel consumption.

Figure 4.12e and Figure 4.12f illustrates the torque and speed provided by the MG2 shaft for all the topologies. MG2 has a significant impact on the total fuel consumption as it is the primary source of power during all the modes and is the only motor to provide regeneration during 0-600 s. The main difference between the operation of MG2 between 2PG-1 and other topologies is in the direction of rotation, as in Figure 4.12d. This negative rotation of MG2 is the reason for the lowest engine fuel consumption in the 2PG-1 topology, as discussed before. From Equation , it is evident that for 2PG-1 topology, the speed of the engine relates to the difference of speeds of MG1 and MG2, while it is the weighted sum of these two speeds for all other topologies. Therefore, EMS of the 2PG-1 topology can choose a high value for the speed of MG1 as a decision variable to reduce the speed of engine. EMS of the 1-PG-topology, on the other hand, should reduce the speed of MG1 at high vehicle speeds to reduce the speed of engine; however, the latter still increases to up to 5000 rpm by high vehicle speed. As a result, the speed and hence power of the engine becomes lower in the 2PG-1 topology at Mode 3 that is applied when the torque demand is high [119].

Table 4.1 shows the results of Software-in-the-loop models developed as ASM models within dSPACE. These results follows the trend of values concluded in Table 3.3, which are the result of the same models which has is a simple model containing dynamic equations of torque, speed, SoC, fuel consumption, and component efficiencies etc, for all the topologies.

## 4.3 Concluding Remarks

The contributions of this section are as follows:

- Evaluation of the impact of the number of PGs on the energy consumption of HEVs using SIL models. It is shown that increasing the number of PGs from one to two and from two to three reduces the energy consumption by 4.6% and 1.8%, respectively.
- Development of five different SIL models using ASM libraries of dSPACE.
- Validation of EMS results with the results of SIL models.

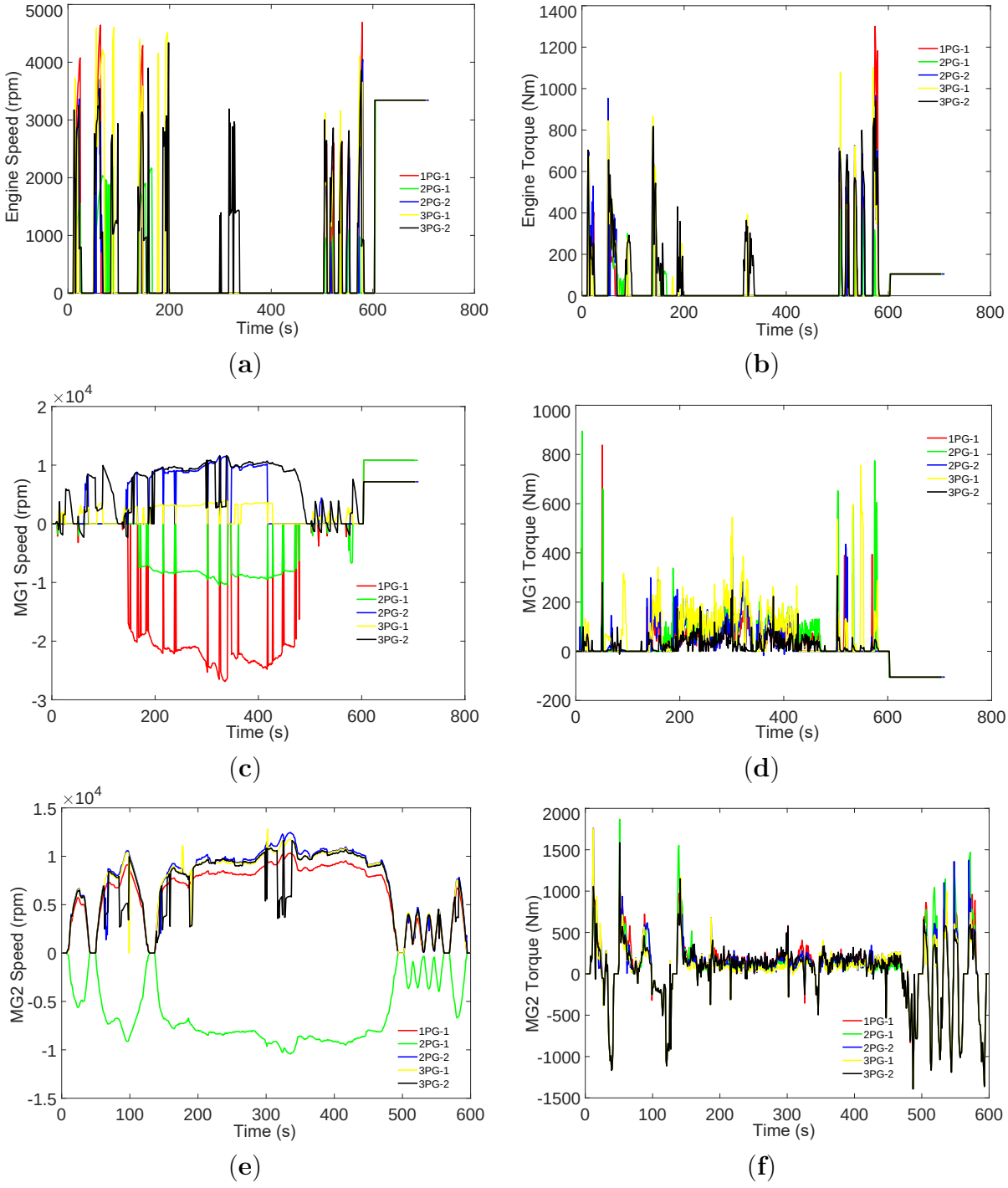


**Figure 4.12:** *Real-time SIL results for all five topologies (**a**) Engine torque, (**b**) Engine speed, (**c**) MG1 speed, (**d**) MG1 torque, (**e**) MG2 speed, (**f**) MG2 torque.*

# Chapter 5

# Conclusion and Future Work

## 5.1 Conclusions

This dissertation focuses on developing an optimal transmission system for hybrid powertrains. Hybrid powertrains consist of one engine, one or more than one motors, and one or more planetary gears. To optimise the efficiency of the powertrain components and energy consumption and an optimal energy management strategy (EMS) is required. The developed optimal transmission system in this work contains a novel EMS which conjointly optimises mode selection, torque distribution and components efficiencies. An EMS with simultaneous mode selection and torque distribution leads to a complex mixed-integer optimisation problem due to the existence of discontinuities caused by changing the mode of operation; i.e. due to engaging and disengaging clutches and switching the operation of the electric motors between motoring and generating. This fact, along with the nonlinearity of components and the existence of algebraic constraints, results in the EMS comprising a mixed-integer nonlin- ear optimal control problem (OCP) with differential and algebraic equations (DAEs).

The EMS is then discretised and then formulated as a mixed-integer non-linear programming (MINLP) problem using the mathematical programming language (AMPL), which is the modelling language adopted by Neos server as the standard interface for solvers. The formulated problem is then solved with Knitro, available in the Neos server, which achieves a local optimal solution at every sampling time. The reliability of the solution of the EMS is assessed by using a real-time simulator which takes into account a full-vehicle model and the environmental disturbances.

To validate and verify the use of the proposed EMS in the real-world scenario, five different simulink-based software in loop (SIL) models emulating hybrid powertrains are developed. The EMS is further integrated into the ECU of the SIL models, and the efficiency of the transmission system of all five powertrains is carried out. The findings of optimal EMS and SIL models are discussed in the section below:

### 5.1.1 Optimal EMS of energy-efficient hybrid powertrains

This work proposed an optimal EMS which performs simultaneous mode selection and torque distribution. The developed EMS is further integrated in to five different hybrid topologies and the minimum energy consumption of hybrid topologies with one, two, and three PGs were compared over the US06 drive cycle.

For each topology, an EMS ensured that the combination of clutch engagements, torque distributions and components' speeds is such that it minimises the total energy consumption. The latter is calculated as the sum of the engine fuel consumption and the equivalent fuel consumption of the battery's discharge energy.

The incorporation of mode selection via clutch engagements into the nonlinear EMS led to a mixed-integer problem, which was then converted into a complementarity constrained problem, and solved using KNITRO using NEOS server.

Simulation results showed that increasing the number of PGs from one to two and from two to three reduces the total fuel consumption by 5% and 1.5%, respectively. The primary reason for lower fuel consumption is the higher power provided by the primary electric motor (MG2). Additional PGs help MG2 to operate at higher speed, where it can provide more power with higher efficiency. This also reduces the power required from the engine, resulting in lower engine fuel consumption. 3PG topologies also benefit from the availability of fixed gear modes, in which MG1 is not involved in regulating the engine speed, therefore avoiding the corresponding power loss. However, when the drive cycle is repeated three times, the total fuel consumption of 3PG topology is increased by 0.02% compared to 2PG topology. The primary reason for the increease in total fuel consumption of 3PG topology is use of fixed gear modes, where the engine provides constant torque and EMS reduces the use of electric motors.

To summarise, increasing the number of PGs reduces total fuel consumption due to the higher rotational speed of MG2 and to the availability of fixed gear modes. However, it is important to note that the rate at which total fuel consumption reduces seems to stagnate as the number of PGs increases. It should also be noted that when the cycle is repeated three times, total fuel consumption by 3PG topology increases.

Design rules are introduced for HEVs with multiple PGs:

1. Electric motors with higher speed give flexibility to improve the engine efficiency and therefore reduce energy consumption. This can happen by both the 2PG and 3PG topologies.

2. Engine can operate within the optimum range of its rotational speed using the fixed-gear modes and without involvement of electric motors. This is possible in 3PG topologies and reduces the electric losses and hence the energy consumption.

### 5.1.2 Software in loop models

Five different SIL models are developed for five different hybrid topolgies namely 1PG-1, 2PG-1, 2PG-2, 3PG-1, and 3PG-2. These models consist of vehicle dynamics, an in-

ternal combustion engine, planetary gearbox including clutches, final drive, two motor-generators labelled MG1 and MG2, batteries and electronics, inner controllers, and the EMS developed in chapter 3. The developed models are simulated over the United States 06 (US06) drive cycle with 80% initial battery SoC and 1 ms sampling time. Different topologies may differ in:

1. The number of PGs in the planetary gearbox block, which varies between one, two, and three;

2. The EMS, which is specific to each topology, solved offline, and stored as a lookup table in the ECU.

The ECU also contains inner controllers for the torques of MG2 and engine, the angular velocity of MG1, and the gearbox clutches.

Real-time simulation results from SIL models showed that increasing the number of PGs from one to two and from two to three reduces the total fuel consumption by 4.6% and 1.8%, respectively. The values of fuel consumption reduction from SIL models has a similar trend as of the EMS results.

Therefore, it can be concluded that using an optimal EMS optimises the transmission system and provides energy efficient operation of powertrains components. This optimal EMS shows that increasing the number of PGs reduces total fuel consumption due to the higher rotational speed of MG2 and to the availability of fixed gear modes. However, it is important to note that the rate at which total fuel consumption reduces seems to stagnate as the number of PGs increases. It should also be noted that when the cycle is repeated three times, total fuel consumption by 3PG topology increases. The overall finding of this work suggests that 2PG topology is best suited for light to heavy-weight cars because of input split, EV, and series modes. Meanwhile, 3PG topology can benefit medium to heavy-duty trucks due to its fixed gear modes.

The methodology developed for this systematic analysis can be applied to different types of electrified powertrains and drive cycles. However, it should be noted that mechanical losses, frictional losses, and the added cost and weight of the powertrains due to increasing the number of PGs were not considered in this study, and are its limitations. The addition of given variables in the cost function of the EMS will increase its complexity and solving such an EMS will be not be possible by MINLP or DP solvers. Moreover, if the mechanical and frictional looses are to taken in to account, 2PG topology may prove to be most fuel economic topology.

## 5.2 Future Work

In this dissertation, we have proposed an EMS which provides optimal transmission System for energy-efficient electrified powertrains. Yet some potential future directions that merit further studies are listed as presented below:

1. Exhaustive search for all possible clutch combination resulting in higher number of modes is not used in this study. This study is limited to the modes which are feasible and reported in literature. There is a possibility that modes which are classified as non-feasible modes, can provide further reduction in fuel consumption.

2. In this dissertation, optimal component sizing is not involved. All five optimal energy efficient powertrains has same component size. Fixing the component size provide a unbiased comparison between different powertrains. But optimisation of component size can further improve optimality of results. The primary reason for not using component size as variable is that it will increase the complexity of the EMS problem. Moreover, different engine bsfc maps, motor efficiency maps, and battery model are not readily available in dSPACE. Therefore, if all the maps are available, then incorporating component sizing in the EMS problem formulation may show improved results.

3. Emissions are not considered in this study. Adding emission models in the proposed EMS can dramatically increase the complexity and computational time of the problem.

4. Mechanical losses, frictional losses, and the added cost and weight of the powertrains due to increasing the number of PGs can be used as variables in the cost function of the EMS.

# Bibliography


[1] "dSPACE website description," http://https://www.dspace.com/en/ltd/home.cfm, accessed: Dec 2018 - Jan 2022.

[2] V. C. Agency, "Co2 emission performance standards for new passenger cars and light commercial vehicles, 2021."

[3] J. Thomas, S. Huff, B. West, and P. Chambon, "Fuel consumption sensitivity of conventional and hybrid electric light-duty gasoline vehicles to driving style," *SAE International Journal of Fuels and Lubricants*, vol. 10, no. 3, aug 2017.

[4] E. H. Wakefield, "History of the electric automobile hybrid electric vehicles," 1998.

[5] J. Liu, H. Peng, and Z. Filipi, "Modeling and control analysis of toyota hybrid system," in *Proceedings, 2005 IEEE/ASME International Conference on Advanced Intelligent Mechatronics.* IEEE.

[6] X. Zhang, S. E. Li, H. Peng, and J. Sun, "Efficient exhaustive search of power-split hybrid powertrains with multiple planetary gears and clutches," *Journal of Dynamic Systems, Measurement, and Control*, vol. 137, no. 12, sep 2015.

[7] A. N. Duhon, K. S. Sevel, S. A. Tarnowsky, and P. J. Savagian, "Chevrolet volt electric utilization," *SAE International Journal of Alternative Powertrains*, vol. 4, no. 2, pp. 269–276, apr 2015.

[8] N. Jalil, N. A. Kheir, and M. Salman, "A rule-based energy management strategy for a series hybrid vehicle," 1997.

[9] A. Brahma, Y. Guezennec, and G. Rizzoni, "Optimal energy management in series hybrid electric vehicles," in *Proceedings of the 2000 American Control Conference. ACC (IEEE Cat. No.00CH36334).* IEEE, 2000.

[10] S. Barsali, C. Miulli, and A. Possenti, "A control strategy to minimize fuel consumption of series hybrid electric vehicles," vol. 19, pp. 187–195, 2004.

[11] Y. J. Kim and Z. Filipi, "Series hydraulic hybrid propulsion for a light truck - optimizing the thermostatic power management."

[12] K. J. Kelly, M. Zolot, G. Glinsky, and A. Hieronymus, "Test results and modeling of the honda insight using advisor."

[13] H. Ogawa, M. Matsuki, and T. Eguchi, "Development of a power train for the hybrid automobile - the civic hybrid."

[14] A. Nedungadi, M. Walls, and D. Dardalis, "A parallel hybrid drivetrain."

[15] C.-C. Lin, H. Peng, J. W. Grizzle, and J.-M. Kang, "Power management strategy for a parallel hybrid electric truck," vol. 11, pp. 839–849, 2003.

[16] A. Sciarretta, M. Back, and L. Guzzella, "Optimal control of parallel hybrid electric vehicles," vol. 12, no. 3, pp. 352–363, may 2004.

[17] T. A. Burress, S. L. Campbell, C. Coomer, C. W. Ayers, A. A. Wereszczak, J. P. Cunningham, L. D. Marlino, L. E. Seiber, and H.-T. Lin, "Evaluation of the 2010 toyota prius hybrid synergy drive system."

[18] K. Rahman, M. Anwar, S. Schulz, E. Kaiser, P. Turnbull, S. Gleason, B. Given, and M. Grimmer, "The voltec 4et50 electric drive system," vol. 4, pp. 323–337.

[19] J. Liu and H. Peng, "Control optimization for a power-split hybrid vehicle," in *2006 American Control Conference*. IEEE, 2006.

[20] J. Liu, H. Peng, and Z. Filipi, "Modeling and control analysis of toyota hybrid system."

[21] A. A. Frank and N. H. Beachley, "Design considerations for flywheel-transmission automobiles."

[22] R. Wohl, T. Long, V. Mucino, and J. E. Smith, "A model for a planetary - cvt mechanism: Analysis and synthesis."

[23] D. K. A. G. Holmes and M. R. Schmidt, "Electrically variable transmissionwith selective input split, compound split neutral and reverse modes," United States-Patent Patent 6 527 658 B2, 2003.

[24] W. Zhuang, X. Zhang, Y. Ding, L. Wang, and X. Hu, "Comparison of multi-mode hybrid powertrains with multiple planetary gears," *Applied energy*, vol. 178, pp. 624–632, 2016.

[25] Z. Qin, Y. Luo, K. Li, and H. Peng, "A new powertrain design approach for power-split hybrid tracked vehicles," in *Volume 2: Mechatronics Estimation and Identification Uncertain Systems and Robustness Path Planning and Motion Control Tracking Control Systems Multi-Agent and Networked Systems Manufacturing Intelligent Transportation and Vehicles Sensors and Actuators Diagnostics and Detection Unmanned, Ground and Surface Robotics Motion and Vibration Control Applications*. American Society of Mechanical Engineers, oct 2017.

[26] W. Zhuang, X. Zhang, D. Zhao, H. Peng, and L. Wang, "Optimal design of three-planetary-gear power-split hybrid powertrains," *International Journal of Automotive Technology, April 2016, Volume 17, Issue 2, pp 299-309*, aug 2017.

[27] X. Zhang, H. Peng, and J. Sun, "A near optimal power management strategy for rapid component sizing of multi mode power split hybrid vehicles," *IEEE Transactions on Control Systems Technology*, vol. 23, no. 2, pp. 609–618, 2015.

[28] P. G. Anselma, Y. Huo, E. Amin, J. Roeleveld, A. Emadi, and G. Belingardi, "Mode-shifting minimization in a power management strategy for rapid component sizing of multimode power split hybrid vehicles," in *SAE Technical Paper Series*. SAE International, apr 2018.

[29] X. Chen, J. Jiang, L. Zheng, H. Tang, and X. Chen, "Study and analysis of a multi-mode power split hybrid transmission," *World Electric Vehicle Journal*, vol. 11, no. 2, p. 46, jun 2020.

[30] D. Rajput, J. M. Herreros, M. S. Innocente, J. Schaub, and A. M. Dizqah, "Electrified powertrain with multiple planetary gears and corresponding energy management strategy," *Vehicles*, vol. 3, no. 3, pp. 341–356, jul 2021.

[31] A. Biswas, P. G. Anselma, A. Rathore, and A. Emadi, "Effect of coordinated control on real-time optimal mode selection for multi-mode hybrid electric powertrain," vol. 289, p. 116695, may 2021.

[32] J. Wu and N. Zhang, "Driving mode shift control for planetary gear based dual motor powertrain in electric vehicles," *Mechanism and Machine Theory*, vol. 158, p. 104217, apr 2021.

[33] M.-A. Beaudoin and B. Boulet, "Fundamental limitations to no-jerk gearshifts of multi-speed transmission architectures in electric vehicles," *Mechanism and Machine Theory*, vol. 160, p. 104290, jun 2021.

[34] Y. Li, J. Han, X. Tang, and X. Hu, "Predictive energy management for dual motor-driven electric vehicles," in *SAE Technical Paper Series*. SAE International, feb 2022.

[35] W.-S. Yao and C.-Y. Lin, "Design of active continuous variable transmission control system with planetary gear," *Electronics*, vol. 11, no. 7, p. 986, mar 2022.

[36] W. Zhuang, S. L. (Eben), X. Zhang, D. Kum, Z. Song, G. Yin, and F. Ju, "A survey of powertrain configuration studies on hybrid electric vehicles," *Applied Energy*, vol. 262, p. 114553, mar 2020.

[37] H. Kim, T. Barhoumi, and D. Kum, "Comprehensive design methodology of compound-split hybrid electric vehicles: Introduction of the compound lever as a design tool," *IEEE Access*, vol. 7, pp. 84 744–84 756, 2019.

[38] W. Wang, R. Song, M. Guo, and S. Liu, "Analysis on compound-split configuration of power-split hybrid electric vehicle," *Mechanism and Machine Theory*, vol. 78, pp. 272–288, aug 2014.

[39] Y. G. Liao and M.-Y. Chen, "Analysis of multi-speed transmission and electrically continuous variable transmission using lever analogy method for speed ratio determination," *Advances in Mechanical Engineering*, vol. 9, no. 8, p. 168781401771294, aug 2017.

[40] H. Ngo and H. Yan, "Configuration synthesis of series–parallel hybrid transmissions," *Proceedings of the Institution of Mechanical Engineers, Part D: Journal of Automobile Engineering*, vol. 230, no. 5, pp. 664–678, jul 2015.

[41] W. Lee, H. Jeoung, D. Park, L. Yang, and N. Kim, "Analysis of powertrain efficiency of a multi-mode hybrid electric vehicle based on operating modes," 2020.

[42] A. T. Zaremba, C. Soto, and M. Jennings, "Methodology for assessment of alternative hybrid electric vehicle powertrain system architectures," vol. 1, pp. 240–248.

[43] A. Gupta and C. Ramanarayanan, "Analysis of circulating power within hybrid electric vehicle transmissions," *Mechanism and Machine Theory*, vol. 64, pp. 131–143, jun 2013.

[44] E. Pennestrì, L. Mariti, P. P. Valentini, and V. H. Mucino, "Efficiency evaluation of gearboxes for parallel hybrid vehicles: Theory and applications," *Mechanism and Machine Theory*, vol. 49, pp. 157–176, mar 2012.

[45] P. Dong, Y. Liu, P. Tenberge, and X. Xu, "Design and analysis of a novel multi-speed automatic transmission with four degrees-of-freedom," *Mechanism and Machine Theory*, vol. 108, pp. 83–96, feb 2017.

[46] D. Rotella, M. Cammalleri, D. Qin, and X. Zhou, "A simple method for the design of hybrid electric power-split cvts: A case study," pp. 70–79, 2019.

[47] A. Rossetti and A. Macor, "Continuous formulation of the layout of a hydromechanical transmission," *Mechanism and Machine Theory*, vol. 133, pp. 545–558, mar 2019.

[48] F. Bottiglione, S. D. Pinto, and G. Mantriota, "Infinitely variable transmissions in neutral gear: Torque ratio and power re-circulation," *Mechanism and Machine Theory*, vol. 74, pp. 285–298, apr 2014.

[49] F. Bottiglione and G. Mantriota, "Power flows and efficiency of output compound e-cvt," vol. 2015, pp. 1–12, 2015.

[50] S. D. Pinto and G. Mantriota, "Power flows in compound transmissions for hybrid vehicles," *Machines*, vol. 7, no. 1, p. 19, mar 2019.

[51] ——, "A simple model for compound split transmissions," *Proceedings of the Institution of Mechanical Engineers, Part D: Journal of Automobile Engineering*, vol. 228, no. 5, pp. 549–564, dec 2013.

[52] H. Pei, X. Hu, Y. Yang, X. Tang, C. Hou, and D. Cao, "Configuration optimization for improving fuel efficiency of power split hybrid powertrains with a single planetary gear," *Applied Energy*, vol. 214, pp. 103–116, mar 2018.

[53] M. Du and L. Yang, "A basis for the computer-aided design of the topological structure of planetary gear trains," *Mechanism and Machine Theory*, vol. 145, p. 103690, mar 2020.

[54] V. Shanmukhasundaram, Y. Rao, and S. Regalla, "Enumeration of displacement graphs of epicyclic gear train from a given rotation graph using concept of building of kinematic units," *Mechanism and Machine Theory*, vol. 134, pp. 393–424, apr 2019.

[55] F. Yang, J. Feng, and H. Zhang, "Power flow and efficiency analysis of multi-flow planetary gear trains," *Mechanism and Machine Theory*, vol. 92, pp. 86–99, oct 2015.

[56] J. R. G. Ayats, U. Diego-Ayala, J. M. Canela, F. Fenollosa, and J. Vivancos, "Hypergraphs for the analysis of complex mechanisms comprising planetary gear trains and other variable or fixed transmissions," vol. 51, pp. 217–229, 2012.

[57] D. Salgado and J. del Castillo, "Analysis of the transmission ratio and efficiency ranges of the four-, five-, and six-link planetary gear trains," *Mechanism and Machine Theory*, vol. 73, pp. 218–243, mar 2014.

[58] X. Zhou, D. Qin, D. Rotella, and M. Cammalleri, "Hybrid electric vehicle powertrain design: Construction of topologies and initial design schemes," pp. 49–60, 2019.

[59] M. Cammalleri and A. Castellano, "Analysis of hybrid vehicle transmissions with any number of modes and planetary gearing: kinematics, power flows, mechanical power losses," *Mechanism and Machine Theory*, vol. 162, p. 104350, aug 2021.

[60] C. Sieg and F. Küçükay, "Benchmarking of dedicated hybrid transmissions," *Vehicles*, vol. 2, no. 1, pp. 100–125, feb 2020.

[61] H. Chen, L. Li, A. Lange, and F. Küçükay, "Innovative dedicated hybrid transmission concepts in the next generation of hybrid powertrains," vol. 8.

[62] Q. Li, X. Zhou, S. Wang, and J. Liang, "Power split transmission with continuously variable planetary ratio," *Mechanism and Machine Theory*, vol. 140, pp. 765–780, oct 2019.

[63] T.-T. Ho and S.-J. Hwang, "Configuration synthesis of novel hybrid transmission systems using a combination of a ravigneaux gear train and a simple planetary gear train," *Energies*, vol. 13, no. 9, p. 2333, may 2020.

[64] M. Sorrentino, G. Rizzo, and I. Arsie, "Analysis of a rule-based control strategy for on-board energy management of series hybrid vehicles," *Control Engineering Practice*, vol. 19, no. 12, pp. 1433–1441, dec 2011.

[65] J. Liang, J. Zhang, H. Zhang, and C. Yin, "Fuzzy energy management optimization for a parallel hybrid electric vehicle using chaotic non-dominated sorting genetic algorithm," *Automatika*, vol. 56, no. 2, pp. 149–163, jan 2015.

[66] V. Gupta, "Ecms based hybrid algorithm for energy management in parallel hybrid electric vehicles," *HCTL Open International Journal of Technology Innovations and Research (IJTIR)*, vol. 14, pp. 2321–1814, 2015.

[67] G. Paganelli, S. Delprat, T.-M. Guerra, J. Rimaux, and J.-J. Santin, "Equivalent consumption minimization strategy for parallel hybrid powertrains," in *Vehicular Technology Conference. IEEE 55th Vehicular Technology Conference. VTC Spring 2002 (Cat. No. 02CH37367)*, vol. 4. IEEE, 2002, pp. 2076–2081.

[68] G. Paganelli, M. Tateno, A. Brahma, G. Rizzoni, and Y. Guezennec, "Control development for a hybrid-electric sport-utility vehicle: strategy, implementation and field test results (i)," in *Proceedings of the American Control Conference*, vol. 2, 2001, pp. 5064–5064.

[69] Y. Zhang, L. Chu, Z. Fu, C. Guo, D. Zhao, Y. Li, Y. Ou, and L. Xu, "An improved adaptive equivalent consumption minimization strategy for parallel plug-in hybrid electric vehicle," *Proceedings of the Institution of Mechanical Engineers, Part D: Journal of Automobile Engineering*, vol. 233, no. 6, pp. 1649–1663, oct 2018.

[70] Y. Hu, W. Li, K. Xu, T. Zahid, F. Qin, and C. Li, "Energy management strategy for a hybrid electric vehicle based on deep reinforcement learning," *Applied Sciences*, vol. 8, no. 2, p. 187, jan 2018.

[71] S. Zhang, R. Xiong, and F. Sun, "Model predictive control for power management in a plug-in hybrid electric vehicle with a hybrid energy storage system," *Applied Energy*, vol. 185, pp. 1654–1662, jan 2017.

[72] F. Zhang, L. Wang, S. Coskun, H. Pang, Y. Cui, and J. Xi, "Energy management strategies for hybrid electric vehicles: Review, classification, comparison, and outlook," *Energies*, vol. 13, no. 13, p. 3352, jun 2020.

[73] H. Borhan, A. Vahidi, A. M. Phillips, M. L. Kuang, I. V. Kolmanovsky, and S. D. Cairano, "MPC-based energy management of a power-split hybrid electric vehicle," vol. 20, no. 3, pp. 593–603, may 2012.

[74] F. Dettù, G. Pozzato, D. M. Rizzo, and S. Onori, "Exergy-based modeling framework for hybrid and electric ground vehicles," *Applied Energy*, vol. 300, p. 117320, oct 2021.

[75] C.-T. Chung, C.-H. Wu, and Y.-H. Hung, "A design methodology for selecting energy-efficient compound split e-CVT hybrid systems with planetary gearsets based on electric circulation," vol. 230, p. 120732, sep 2021.

[76] A. M. Dizqah, B. L. Ballard, M. V. Blundell, S. Kanarachos, and M. S. Innocente, "A non-convex control allocation strategy as energy-efficient torque distributors for on-road and off-road vehicles," *Control Engineering Practice*, vol. 95, p. 104256, 2020.

[77] S. Nazari, J. Siegel, and A. Stefanopoulou, "Optimal energy management for a mild hybrid vehicle with electric and hybrid engine boosting systems," *IEEE Transactions on Vehicular Technology*, vol. 68, no. 4, pp. 3386–3399, apr 2019.

[78] C. Sun, F. Sun, and H. He, "Investigating adaptive-ECMS with velocity forecast ability for hybrid electric vehicles," vol. 185, pp. 1644–1653, jan 2017.

[79] O. H. Dagci, H. Peng, and J. W. Grizzle, "Hybrid electric powertrain design methodology with planetary gear sets for performance and fuel economy," *IEEE Access*, vol. 6, pp. 9585–9602, 2018.

[80] S. Sarvaiya, S. Ganesh, and B. Xu, "Comparative analysis of hybrid vehicle energy management strategies with optimization of fuel economy and battery life," *Energy*, vol. 228, p. 120604, aug 2021.

[81] D. Shi, S. Liu, Y. Cai, S. Wang, H. Li, and L. Chen, "Pontryagin's minimum principle based fuzzy adaptive energy management for hybrid electric vehicle using real-time traffic information," *Applied Energy*, vol. 286, p. 116467, mar 2021.

[82] J. Zhou, S. Xue, Y. Xue, Y. Liao, J. Liu, and W. Zhao, "A novel energy management strategy of hybrid electric vehicle via an improved TD3 deep reinforcement learning," vol. 224, p. 120118, jun 2021.

[83] W. Li, H. Cui, T. Nemeth, J. Jansen, C. Ünlübayir, Z. Wei, X. Feng, X. Han, M. Ouyang, H. Dai, X. Wei, and D. U. Sauer, "Cloud-based health-conscious energy management of hybrid battery systems in electric vehicles with deep reinforcement learning," *Applied Energy*, vol. 293, p. 116977, jul 2021.

[84] Y. Wang, X. Jiao, Z. Sun, and P. Li, "Energy management strategy in consideration of battery health for PHEV via stochastic control and particle swarm optimization algorithm," *Energies*, vol. 10, no. 11, p. 1894, nov 2017.

[85] X. Hu, X. Zhang, X. Tang, and X. Lin, "Model predictive control of hybrid electric vehicles for fuel economy, emission reductions, and inter-vehicle safety in car-following scenarios," *Energy*, vol. 196, p. 117101, apr 2020.

[86] H. Zhang, Q. Fan, S. Liu, S. E. Li, J. Huang, and Z. Wang, "Hierarchical energy management strategy for plug-in hybrid electric powertrain integrated with dual-mode combustion engine," *Applied Energy*, vol. 304, p. 117869, dec 2021.

[87] B. Zhang, J. Zhang, and T. Shen, "Optimal control design for comfortable-driving of hybrid electric vehicles in acceleration mode," *Applied Energy*, vol. 305, p. 117885, jan 2022.

[88] S. Trilochana, B. Jyothi, and N. Ramchandra, "A comparative study on different types of drive train systems of hybrid and plug-in hybrid electric vehicle," in *Lecture Notes in Mechanical Engineering*. Springer Nature Singapore, 2022, pp. 273–283.

[89] C. T. Nguyen, P. D. Walker, S. Zhou, and N. Zhang, "Optimal sizing and energy management of an electric vehicle powertrain equipped with two motors and multi-gear ratios," *Mechanism and Machine Theory*, vol. 167, p. 104513, jan 2022.

[90] Q. Li, Z. Zhang, J. Bai, T. Zhang, and F. Gai, "Development of a compound power-split hybrid power system for commercial vehicles," *International Journal of Automotive Technology*, vol. 23, no. 1, pp. 135–147, feb 2022.

[91] M. Zeraoulia, M. E. H. Benbouzid, and D. Diallo, "Electric motor drive selection issues for HEV propulsion systems: A comparative study," *IEEE Transactions on Vehicular Technology*, vol. 55, no. 6, pp. 1756–1764, nov 2006.

[92] M. Ehsani, Y. Gao, and J. M. Miller, "Hybrid electric vehicles: Architecture and motor drives," *Proceedings of the IEEE*, vol. 95, no. 4, pp. 719–728, apr 2007.

[93] B. Huang, M. Hu, L. Zeng, G. Fu, and Q. Jia, "Design method for hybrid electric vehicle powertrain configuration with a single motor," *Sustainability*, vol. 14, no. 13, p. 8225, jul 2022.

[94] J. Walters, H. Husted, and K. Rajashekara, "Comparative study of hybrid powertrain strategies," *SAE Transactions*, vol. 110, pp. 1944–1953, 2001. [Online]. Available: http://www.jstor.org/stable/44724452

[95] S. Ebbesen, P. Elbert, and L. Guzzella, "Battery state-of-health perceptive energy management for hybrid electric vehicles," *IEEE Transactions on Vehicular Technology*, vol. 61, no. 7, pp. 2893–2900, sep 2012.

[96] T. Markel and A. Simpson, "Energy storage systems considerations for grid-charged hybrid electric vehicles."

[97] F. Martel, Y. Dubé, S. Kelouwani, J. Jaguemont, and K. Agbossou, "Long-term assessment of economic plug-in hybrid electric vehicle battery lifetime degradation management through near optimal fuel cell load sharing," *Journal of Power Sources*, vol. 318, pp. 270–282, jun 2016.

[98] Z. Chen, C. C. Mi, R. Xiong, J. Xu, and C. You, "Energy management of a power-split plug-in hybrid electric vehicle based on genetic algorithm and quadratic programming," *Journal of Power Sources*, vol. 248, pp. 416–426, feb 2014.

[99] X. Hu, C. M. Martinez, and Y. Yang, "Charging, power management, and battery degradation mitigation in plug-in hybrid electric vehicles: A unified cost-optimal approach," *Mechanical Systems and Signal Processing*, vol. 87, pp. 4–16, mar 2017.

[100] Z. Song, J. Li, X. Han, L. Xu, L. Lu, M. Ouyang, and H. Hofmann, "Multi-objective optimization of a semi-active battery/supercapacitor energy storage system for electric vehicles," *Applied Energy*, vol. 135, pp. 212–224, dec 2014.

[101] M. Hannan, M. Hoque, A. Mohamed, and A. Ayob, "Review of energy storage systems for electric vehicle applications: Issues and challenges," *Renewable and Sustainable Energy Reviews*, vol. 69, pp. 771–789, mar 2017.

[102] S. J. Moura, J. L. Stein, and H. K. Fathy, "Battery-health conscious power management in plug-in hybrid electric vehicles via electrochemical modeling and stochastic control," *IEEE Transactions on Control Systems Technology*, vol. 21, no. 3, pp. 679–694, may 2013.

[103] J. Li, H. He, Z. Wei, and X. Zhang, "Hierarchical sizing and power distribution strategy for hybrid energy storage system," vol. 4, pp. 440–447, 2021.

[104] W. Gu, Z. Sun, X. Wei, and H. Dai, "A capacity fading model of lithium-ion battery cycle life based on the kinetics of side reactions for electric vehicle applications," *Electrochimica Acta*, vol. 133, pp. 107–116, jul 2014.

[105] Y. Song, D. Liu, L. Li, and Y. Peng, "Lithium-ion battery pack on-line degradation state prognosis based on the empirical model," in *2018 International Conference on Sensing,Diagnostics, Prognostics, and Control (SDPC)*. IEEE, aug 2018.

[106] J. Wu, Z. Wei, K. Liu, Z. Quan, and Y. Li, "Battery-involved energy management for hybrid electric bus based on expert-assistance deep deterministic policy gradient algorithm," *IEEE Transactions on Vehicular Technology*, vol. 69, no. 11, pp. 12 786–12 796, nov 2020.

[107] J. Wu, Z. Wei, W. Li, Y. Wang, Y. Li, and D. U. Sauer, "Battery thermal- and health-constrained energy management for hybrid electric bus based on soft actor-critic DRL algorithm," *IEEE Transactions on Industrial Informatics*, vol. 17, no. 6, pp. 3751–3761, jun 2021.

[108] A. Jarushi and N. Schofield, "Battery and supercapacitor combination for a series hybrid electric vehicle," in *5th IET International Conference on Power Electronics, Machines and Drives (PEMD 2010)*. Institution of Engineering and Technology, 2010.

[109] B. M. Conlon, T. Blohm, M. Harpster, A. Holmes, M. Palardy, S. Tarnowsky, and L. Zhou, "The next generation "voltec" extended range EV propulsion system," *SAE International Journal of Alternative Powertrains*, vol. 4, no. 2, pp. 248–259, apr 2015.

[110] W. Zhuang, X. Zhang, D. Li, L. Wang, and G. Yin, "Mode shift map design and integrated energy management control of a multi-mode hybrid electric vehicle," *Applied Energy*, vol. 204, pp. 476–488, oct 2017.

[111] R. Fourer, D. M. Gay, and B. W. Kernighan, "Ampl: A mathematical programing language," pp. 150–151, 1989.

[112] L. T. Biegler, *Nonlinear Programming*. Society for Industrial and Applied Mathematics, jan 2010.

[113] E. D. Dolan, R. Fourer, J.-P. Goux, T. S. Munson, and J. Sarich, "Kestrel: An interface from optimization modeling systems to the neos server," vol. 20, pp. 525–538, 2008.

[114] R. H. Byrd, J. Nocedal, and R. A. Waltz, "Knitro an integrated package for nonlinear optimization," in *Nonconvex Optimization and Its Applications*. Springer US, 2006, pp. 35–59.

[115] "NEOS server," https://neos-server.org/neos/solvers/index.html.

[116] "Morgridge Institute for Research server," https://morgridge.org/.

[117] "Wisconsin Alumni Research Foundation server," https://www.warf.org/about-warf/discovery-building/.

[118] T. M. Grewe, B. M. Conlon, and A. G. Holmes, "Defining the general motors 2-mode hybrid transmission."

[119] D. Rajput, A. M. Dizqah, J. M. Herreros, and M. Innocente, "Effect of number of planetary gears on fuel consumption and vehicle performance in the hybrid powertrain of a passenger car," in *The Future Powertrain Conference*, 2020.

# Appendices

# Appendix A

# AMPL codes all powertrain topologies considered

This appendix provides the AMPL codes for all five topologies. The energy management strategy problem discussed in chapter 3 is written using AMPL. The parameter file, data file (US06 drive cycle), and solver are same for all topologies, only model file is different.

### A.0.1 Variables

$$\begin{aligned} varacc\{V\}; \\ varz\{V\}; \\ varM_{shift}\{V\}; \\ varTreq\{V\}; \\ varemg2\{V\}; \\ varemg1\{V\}; \\ varebth\{V\}; \\ varPbatt\{V\}; \\ varTeng\{V\}; \end{aligned} \tag{A.1}$$

$$
\begin{aligned}
-1300 \leq varWmg2\{V\} \leq 1300;\\
-400 \leq varWmg1\{V\} \leq 4000;\\
0 \leq varWe\{V\} \leq 500;\\
-200 \leq varTmg2\{V\} \leq 200;\\
-200 \leq varTmg1\{V\} \leq 200;\\
0 \leq varTe\{V\} \leq 142;\\
varQ\{V\} \leq 0;\\
varMice\{V\} \leq 0;\\
varMeqv\{V\} \leq 0;\\
varMT\{V\} \leq 0;\\
vardelta\{V\} \leq 0;\\
0 \leq varsoc\{V\} \leq 1;\\
vars_i\{V\} \leq 1;
\end{aligned}
\tag{A.2}
$$

### A.0.2 Parameters

$$
\begin{aligned}
param \quad g = 9.8;\\
param \quad f0 = 0.015;\\
param \quad f2 = 10^{(-6)};\\
param \quad c_d = 0.3;\\
param \quad A_d = 2.1;\\
param \quad rho_{air} = 1.225;\\
param \quad theta = 0;\\
param \quad I_e = 0.5;\\
param \quad I_{mg1} = 0.2;\\
param \quad I_{mg2} = 0.2;\\
param \quad alpha = 0.02;
\end{aligned}
\tag{A.3}
$$

$$
\begin{aligned}
param \quad & v = 8; \quad (velocity) \\
set \quad & V = 1..v; \\
param \quad & m = 9; \\
param \quad & R_1 = 0.26; \\
param \quad & S_1 = 0.1; \\
param \quad & R_2 = 0.26; \\
param \quad & S_2 = 0.1; \\
param \quad & R_3 = 0.2; \\
param \quad & S_3 = 0.1; \\
param \quad & Diff_{GR} = 3.95; \\
param \quad & R_{eff} = 0.33; \\
param \quad & mass = 1450; \\
param \quad & p00 = 3.564; \\
param \quad & p10 = -0.0001743; \\
param \quad & p01 = -0.1142; \\
param \quad & p20 = -5.059 \times 10^{(-7)}; \\
param \quad & p11 = 6.839 \times 10^{(-5)}; \\
param \quad & p02 = 0.008514; \\
param \quad & p30 = 1.181 \times 10^{(-10)}; \\
param \quad & p21 = 3.371 \times 10^{(-8)}; \\
param \quad & p12 = -4.526 \times 10^{(-6)}; \\
param \quad & p03 = -8.259 \times 10^{(-5)}; \\
param \quad & p40 = -1.491 * 10^{(-14)}; \\
param \quad & p31 = -5.748 * 10^{(-12)}; \\
param \quad & p22 = 1.135 \times 10^{(-10)}; \\
param \quad & p13 = 4.176 \times 10^{(-08)}; \\
param \quad & p04 = 2.948 \times 10^{(-7)}; \\
param \quad & p50 = 1.221 \times 10^{(-18)}; \\
param \quad & p41 = 8.305 \times 10^{(-17)}; \\
param \quad & p32 = 2.738 \times 10^{(-14)}; \\
param \quad & p23 = -1.97 \times 10^{(-12)}; \\
param \quad & p14 = -9.843 * 10^{(-11)}; \\
param \quad & p05 = -2.164 \times 10^{(-10)};
\end{aligned}
\tag{A.4}
$$

### A.0.3 Solver

1.

$$option \quad knitro \quad maxit = 0, \quad xtol = 0, \quad bar\_initpi\_mpec = -1, par\_msnumthreads = 4"; \tag{A.5}$$

2. solve;
3. display fuel;
4. display _varname, _var;
5. display _conname, _con.slack;

### A.0.4 Data

The data files has the velocity points of US06 drive cycles at every 1 second.

```
data;
param:    Vel :=
1    0
2    0
3    0
4    0
5    0
6    0
7    0
8    0
9    1.77028
10    2.73588
11    9.65606
12    22.3699
13    32.9916
14    41.3601
15    40.2336
16    45.7054
17    51.9818
18    55.6833
19    58.7411
20    61.7988
21    64.2128
22    67.9143
23    70.4893
24    71.133
25    69.8455
26    68.5581
27    64.8566
28    63.0863
29    61.7988
30    61.7988
31    63.0863
32    62.4425
33    62.4425
34    58.7411
35    51.9818
36    44.4179
.....................
600    0;
```

### A.0.5 Model of 1PG-1

Objective function:

Minimise fuel:

$$sum\{i \quad in \quad V\}(\frac{0.5 \times MT[i]}{190} + 0.1 \times M\_shift[i]/1 + 0.4 \times (0.8 - soc[i])^2); \quad (A.6)$$

Constraint equations:

$$c1\{i \quad in \quad V\}: \quad 0 \leq s4[i] \quad complements \quad s1[i] \leq 0; \quad (A.7)$$
$$c2\{i \quad in \quad V\}: \quad 0 \leq s4[i] \quad complements \quad s2[i] \leq 0; \quad (A.8)$$
$$c3\{i \quad in \quad V\}: \quad 0 \leq s4[i] \quad complements \quad s3[i] \leq 0; \quad (A.9)$$
$$c4\{i \quad in \quad V\}: \quad 0 \leq s3[i] \quad complements \quad s1[i] \leq 0; \quad (A.10)$$
$$c5\{i \quad in \quad V\}: \quad 0 \leq s3[i] \quad complements \quad s2[i] \leq 0; \quad (A.11)$$
$$c6\{i \quad in \quad V\}: \quad 0 \leq s2[i] \quad complements \quad s1[i] \leq 0; \quad (A.12)$$
$$c7\{i \quad in \quad V\}: \quad s1[i] + s2[i] + s3[i] + s4[i] = 1; \quad (A.13)$$

$$torque\_mg2\{i \quad in \quad V\}: \quad Tmg2[i] = \frac{S_1}{R_1}\Big( - \frac{R_2}{S_2} T_{mg2[i]} z[i] + \frac{T_{req}[i]}{D_{GR}}\Big) s1[i] + \frac{T_{req}[i]}{D_{GR}} s2[i] + -R_1\Big(\frac{T_{e[i]}}{R_1 + S_1} z[i] + \frac{T_{req}[i]}{D_{GR}} s3[i]\Big) + \frac{T_{req}[i]}{D_{GR}} s4[i]; \quad (A.14)$$

$$torque\_mg1\{i \quad in \quad V\}: \quad Tmg1[i] = \frac{S_1}{R_1}\Big(T_{mg2}[i] + \frac{T_{req}[i]}{D_{GR}}\Big) s1[i] + \frac{S_1 T_e[i]}{(R_1 + S_1)} s2[i]; \quad (A.15)$$

$$torque\_req\{i \quad in \quad V\}: \quad Treq[i] = mass \times acc[i] + mass \times g \times sin\theta + 0.5 \times rho_{air} \times c_d \times A_d \times \big(\frac{vel[i]}{3.6}\big)^2; \quad (A.16)$$

$$Z\_sign\{i \quad in \quad V\}: T_{req}[i](2z[i] - 1) = T_{req}[i] tanh\big(\frac{T_{req}[i]}{0.01}\big); \quad (A.17)$$

$$\omega\_mg2\{i \quad in \quad V\}: W_{mg2}[i] = \frac{Vel[i] Diff_{GR}}{3.6 R_{eff}}; \quad (A.18)$$

$$\omega\_mg1\{i \quad in \quad V\}: W_{mg1}[i] = \frac{R_1}{S_1} - W_{mg2}[i] s[1] z[i] + \frac{R_1 + S_1}{S_1} W_e s2[i] z[i]; \quad (A.19)$$

$$\omega\_e\{i \quad in \quad V\} : W_e[i] = \frac{R_1 + S_1}{S_1} W_{mg1} s2[i] z[i] + (\frac{R_1 + S_1}{R_1} W_{mg2} + \frac{R_1 + S_1}{S_1} W_{mg1} z[i]) s3[i]; \tag{A.20}$$

$$\begin{aligned} Fuel\_flow\_rate\{i \quad in \quad V\} : Q[i] = & p00 + \\ & p10\omega_e[i] + p01T_e[i] + \\ & p20\omega_{e^2}[i] + p11\omega_e[i]T_e[i] + p02T_{e^2}[i] + \\ & p30\omega_{e^3}[i] + p21\omega_{e_k}[i]T_e[i] + p12\omega_e[i]T_{e^2}[i] + p03T_{e^3}[i] + \\ & p40\omega_{e^4}[i] + p31\omega_{e^3}[i]T_e[i] + p22\omega_{e^2}[i]T_{e^2}[i] + p13\omega_e[i]T_{e^3}[i] + p04T_{e^4}[i] + \\ & p50\omega_{e^5}[i] + p41\omega_{e^4}[i]T_e[i] + p32\omega_{e^3}[i]T_{e^2}[i] + \\ & \quad p23\omega_{e^2}[i]T_{e^3}[i] + p14\omega_e[i]T_{e^4}[i] + p05\omega_{e^5}[i]; \end{aligned} \tag{A.21}$$

$$Fuel\_eng\{i \quad in \quad V\} : M_{ice}[i] = \frac{Q[i]W_e[i]780}{120}; \tag{A.22}$$

$$\begin{aligned} Fuel\_eqv\{i \quad in \quad V\} : M_{eqv}[i] = max(0, & (\frac{T_{mg2}[i]W_{mg2}[i]}{emg2[i]}) \times 0.75 \times 0.00002381 \times \frac{1}{0.35} s4[i]z[i] + \\ & (\frac{T_{mg2}[i]W_{mg2}[i]}{emg2[i]} + \frac{T_{mg1}[i]W_{mg1}[i]}{emg1[i]}) \times 0.75 \times 0.00002381 \times \frac{1}{0.35} s1[i]z[i] + \\ & \frac{T_{mg2}[i]W_{mg2}[i]}{emg2[i]}) \times 0.75 \times 0.00002381 \times \frac{1}{0.35} s2[i]z[i] + \\ & \frac{T_{mg2}[i]W_{mg2}[i]}{emg2[i]}) \times 0.75 \times 0.00002381 \times \frac{1}{0.35} s3[i]z[i]); \end{aligned} \tag{A.23}$$

$$Fuel\_total\{i \quad in \quad V\} : M_T[i] = M_{ice}[i] + M_{eqv}[i]; \tag{A.24}$$

$$eff\_mg2\{i \quad in \quad V\} : emg2[i] = abs(\frac{T_{mg2}[i]W_{mg2}[i])}{abs(T_{mg2}[i]W_{mg2}[i])}) + (abs\frac{T_{mg2}[i]}{0.45})^2 \times 0.75; \tag{A.25}$$

$$eff\_mg1\{i \quad in \quad V\} : emg1[i] = abs(\frac{T_{mg1}[i]W_{mg1}[i])}{abs(T_{mg1}[i]W_{mg1}[i])}) + (abs\frac{T_{mg1}[i]}{0.45})^2 \times 0.75; \tag{A.26}$$

$$eff\_bth\{i \quad in \quad V\} : ebth[i] = (\frac{3.14 \times T_e[i]}{780 \times Q[i] \times 46000 \times 2}) \times 10^6; \tag{A.27}$$

$$\begin{aligned} battery\_power\{i \quad in \quad V\} : Pbatt[i] = {} & \frac{T_{mg2}[i]W_{mg2}[i]}{e_{mg2}[i]}s4[i](1 - z[i]) + \frac{T_{mg2}[i]W_{mg2}[i]}{e_{mg2}[i]}s4[i]z[i] + \\ & \frac{T_{mg2}[i]W_{mg2}[i]}{e_{mg2}[i]}s1[i]z[i] + \frac{T_{mg1}[i]W_{mg1}[i]}{e_{mg1}[i]}s1[i]z[i] + \frac{T_{mg2}[i]W_{mg2}[i]}{e_{mg2}[i]}s1[i](1 - z[i]) + \\ & \frac{T_{mg2}[i]W_{mg2}[i]}{e_{mg2}[i]}s2[i](1 - z[i]) + \frac{T_{mg2}[i]W_{mg2}[i]}{e_{mg2}[i]}s2[i]z[i] + \frac{T_{mg1}[i]W_{mg1}[i]}{e_{mg1}[i]}s2[i]z[i] + \\ & \frac{T_{mg1}[i]W_{mg1}[i]}{e_{mg1}[i]}s2[i](1 - z[i]) + \frac{T_{mg2}[i]W_{mg2}[i]}{e_{mg2}[i]}s3[i](1 - z[i]) + \frac{T_{mg2}[i]W_{mg2}[i]}{e_{mg2}[i]}s3[i]z[i]; \end{aligned} \tag{A.28}$$

$$SoC\_ode\{i \quad in \quad V \quad diff\{V\}\} : SOC[i+1] = SOC[i] - \frac{Pbatt[i]}{27000 \times 3600}; \tag{A.29}$$

$$acc\_eq\{i \quad in \quad V \quad diff\{1\}\} : acc[i] = \frac{vel[i] - vel[i-1]}{3.6}; \tag{A.30}$$

$$SOC\_init : SOC[1] = 0.80; \tag{A.31}$$
$$acc\_init : acc[1] = 0; \tag{A.32}$$
$$Shift1\_init : M_{shift}[1] = 0; \tag{A.33}$$
$$delta\_init : delta[1] = 0; \tag{A.34}$$
$$mode1\_init : s1[1] = 1; \tag{A.35}$$
$$mode2\_init : s2[1] = 0; \tag{A.36}$$
$$mode3\_init : s3[1] = 0; \tag{A.37}$$
$$mode4\_init : s4[1] = 0; \tag{A.38}$$
$$constraint\_enginetorque\{i \quad in \quad V\} : T_e[i] = \frac{Teng[i]floor(W_e[i])}{W_e[i] + 10^{-6}}; \tag{A.39}$$
$$constraint\_enginespeed\{i \quad in \quad V\} : W_e[i] \geq 75 \times s2[i] + 75 \times s3[i]; \tag{A.40}$$

$$\begin{aligned} delta\_shift\{i \quad in \quad V \quad diff\{1\}\} : delta[i] = abs(s1[i] - s1[i-1]) + \\ abs(s2[i] - s2[i-1]) + abs(s3[i] - s3[i-1]) + abs(s4[i] - s4[i-1]); \end{aligned} \tag{A.41}$$

$$\begin{aligned} Mode\_shift\{i \quad in \quad V \quad diff\{1\}\} : M_{shift}[i] = delta[i] \times alpha \times 0.5 \\ (I_e(W_e[i] - W_e[i-1])^2 + I_{mg1}(W_{mg1}[i] - W_{mg1}[i-1])^2); \end{aligned} \tag{A.42}$$

$$motor2\{i \quad in \quad V\} : T_{mg2}[i]W_{mg2}[i] \leq 60000; \tag{A.43}$$
$$motor1\{i \quad in \quad V\} : T_{mg1}[i]W_{mg1}[i] \leq 42000; \tag{A.44}$$
$$\tag{A.45}$$

$$\begin{aligned} engine1\{i \quad in \quad V\} : T_e[i] \leq max(0, (-3.002 \times 10^{(-14)} \times W_e[i]^6 + \\ +6.96 \times 10^{(-11)} \times W_e[i]^5 - 5.712 \times 10^{(-08)} \times W_e[i]^4 + \\ 1.885 \times 10^{(-05)} \times W_e[i]^3 - 0.001907 \times W_e[i]^2 + 0.05586 \times W_e[i] + 91.09; \end{aligned} \tag{A.46}$$

### A.0.6 Model of 2PG-1

Objective function:

Minimise fuel:

$$sum\{i \quad in \quad V\}(\frac{0.5 \times MT[i]}{190} + 0.1 \times M\_shift[i]/1 + 0.4 \times (0.8 - soc[i])^2); \quad (A.47)$$

Constraint equations:

$$c1\{i \quad in \quad V\}: \quad 0 \leq s4[i] \quad complements \quad s1[i] \leq 0; \quad (A.48)$$
$$c2\{i \quad in \quad V\}: \quad 0 \leq s4[i] \quad complements \quad s2[i] \leq 0; \quad (A.49)$$
$$c3\{i \quad in \quad V\}: \quad 0 \leq s4[i] \quad complements \quad s3[i] \leq 0; \quad (A.50)$$
$$c4\{i \quad in \quad V\}: \quad 0 \leq s3[i] \quad complements \quad s1[i] \leq 0; \quad (A.51)$$
$$c5\{i \quad in \quad V\}: \quad 0 \leq s3[i] \quad complements \quad s2[i] \leq 0; \quad (A.52)$$
$$c6\{i \quad in \quad V\}: \quad 0 \leq s2[i] \quad complements \quad s1[i] \leq 0; \quad (A.53)$$
$$c7\{i \quad in \quad V\}: \quad s1[i] + s2[i] + s3[i] + s4[i] = 1; \quad (A.54)$$

$$torque\_mg2\{i \quad in \quad V\}: \quad Tmg2[i] = \frac{S_1}{R_1}\Big( - \frac{R_2}{S_2} T_{mg2[i]} z[i] + \frac{T_{req}[i]}{D_{GR}}\Big) s1[i] + \frac{T_{req}[i]}{D_{GR}} s2[i] + -R_1\Big(\frac{T_{e[i]}}{R_1 + S_1} z[i] + \frac{T_{req}[i]}{D_{GR}} s3[i]\Big) + \frac{T_{req}[i]}{D_{GR}} s4[i]; \quad (A.55)$$

$$torque\_mg1\{i \quad in \quad V\}: \quad Tmg1[i] = \frac{S_1}{R_1}\Big(T_{mg2}[i] + \frac{T_{req}[i]}{D_{GR}}\Big) s1[i] + \frac{S_1 T_e[i]}{(R_1 + S_1)} s2[i]; \quad (A.56)$$

$$torque\_req\{i \quad in \quad V\}: \quad Treq[i] = mass \times acc[i] + mass \times g \times sin\theta + 0.5 \times rho_{air} \times c_d \times A_d \times \big(\frac{vel[i]}{3.6}\big)^2; \quad (A.57)$$

$$Z\_sign\{i \quad in \quad V\}: T_{req}[i](2z[i] - 1) = T_{req}[i] tanh\big(\frac{T_{req}[i]}{0.01}\big); \quad (A.58)$$

$$\omega\_mg2\{i \quad in \quad V\}: W_{mg2}[i] = \frac{Vel[i] Diff_{GR}}{3.6 R_{eff}}; \quad (A.59)$$

$$\omega\_mg1\{i \quad in \quad V\}: W_{mg1}[i] = \frac{R_1}{S_1} - W_{mg2}[i] s[1] z[i] + \frac{R_1 + S_1}{S_1} W_e s2[i] z[i]; \quad (A.60)$$

$$\omega\_e\{i \quad in \quad V\} : W_e[i] = \frac{R_1 + S_1}{S_1} W_{mg1} s2[i] z[i] + (\frac{R_1 + S_1}{R_1} W_{mg2} + \frac{R_1 + S_1}{S_1} W_{mg1} z[i]) s3[i]; \tag{A.61}$$

$$\begin{aligned} Fuel\_flow\_rate\{i \quad in \quad V\} : Q[i] = & p00 + \\ & p10\omega_e[i] + p01T_e[i] + \\ & p20\omega_{e^2}[i] + p11\omega_e[i]T_e[i] + p02T_{e^2}[i] + \\ & p30\omega_{e^3}[i] + p21\omega_{e_k}[i]T_e[i] + p12\omega_e[i]T_{e^2}[i] + p03T_{e^3}[i] + \\ & p40\omega_{e^4}[i] + p31\omega_{e^3}[i]T_e[i] + p22\omega_{e^2}[i]T_{e^2}[i] + p13\omega_e[i]T_{e^3}[i] + p04T_{e^4}[i] + \\ & p50\omega_{e^5}[i] + p41\omega_{e^4}[i]T_e[i] + p32\omega_{e^3}[i]T_{e^2}[i] + \\ & \quad p23\omega_{e^2}[i]T_{e^3}[i] + p14\omega_e[i]T_{e^4}[i] + p05\omega_{e^5}[i]; \end{aligned} \tag{A.62}$$

$$Fuel\_eng\{i \quad in \quad V\} : M_{ice}[i] = \frac{Q[i]W_e[i]780}{120}; \tag{A.63}$$

$$\begin{aligned} Fuel\_eqv\{i \quad in \quad V\} : M_{eqv}[i] = max(0, & (\frac{T_{mg2}[i]W_{mg2}[i]}{emg2[i]}) \times 0.75 \times 0.00002381 \times \frac{1}{0.35} s4[i]z[i] + \\ & (\frac{T_{mg2}[i]W_{mg2}[i]}{emg2[i]} + \frac{T_{mg1}[i]W_{mg1}[i]}{emg1[i]}) \times 0.75 \times 0.00002381 \times \frac{1}{0.35} s1[i]z[i] + \\ & \frac{T_{mg2}[i]W_{mg2}[i]}{emg2[i]}) \times 0.75 \times 0.00002381 \times \frac{1}{0.35} s2[i]z[i] + \\ & \frac{T_{mg2}[i]W_{mg2}[i]}{emg2[i]}) \times 0.75 \times 0.00002381 \times \frac{1}{0.35} s3[i]z[i]); \end{aligned} \tag{A.64}$$

$$Fuel\_total\{i \quad in \quad V\} : M_T[i] = M_{ice}[i] + M_{eqv}[i]; \tag{A.65}$$

$$eff\_mg2\{i \quad in \quad V\} : emg2[i] = abs(\frac{T_{mg2}[i]W_{mg2}[i])}{abs(T_{mg2}[i]W_{mg2}[i])}) + (abs\frac{T_{mg2}[i]}{0.45})^2 \times 0.75; \tag{A.66}$$

$$eff\_mg1\{i \quad in \quad V\} : emg1[i] = abs(\frac{T_{mg1}[i]W_{mg1}[i])}{abs(T_{mg1}[i]W_{mg1}[i])}) + (abs\frac{T_{mg1}[i]}{0.45})^2 \times 0.75; \tag{A.67}$$

$$eff\_bth\{i \quad in \quad V\} : ebth[i] = (\frac{3.14 \times T_e[i]}{780 \times Q[i] \times 46000 \times 2}) \times 10^6; \tag{A.68}$$

$$\begin{aligned} battery\_power\{i \quad in \quad V\} : Pbatt[i] = {} & \frac{T_{mg2}[i]W_{mg2}[i]}{e_{mg2}[i]}s4[i](1 - z[i]) + \frac{T_{mg2}[i]W_{mg2}[i]}{e_{mg2}[i]}s4[i]z[i] + \\ & \frac{T_{mg2}[i]W_{mg2}[i]}{e_{mg2}[i]}s1[i]z[i] + \frac{T_{mg1}[i]W_{mg1}[i]}{e_{mg1}[i]}s1[i]z[i] + \frac{T_{mg2}[i]W_{mg2}[i]}{e_{mg2}[i]}s1[i](1 - z[i]) + \\ & \frac{T_{mg2}[i]W_{mg2}[i]}{e_{mg2}[i]}s2[i](1 - z[i]) + \frac{T_{mg2}[i]W_{mg2}[i]}{e_{mg2}[i]}s2[i]z[i] + \frac{T_{mg1}[i]W_{mg1}[i]}{e_{mg1}[i]}s2[i]z[i] + \\ & \frac{T_{mg1}[i]W_{mg1}[i]}{e_{mg1}[i]}s2[i](1 - z[i]) + \frac{T_{mg2}[i]W_{mg2}[i]}{e_{mg2}[i]}s3[i](1 - z[i]) + \frac{T_{mg2}[i]W_{mg2}[i]}{e_{mg2}[i]}s3[i]z[i]; \end{aligned} \tag{A.69}$$

$$SoC\_ode\{i \quad in \quad V \quad diff\{V\}\} : SOC[i+1] = SOC[i] - \frac{Pbatt[i]}{27000 \times 3600}; \tag{A.70}$$

$$acc\_eq\{i \quad in \quad V \quad diff\{1\}\} : acc[i] = \frac{vel[i] - vel[i-1]}{3.6}; \tag{A.71}$$

$$SOC\_init : SOC[1] = 0.80; \tag{A.72}$$
$$acc\_init : acc[1] = 0; \tag{A.73}$$
$$Shift1\_init : M_{shift}[1] = 0; \tag{A.74}$$
$$delta\_init : delta[1] = 0; \tag{A.75}$$
$$mode1\_init : s1[1] = 1; \tag{A.76}$$
$$mode2\_init : s2[1] = 0; \tag{A.77}$$
$$mode3\_init : s3[1] = 0; \tag{A.78}$$
$$mode4\_init : s4[1] = 0; \tag{A.79}$$
$$constraint\_enginetorque\{i \quad in \quad V\} : T_e[i] = \frac{Teng[i]floor(W_e[i])}{W_e[i] + 10^{-6}}; \tag{A.80}$$
$$constraint\_enginespeed\{i \quad in \quad V\} : W_e[i] \geq 75 \times s2[i] + 75 \times s3[i]; \tag{A.81}$$

$$\begin{aligned} delta\_shift\{i \quad in \quad V \quad diff\{1\}\} : delta[i] = abs(s1[i] - s1[i-1]) + \\ abs(s2[i] - s2[i-1]) + abs(s3[i] - s3[i-1]) + abs(s4[i] - s4[i-1]); \end{aligned} \tag{A.82}$$

$$\begin{aligned} Mode\_shift\{i \quad in \quad V \quad diff\{1\}\} : M_{shift}[i] = delta[i] \times alpha \times 0.5 \\ (I_e(W_e[i] - W_e[i-1])^2 + I_{mg1}(W_{mg1}[i] - W_{mg1}[i-1])^2); \end{aligned} \tag{A.83}$$

$$motor2\{i \quad in \quad V\} : T_{mg2}[i]W_{mg2}[i] \leq 60000; \tag{A.84}$$
$$motor1\{i \quad in \quad V\} : T_{mg1}[i]W_{mg1}[i] \leq 42000; \tag{A.85}$$
$$\tag{A.86}$$

$$\begin{aligned} engine1\{i \quad in \quad V\} : T_e[i] \leq max(0, (-3.002 \times 10^{(-14)} \times W_e[i]^6 + \\ +6.96 \times 10^{(-11)} \times W_e[i]^5 - 5.712 \times 10^{(-08)} \times W_e[i]^4 + \\ 1.885 \times 10^{(-05)} \times W_e[i]^3 - 0.001907 \times W_e[i]^2 + 0.05586 \times W_e[i] + 91.09; \end{aligned} \tag{A.87}$$

### A.0.7 Model of 2PG-2

Objective function:

Minimise fuel:

$$sum\{i \quad in \quad V\}\frac{0.5 \times MT[i]}{190} + 0.1 \times M\_shift[i]/1 + 0.4 \times (0.8 - soc[i])^2); \quad \text{(A.88)}$$

Constraint equations:

$$c1\{i \quad in \quad V\}: \quad 0 \leq s4[i] \quad complements \quad s1[i] \leq 0; \quad \text{(A.89)}$$
$$c2\{i \quad in \quad V\}: \quad 0 \leq s4[i] \quad complements \quad s2[i] \leq 0; \quad \text{(A.90)}$$
$$c3\{i \quad in \quad V\}: \quad 0 \leq s4[i] \quad complements \quad s3[i] \leq 0; \quad \text{(A.91)}$$
$$c4\{i \quad in \quad V\}: \quad 0 \leq s3[i] \quad complements \quad s1[i] \leq 0; \quad \text{(A.92)}$$
$$c5\{i \quad in \quad V\}: \quad 0 \leq s3[i] \quad complements \quad s2[i] \leq 0; \quad \text{(A.93)}$$
$$c6\{i \quad in \quad V\}: \quad 0 \leq s2[i] \quad complements \quad s1[i] \leq 0; \quad \text{(A.94)}$$
$$c7\{i \quad in \quad V\}: \quad 0 \leq s5[i] \quad complements \quad s1[i] \leq 0; \quad \text{(A.95)}$$
$$c8\{i \quad in \quad V\}: \quad 0 \leq s5[i] \quad complements \quad s2[i] \leq 0; \quad \text{(A.96)}$$
$$c9\{i \quad in \quad V\}: \quad 0 \leq s5[i] \quad complements \quad s3[i] \leq 0; \quad \text{(A.97)}$$
$$c10\{i \quad in \quad V\}: \quad 0 \leq s5[i] \quad complements \quad s4[i] \leq 0; \quad \text{(A.98)}$$
$$c11\{i \quad in \quad V\}: \quad s1[i] + s2[i] + s3[i] + s4[i] + s5[i] = 1; \quad \text{(A.99)}$$

$$torque\_mg2\{i \quad in \quad V\}: \quad Tmg2[i] = \frac{S_2}{(R_2 + S_2)}\Big( - \frac{(R_1 + S_1)}{S_1}T_{mg2[i]}z[i] + \frac{T_{req}[i]}{D_{GR}}\Big)s1[i] + \frac{T_{req}[i]}{D_{GR}}s2[i] +$$
$$-R_1\frac{S_2}{(R_2 + S_2)}\Big(\frac{T_{e[i]}}{R_1 + S_1}z[i] + \frac{T_{req}[i]}{D_{GR}}s3[i]\Big) + \frac{T_{req}[i]}{D_{GR}}s4[i] + \Big(\frac{T_{req}[i]}{D_{GR}} - T_{e[i]}z[i] - T_{mg1[i]}z[i]\Big)s5[i]; \quad \text{(A.100)}$$

$$torque\_mg1\{i \quad in \quad V\}: \quad Tmg1[i] = \frac{S_1}{(R_1 + S_1)}\Big( - \frac{(R_2 + S_2)}{S_2}T_{mg2}[i] + \frac{T_{req}[i]}{D_{GR}}\Big)s1[i] + \frac{S_1T_e[i]}{(R_1 + S_1)}s2[i] +$$
$$\Big(\frac{T_{req}[i]}{D_{GR}} - T_{e[i]}z[i] - T_{mg2[i]}z[i]\Big)s5[i]; \quad \text{(A.101)}$$

$$torque\_req\{i \quad in \quad V\}: \quad Treq[i] = mass \times acc[i] + mass \times g \times sin\theta + 0.5 \times rho_{air} \times c_d \times A_d \times \big(\frac{vel[i]}{3.6}\big)^2; \quad \text{(A.102)}$$

$$Z\_sign\{i \quad in \quad V\}: T_{req}[i](2z[i] - 1) = T_{req}[i]tanh\big(\frac{T_{req}[i]}{0.01}\big); \quad \text{(A.103)}$$

$$\omega\_mg2\{i \quad in \quad V\} : W_{mg2}[i] = \frac{Vel[i]Diff_{GR}}{3.6R_{eff}} \frac{(R_2 + S_2)}{S_2}; \tag{A.104}$$

$$\omega\_mg1\{i \quad in \quad V\} : W_{mg1}[i] = \frac{S_2}{S_1} W_{mg2}[i]s[1]z[i] + \frac{R_1 + S_1}{S_1} W_e s2[i]z[i]; \tag{A.105}$$

$$\omega\_e\{i \quad in \quad V\} : W_e[i] = \frac{R_1 + S_1}{S_1} W_{mg1} s2[i]z[i] + (\frac{R_2 + S_2}{R_2} W_{mg2} + \frac{R_1 + S_1}{S_1} W_{mg1}) s3[i]z[i] + (\frac{S_2}{R_2} W_{mg2} + \frac{R_1}{S_1} W_{mg1}) s5[i]z[i]; \tag{A.106}$$

$$\begin{aligned} Fuel\_flow\_rate\{i \quad in \quad V\} : Q[i] = & p00 + \\ & p10\omega_e[i] + p01T_e[i] + \\ & p20\omega_{e^2}[i] + p11\omega_e[i]T_e[i] + p02T_{e^2}[i] + \\ & p30\omega_{e^3}[i] + p21\omega_{e_k}[i]T_e[i] + p12\omega_e[i]T_{e^2}[i] + p03T_{e^3}[i] + \\ & p40\omega_{e^4}[i] + p31\omega_{e^3}[i]T_e[i] + p22\omega_{e^2}[i]T_{e^2}[i] + p13\omega_e[i]T_{e^3}[i] + p04T_{e^4}[i] + \\ & p50\omega_{e^5}[i] + p41\omega_{e^4}[i]T_e[i] + p32\omega_{e^3}[i]T_{e^2}[i] + \\ & \quad p23\omega_{e^2}[i]T_{e^3}[i] + p14\omega_e[i]T_{e^4}[i] + p05\omega_{e^5}[i]; \end{aligned} \tag{A.107}$$

$$Fuel\_eng\{i \quad in \quad V\} : M_{ice}[i] = \frac{Q[i]W_e[i]780}{120}; \tag{A.108}$$

$$\begin{aligned} Fuel\_eqv\{i \quad in \quad V\} : M_{eqv}[i] = max(0, & (\frac{T_{mg2}[i]W_{mg2}[i]}{emg2[i]}) \times 0.75 \times 0.00002381 \times \frac{1}{0.35} s4[i]z[i] + \\ & (\frac{T_{mg2}[i]W_{mg2}[i]}{emg2[i]} + \frac{T_{mg1}[i]W_{mg1}[i]}{emg1[i]}) \times 0.75 \times 0.00002381 \times \frac{1}{0.35} s1[i]z[i] + \\ & \frac{T_{mg2}[i]W_{mg2}[i]}{emg2[i]}) \times 0.75 \times 0.00002381 \times \frac{1}{0.35} s2[i]z[i] + \\ & \frac{T_{mg2}[i]W_{mg2}[i]}{emg2[i]}) \times 0.75 \times 0.00002381 \times \frac{1}{0.35} s3[i]z[i]) + \\ & (\frac{T_{mg2}[i]W_{mg2}[i]}{emg2[i]} + \frac{T_{mg1}[i]W_{mg1}[i]}{emg1[i]}) \times 0.75 \times 0.00002381 \times \frac{1}{0.35} s5[i]z[i]; \end{aligned} \tag{A.109}$$

$$Fuel\_total\{i \quad in \quad V\} : M_T[i] = M_{ice}[i] + M_{eqv}[i]; \tag{A.110}$$

$$eff\_mg2\{i \quad in \quad V\} : emg2[i] = abs(\frac{T_{mg2}[i]W_{mg2}[i])}{abs(T_{mg2}[i]W_{mg2}[i])}) + (abs\frac{T_{mg2}[i]}{0.45})^2 \times 0.75; \tag{A.111}$$

$$eff\_mg1\{i \quad in \quad V\} : emg1[i] = abs(\frac{T_{mg1}[i]W_{mg1}[i])}{abs(T_{mg1}[i]W_{mg1}[i])}) + (abs\frac{T_{mg1}[i]}{0.45})^2 \times 0.75; \tag{A.112}$$

$$eff\_bth\{i \quad in \quad V\} : ebth[i] = (\frac{3.14 \times T_e[i]}{780 \times Q[i] \times 46000 \times 2}) \times 10^6; \tag{A.113}$$

$$\begin{aligned} battery\_power\{i \quad in \quad V\} : Pbatt[i] = {} & \frac{T_{mg2}[i]W_{mg2}[i]}{e_{mg2}[i]}s4[i](1-z[i]) + \frac{T_{mg2}[i]W_{mg2}[i]}{e_{mg2}[i]}s4[i]z[i] + \\ & \frac{T_{mg2}[i]W_{mg2}[i]}{e_{mg2}[i]}s1[i]z[i] + \frac{T_{mg1}[i]W_{mg1}[i]}{e_{mg1}[i]}s1[i]z[i] + \frac{T_{mg2}[i]W_{mg2}[i]}{e_{mg2}[i]}s1[i](1-z[i]) + \\ & \frac{T_{mg2}[i]W_{mg2}[i]}{e_{mg2}[i]}s2[i](1-z[i]) + \frac{T_{mg2}[i]W_{mg2}[i]}{e_{mg2}[i]}s2[i]z[i] + \frac{T_{mg1}[i]W_{mg1}[i]}{e_{mg1}[i]}s2[i]z[i] + \\ & \frac{T_{mg1}[i]W_{mg1}[i]}{e_{mg1}[i]}s2[i](1-z[i]) + \frac{T_{mg2}[i]W_{mg2}[i]}{e_{mg2}[i]}s3[i](1-z[i]) + \frac{T_{mg2}[i]W_{mg2}[i]}{e_{mg2}[i]}s3[i]z[i] + \\ & \frac{T_{mg2}[i]W_{mg2}[i]}{e_{mg2}[i]}s1[i]z[i] + \frac{T_{mg1}[i]W_{mg1}[i]}{e_{mg1}[i]}s1[i]z[i] + \frac{T_{mg2}[i]W_{mg2}[i]}{e_{mg2}[i]}s5[i](1-z[i]); \end{aligned} \tag{A.114}$$

$$SoC\_ode\{i \quad in \quad V \quad diff\{V\}\} : SOC[i+1] = SOC[i] - \frac{Pbatt[i]}{27000 \times 3600}; \tag{A.115}$$

$$acc\_eq\{i \quad in \quad V \quad diff\{1\}\} : acc[i] = \frac{vel[i] - vel[i-1]}{3.6}; \tag{A.116}$$

$$SOC\_init : SOC[1] = 0.80; \tag{A.117}$$
$$acc\_init : acc[1] = 0; \tag{A.118}$$
$$Shift1\_init : M_{shift}[1] = 0; \tag{A.119}$$
$$delta\_init : delta[1] = 0; \tag{A.120}$$
$$mode1\_init : s1[1] = 1; \tag{A.121}$$
$$mode2\_init : s2[1] = 0; \tag{A.122}$$
$$mode3\_init : s3[1] = 0; \tag{A.123}$$
$$mode4\_init : s4[1] = 0; \tag{A.124}$$
$$mode5\_init : s5[1] = 0; \tag{A.125}$$
$$mode6\_init : s6[1] = 0; \tag{A.126}$$
$$mode7\_init : s7[1] = 0; \tag{A.127}$$
$$mode8\_init : s8[1] = 0; \tag{A.128}$$
$$constraint\_enginetorque\{i \quad in \quad V\} : T_e[i] = \frac{Teng[i]floor(W_e[i])}{W_e[i] + 10^{-6}}; \tag{A.129}$$
$$constraint\_enginespeed\{i \quad in \quad V\} : W_e[i] \geq 75 \times s2[i] + 75 \times s3[i] + 75 \times s5[i]; \tag{A.130}$$

$$\begin{aligned} delta\_shift\{i \quad in \quad V \quad diff\{1\}\} : delta[i] = abs(s1[i] - s1[i-1]) + \\ abs(s2[i] - s2[i-1]) + abs(s3[i] - s3[i-1]) + abs(s4[i] - s4[i-1]) + \\ + abs(s5[i] - s5[i-1]); \end{aligned} \tag{A.131}$$

$$\begin{aligned} Mode\_shift\{i \quad in \quad V \quad diff\{1\}\} : M_{shift}[i] = delta[i] \times alpha \times 0.5 \\ (I_e(W_e[i] - W_e[i-1])^2 + I_{mg1}(W_{mg1}[i] - W_{mg1}[i-1])^2); \end{aligned} \tag{A.132}$$

$$motor2\{i \quad in \quad V\} : T_{mg2}[i]W_{mg2}[i] \leq 60000; \tag{A.133}$$
$$motor1\{i \quad in \quad V\} : T_{mg1}[i]W_{mg1}[i] \leq 42000; \tag{A.134}$$
$$\tag{A.135}$$

$$\begin{aligned} engine1\{i \quad in \quad V\} : T_e[i] \leq max(0, (-3.002 \times 10^{(-14)} \times W_e[i]^6 + \\ + 6.96 \times 10^{(-11)} \times W_e[i]^5 - 5.712 \times 10^{(-08)} \times W_e[i]^4 + \\ 1.885 \times 10^{(-05)} \times W_e[i]^3 - 0.001907 \times W_e[i]^2 + 0.05586 \times W_e[i] + 91.09; \end{aligned} \tag{A.136}$$

### A.0.8 Model of 3PG-1

Objective function:

Minimise fuel:

$$sum\{i \quad in \quad V\}\frac{0.5 \times MT[i]}{190} + 0.1 \times M\_shift[i]/1 + 0.4 \times (0.8 - soc[i])^2); \quad \text{(A.137)}$$

Constraint equations:

$$c1\{i \quad in \quad V\}: \quad 0 \leq s4[i] \quad complements \quad s1[i] \leq 0; \quad \text{(A.138)}$$
$$c2\{i \quad in \quad V\}: \quad 0 \leq s4[i] \quad complements \quad s2[i] \leq 0; \quad \text{(A.139)}$$
$$c3\{i \quad in \quad V\}: \quad 0 \leq s4[i] \quad complements \quad s3[i] \leq 0; \quad \text{(A.140)}$$
$$c4\{i \quad in \quad V\}: \quad 0 \leq s3[i] \quad complements \quad s1[i] \leq 0; \quad \text{(A.141)}$$
$$c5\{i \quad in \quad V\}: \quad 0 \leq s3[i] \quad complements \quad s2[i] \leq 0; \quad \text{(A.142)}$$
$$c6\{i \quad in \quad V\}: \quad 0 \leq s2[i] \quad complements \quad s1[i] \leq 0; \quad \text{(A.143)}$$
$$c8\{i \quad in \quad V\}: \quad 0 \leq s5[i] \quad complements \quad s2[i] \leq 0; \quad \text{(A.144)}$$
$$c9\{i \quad in \quad V\}: \quad 0 \leq s5[i] \quad complements \quad s3[i] \leq 0; \quad \text{(A.145)}$$
$$c10\{i \quad in \quad V\}: \quad 0 \leq s5[i] \quad complements \quad s4[i] \leq 0; \quad \text{(A.146)}$$
$$c11\{i \quad in \quad V\}: \quad 0 \leq s5[i] \quad complements \quad s6[i] \leq 0; \quad \text{(A.147)}$$
$$c12\{i \quad in \quad V\}: \quad 0 \leq s5[i] \quad complements \quad s7[i] \leq 0; \quad \text{(A.148)}$$
$$c13\{i \quad in \quad V\}: \quad 0 \leq s5[i] \quad complements \quad s8[i] \leq 0; \quad \text{(A.149)}$$
$$c14\{i \quad in \quad V\}: \quad 0 \leq s1[i] \quad complements \quad s6[i] \leq 0; \quad \text{(A.150)}$$
$$c15\{i \quad in \quad V\}: \quad 0 \leq s1[i] \quad complements \quad s7[i] \leq 0; \quad \text{(A.151)}$$
$$c16\{i \quad in \quad V\}: \quad 0 \leq s1[i] \quad complements \quad s8[i] \leq 0; \quad \text{(A.152)}$$
$$. \quad \text{(A.153)}$$
$$. \quad \text{(A.154)}$$
$$. \quad \text{(A.155)}$$
$$c29\{i \quad in \quad V\}: \quad s1[i] + s2[i] + s3[i] + s4[i] + s5[i] + s6[i] + s7[i] + s8[i] = 1; \quad \text{(A.156)}$$

$$torque\_mg2\{i \quad in \quad V\}: \quad Tmg2[i] = \frac{S_3}{(R_3 + S_3)}\Big( - \frac{R_2}{S_2}T_{mg1[i]}z[i] + \frac{T_{req}[i]}{D_{GR}}\Big)s1[i] + \frac{T_{req}[i]}{D_{GR}}s2[i] +$$
$$\Big(\frac{-T_{e[i]}}{z}[i] + \frac{T_{req}[i]}{D_{GR}}\frac{S_3}{(R_3 + S_3)}s3[i]\Big) + \frac{T_{req}[i]}{D_{GR}}s4[i] +$$
$$\Big( - T_e[i]z[i] - T_{mg1}[i]z[i] + \frac{T_{req}[i]}{D_{GR}}\Big)s5[i] +$$
$$\Big( - T_e[i]z[i] - T_{mg1}[i]z[i] + \frac{T_{req}[i]}{D_{GR}}\Big)s6[i] +$$
$$\Big( - T_e[i]z[i] - T_{mg1}[i]z[i] + \frac{T_{req}[i]}{D_{GR}}\Big)s9[i]; \quad \text{(A.157)}$$

$$torque\_mg1\{i \quad in \quad V\}: \quad Tmg1[i] = \frac{S_1}{R_1}\Big(T_{mg2}[i] + \frac{T_{req}[i]}{D_{GR}}\Big)s1[i] + \frac{S_1 T_e[i]}{(R_1+S_1)}s2[i]; \tag{A.158}$$

$$\begin{aligned} torque\_req\{i \quad in \quad V\}: \quad Treq[i] = mass \times acc[i] + mass \times g \times sin\theta + \\ 0.5 \times rho_{air} \times c_d \times A_d \times \big(\frac{vel[i]}{3.6}\big)^2; \end{aligned} \tag{A.159}$$

$$Z\_sign\{i \quad in \quad V\}: T_{req}[i](2z[i]-1) = T_{req}[i]tanh\big(\frac{T_{req}[i]}{0.01}\big); \tag{A.160}$$

$$\omega\_mg2\{i \quad in \quad V\}: W_{mg2}[i] = \frac{Vel[i]Diff_{GR}}{3.6R_{eff}}; \tag{A.161}$$

$$\begin{aligned} \omega\_mg1\{i \quad in \quad V\}: W_{mg1}[i] = \frac{R_1}{S_1} - W_{mg2}[i]s[1]z[i] + \frac{R_1+S_1}{S_1}W_e s2[i]z[i] + \\ \frac{R_1+S_1}{S_1}\big(W_e[i] - \frac{R_1 W_{mg2}[i]}{R_1+S_1}\big)s3[i]z[i]; \end{aligned} \tag{A.162}$$

$$\omega\_e\{i \quad in \quad V\}: W_e[i] = \frac{R_1+S_1}{S_1}W_{mg1}s2[i]z[i] + (\frac{R_1+S_1}{R_1}W_{mg2} + \frac{R_1+S_1}{S_1}W_{mg1}z[i])s3[i]; \tag{A.163}$$

$$\begin{aligned} Fuel\_flow\_rate\{i \quad in \quad V\}: Q[i] = & p00 + \\ & p10\omega_e[i] + p01T_e[i] + \\ & p20\omega_{e^2}[i] + p11\omega_e[i]T_e[i] + p02T_{e^2}[i] + \\ & p30\omega_{e^3}[i] + p21\omega_{e_k}[i]T_e[i] + p12\omega_e[i]T_{e^2}[i] + p03T_{e^3}[i] + \\ & p40\omega_{e^4}[i] + p31\omega_{e^3}[i]T_e[i] + p22\omega_{e^2}[i]T_{e^2}[i] + p13\omega_e[i]T_{e^3}[i] + p04T_{e^4}[i] + \\ & p50\omega_{e^5}[i] + p41\omega_{e^4}[i]T_e[i] + p32\omega_{e^3}[i]T_{e^2}[i] + \\ & \quad p23\omega_{e^2}[i]T_{e^3}[i] + p14\omega_e[i]T_{e^4}[i] + p05\omega_{e^5}[i]; \end{aligned} \tag{A.164}$$

$$Fuel\_eng\{i \quad in \quad V\}: M_{ice}[i] = \frac{Q[i]W_e[i]780}{120}; \tag{A.165}$$

$$
\begin{aligned}
Fuel\_eqv\{i \quad in \quad V\} : M_{eqv}[i] = max(0, (\frac{T_{mg2}[i]W_{mg2}[i]}{emg2[i]}) \times 0.75 \times 0.00002381 \times \frac{1}{0.35} s4[i]z[i] + \\
(\frac{T_{mg2}[i]W_{mg2}[i]}{emg2[i]} + \frac{T_{mg1}[i]W_{mg1}[i]}{emg1[i]}) \times 0.75 \times 0.00002381 \times \frac{1}{0.35} s1[i]z[i] + \\
\frac{T_{mg2}[i]W_{mg2}[i]}{emg2[i]}) \times 0.75 \times 0.00002381 \times \frac{1}{0.35} s2[i]z[i] + \\
\frac{T_{mg2}[i]W_{mg2}[i]}{emg2[i]}) \times 0.75 \times 0.00002381 \times \frac{1}{0.35} s3[i]z[i]);
\end{aligned}
\tag{A.166}
$$

$$Fuel\_total\{i \quad in \quad V\} : M_T[i] = M_{ice}[i] + M_{eqv}[i]; \tag{A.167}$$

$$eff\_mg2\{i \quad in \quad V\} : emg2[i] = abs(\frac{T_{mg2}[i]W_{mg2}[i])}{abs(T_{mg2}[i]W_{mg2}[i])}) + (abs\frac{T_{mg2}[i]}{0.45})^2 \times 0.75; \tag{A.168}$$

$$eff\_mg1\{i \quad in \quad V\} : emg1[i] = abs(\frac{T_{mg1}[i]W_{mg1}[i])}{abs(T_{mg1}[i]W_{mg1}[i])}) + (abs\frac{T_{mg1}[i]}{0.45})^2 \times 0.75; \tag{A.169}$$

$$eff\_bth\{i \quad in \quad V\} : ebth[i] = (\frac{3.14 \times T_e[i]}{780 \times Q[i] \times 46000 \times 2}) \times 10^6; \tag{A.170}$$

$$\begin{aligned} battery\_power\{i \quad in \quad V\} : Pbatt[i] = {} & \frac{T_{mg2}[i]W_{mg2}[i]}{e_{mg2}[i]}s4[i](1 - z[i]) + \frac{T_{mg2}[i]W_{mg2}[i]}{e_{mg2}[i]}s4[i]z[i] + \\ & \frac{T_{mg2}[i]W_{mg2}[i]}{e_{mg2}[i]}s1[i]z[i] + \frac{T_{mg1}[i]W_{mg1}[i]}{e_{mg1}[i]}s1[i]z[i] + \frac{T_{mg2}[i]W_{mg2}[i]}{e_{mg2}[i]}s1[i](1 - z[i]) + \\ & \frac{T_{mg2}[i]W_{mg2}[i]}{e_{mg2}[i]}s2[i](1 - z[i]) + \frac{T_{mg2}[i]W_{mg2}[i]}{e_{mg2}[i]}s2[i]z[i] + \frac{T_{mg1}[i]W_{mg1}[i]}{e_{mg1}[i]}s2[i]z[i] + \\ & \frac{T_{mg1}[i]W_{mg1}[i]}{e_{mg1}[i]}s2[i](1 - z[i]) + \frac{T_{mg2}[i]W_{mg2}[i]}{e_{mg2}[i]}s3[i](1 - z[i]) + \frac{T_{mg2}[i]W_{mg2}[i]}{e_{mg2}[i]}s3[i]z[i]; \end{aligned} \tag{A.171}$$

$$SoC\_ode\{i \quad in \quad V \quad diff\{V\}\} : SOC[i+1] = SOC[i] - \frac{Pbatt[i]}{27000 \times 3600}; \tag{A.172}$$

$$acc\_eq\{i \quad in \quad V \quad diff\{1\}\} : acc[i] = \frac{vel[i] - vel[i-1]}{3.6}; \tag{A.173}$$

$$SOC\_init : SOC[1] = 0.80; \tag{A.174}$$
$$acc\_init : acc[1] = 0; \tag{A.175}$$
$$Shift1\_init : M_{shift}[1] = 0; \tag{A.176}$$
$$delta\_init : delta[1] = 0; \tag{A.177}$$
$$mode1\_init : s1[1] = 1; \tag{A.178}$$
$$mode2\_init : s2[1] = 0; \tag{A.179}$$
$$mode3\_init : s3[1] = 0; \tag{A.180}$$
$$mode4\_init : s4[1] = 0; \tag{A.181}$$
$$mode5\_init : s5[1] = 0; \tag{A.182}$$
$$mode6\_init : s6[1] = 0; \tag{A.183}$$
$$mode7\_init : s7[1] = 0; \tag{A.184}$$
$$mode8\_init : s8[1] = 0; \tag{A.185}$$
$$mode9\_init : s9[1] = 0; \tag{A.186}$$
$$constraint\_enginetorque\{i \quad in \quad V\} : T_e[i] = \frac{Teng[i]floor(W_e[i])}{W_e[i] + 10^{-6}}; \tag{A.187}$$
$$constraint\_enginespeed\{i \quad in \quad V\} : W_e[i] \geq 75 \times s2[i] + 75 \times s3[i]; \tag{A.188}$$

$$\begin{aligned} delta\_shift\{i \quad in \quad V \quad diff\{1\}\} : delta[i] = abs(s1[i] - s1[i-1]) + \\ abs(s2[i] - s2[i-1]) + abs(s3[i] - s3[i-1]) + abs(s4[i] - s4[i-1]); \end{aligned} \tag{A.189}$$

$$\begin{aligned} Mode\_shift\{i \quad in \quad V \quad diff\{1\}\} : M_{shift}[i] = delta[i] \times alpha \times 0.5 \\ (I_e(W_e[i] - W_e[i-1])^2 + I_{mg1}(W_{mg1}[i] - W_{mg1}[i-1])^2); \end{aligned} \tag{A.190}$$

$$motor2\{i \quad in \quad V\} : T_{mg2}[i]W_{mg2}[i] \leq 60000; \tag{A.191}$$
$$motor1\{i \quad in \quad V\} : T_{mg1}[i]W_{mg1}[i] \leq 42000; \tag{A.192}$$
$$\tag{A.193}$$

$$\begin{aligned} engine1\{i \quad in \quad V\} : T_e[i] \leq max(0, (-3.002 \times 10^{(-14)} \times W_e[i]^6 + \\ +6.96 \times 10^{(-11)} \times W_e[i]^5 - 5.712 \times 10^{(-08)} \times W_e[i]^4 + \\ 1.885 \times 10^{(-05)} \times W_e[i]^3 - 0.001907 \times W_e[i]^2 + 0.05586 \times W_e[i] + 91.09; \end{aligned} \tag{A.194}$$

### A.0.9 Model of 3PG-2

Objective function:

Minimise fuel:

$$sum\{i \quad in \quad V\}\frac{0.5 \times MT[i]}{190} + 0.1 \times M\_shift[i]/1 + 0.4 \times (0.8 - soc[i])^2); \quad \text{(A.195)}$$

Constraint equations:

$$c1\{i \quad in \quad V\}: \quad 0 \leq s4[i] \quad complements \quad s1[i] \leq 0; \quad \text{(A.196)}$$
$$c2\{i \quad in \quad V\}: \quad 0 \leq s4[i] \quad complements \quad s2[i] \leq 0; \quad \text{(A.197)}$$
$$c3\{i \quad in \quad V\}: \quad 0 \leq s4[i] \quad complements \quad s3[i] \leq 0; \quad \text{(A.198)}$$
$$c4\{i \quad in \quad V\}: \quad 0 \leq s3[i] \quad complements \quad s1[i] \leq 0; \quad \text{(A.199)}$$
$$c5\{i \quad in \quad V\}: \quad 0 \leq s3[i] \quad complements \quad s2[i] \leq 0; \quad \text{(A.200)}$$
$$c6\{i \quad in \quad V\}: \quad 0 \leq s2[i] \quad complements \quad s1[i] \leq 0; \quad \text{(A.201)}$$
$$c8\{i \quad in \quad V\}: \quad 0 \leq s5[i] \quad complements \quad s2[i] \leq 0; \quad \text{(A.202)}$$
$$c9\{i \quad in \quad V\}: \quad 0 \leq s5[i] \quad complements \quad s3[i] \leq 0; \quad \text{(A.203)}$$
$$c10\{i \quad in \quad V\}: \quad 0 \leq s5[i] \quad complements \quad s4[i] \leq 0; \quad \text{(A.204)}$$
$$c11\{i \quad in \quad V\}: \quad 0 \leq s5[i] \quad complements \quad s6[i] \leq 0; \quad \text{(A.205)}$$
$$c12\{i \quad in \quad V\}: \quad 0 \leq s5[i] \quad complements \quad s7[i] \leq 0; \quad \text{(A.206)}$$
$$c13\{i \quad in \quad V\}: \quad 0 \leq s5[i] \quad complements \quad s8[i] \leq 0; \quad \text{(A.207)}$$
$$c14\{i \quad in \quad V\}: \quad 0 \leq s1[i] \quad complements \quad s6[i] \leq 0; \quad \text{(A.208)}$$
$$c15\{i \quad in \quad V\}: \quad 0 \leq s1[i] \quad complements \quad s7[i] \leq 0; \quad \text{(A.209)}$$
$$c16\{i \quad in \quad V\}: \quad 0 \leq s1[i] \quad complements \quad s8[i] \leq 0; \quad \text{(A.210)}$$
$$c17\{i \quad in \quad V\}: \quad 0 \leq s1[i] \quad complements \quad s9[i] \leq 0; \quad \text{(A.211)}$$
$$c18\{i \quad in \quad V\}: \quad 0 \leq s2[i] \quad complements \quad s9[i] \leq 0; \quad \text{(A.212)}$$
$$. \quad \text{(A.213)}$$
$$. \quad \text{(A.214)}$$
$$. \quad \text{(A.215)}$$
$$c29\{i \quad in \quad V\}: \quad s1[i] + s2[i] + s3[i] + s4[i] + s5[i] + s6[i] + s7[i] + s8[i] + s9[i] = 1; \quad \text{(A.216)}$$

$$torque\_mg2\{i \quad in \quad V\}: \quad Tmg2[i] = \frac{S_1}{R_1}\Big( - \frac{R_2}{S_2}T_{mg2[i]}z[i] + \frac{T_{req}[i]}{D_{GR}}\Big)s1[i] + \frac{T_{req}[i]}{D_{GR}}s2[i] + \\ -R_1\Big(\frac{T_{e[i]}}{R_1+S_1}z[i] + \frac{T_{req}[i]}{D_{GR}}s3[i]\Big) + \frac{T_{req}[i]}{D_{GR}}s4[i] + \\ \Big( - T_e[i]z[i] - T_{mg1}[i]z[i] + \frac{T_{req}[i]}{D_{GR}}\Big)s5[i] + \\ \Big( - T_e[i]z[i] - T_{mg1}[i]z[i] + \frac{T_{req}[i]}{D_{GR}}\Big)s7[i] + \\ \Big( - T_e[i]z[i] - T_{mg1}[i]z[i] + \frac{T_{req}[i]}{D_{GR}}\Big)s9[i]; \tag{A.217}$$

$$torque\_mg1\{i \quad in \quad V\}: \quad Tmg1[i] = \frac{S_1}{R_1}\Big(T_{mg2}[i] + \frac{T_{req}[i]}{D_{GR}}\Big)s1[i] + \frac{S_1T_e[i]}{(R_1+S_1)}s2[i]; \tag{A.218}$$

$$torque\_req\{i \quad in \quad V\}: \quad Treq[i] = mass \times acc[i] + mass \times g \times sin\theta + \\ 0.5 \times rho_{air} \times c_d \times A_d \times \big(\frac{vel[i]}{3.6}\big)^2; \tag{A.219}$$

$$Z\_sign\{i \quad in \quad V\}: T_{req}[i](2z[i]-1) = T_{req}[i]tanh\big(\frac{T_{req}[i]}{0.01}\big); \tag{A.220}$$

$$\omega\_mg2\{i \quad in \quad V\}: W_{mg2}[i] = \frac{Vel[i]Diff_{GR}}{3.6R_{eff}}; \tag{A.221}$$

$$\omega\_mg1\{i \quad in \quad V\}: W_{mg1}[i] = \frac{R_1}{S_1} - W_{mg2}[i]s[1]z[i] + \frac{R_1+S_1}{S_1}W_e s2[i]z[i] + \\ \frac{R_1+S_1}{S_1}\big(W_e[i] - \frac{R_1W_{mg2}[i]}{R_1+S_1}\big)s3[i]z[i]; \tag{A.222}$$

$$\omega\_e\{i \quad in \quad V\}: W_e[i] = \frac{R_1+S_1}{S_1}W_{mg1}s2[i]z[i] + (\frac{R_1+S_1}{R_1}W_{mg2} + \frac{R_1+S_1}{S_1}W_{mg1}z[i])s3[i]; \tag{A.223}$$

$$\begin{aligned}Fuel\_flow\_rate\{i \quad in \quad V\} : Q[i] = & p00+ \\ & p10\omega_e[i] + p01T_e[i]+ \\ & p20\omega_{e^2}[i] + p11\omega_e[i]T_e[i] + p02T_{e^2}[i]+ \\ & p30\omega_{e^3}[i] + p21\omega_{e_k}[i]T_e[i] + p12\omega_e[i]T_{e^2}[i] + p03T_{e^3}[i]+ \\ & p40\omega_{e^4}[i] + p31\omega_{e^3}[i]T_e[i] + p22\omega_{e^2}[i]T_{e^2}[i] + p13\omega_e[i]T_{e^3}[i] + p04T_{e^4}[i]+ \\ & p50\omega_{e^5}[i] + p41\omega_{e^4}[i]T_e[i] + p32\omega_{e^3}[i]T_{e^2}[i]+ \\ & \quad p23\omega_{e^2}[i]T_{e^3}[i] + p14\omega_e[i]T_{e^4}[i] + p05\omega_{e^5}[i];\end{aligned} \tag{A.224}$$

$$Fuel\_eng\{i \quad in \quad V\} : M_{ice}[i] = \frac{Q[i]W_e[i]780}{120}; \tag{A.225}$$

$$\begin{aligned}Fuel\_eqv\{i \quad in \quad V\} : M_{eqv}[i] = max(0, ( & \frac{T_{mg2}[i]W_{mg2}[i]}{emg2[i]}) \times 0.75 \times 0.00002381 \times \frac{1}{0.35}s4[i]z[i]+ \\ ( & \frac{T_{mg2}[i]W_{mg2}[i]}{emg2[i]} + \frac{T_{mg1}[i]W_{mg1}[i]}{emg1[i]}) \times 0.75 \times 0.00002381 \times \frac{1}{0.35}s1[i]z[i]+ \\ & \frac{T_{mg2}[i]W_{mg2}[i]}{emg2[i]}) \times 0.75 \times 0.00002381 \times \frac{1}{0.35}s2[i]z[i]+ \\ & \frac{T_{mg2}[i]W_{mg2}[i]}{emg2[i]}) \times 0.75 \times 0.00002381 \times \frac{1}{0.35}s3[i]z[i]);\end{aligned} \tag{A.226}$$

$$Fuel\_total\{i \quad in \quad V\} : M_T[i] = M_{ice}[i] + M_{eqv}[i]; \tag{A.227}$$

$$eff\_mg2\{i \quad in \quad V\} : emg2[i] = abs(\frac{T_{mg2}[i]W_{mg2}[i])}{abs(T_{mg2}[i]W_{mg2}[i])}) + (abs\frac{T_{mg2}[i]}{0.45})^2 \times 0.75; \tag{A.228}$$

$$eff\_mg1\{i \quad in \quad V\} : emg1[i] = abs(\frac{T_{mg1}[i]W_{mg1}[i])}{abs(T_{mg1}[i]W_{mg1}[i])}) + (abs\frac{T_{mg1}[i]}{0.45})^2 \times 0.75; \tag{A.229}$$

$$eff\_bth\{i \quad in \quad V\} : ebth[i] = (\frac{3.14 \times T_e[i]}{780 \times Q[i] \times 46000 \times 2}) \times 10^6; \tag{A.230}$$

$$\begin{aligned} battery\_power\{i \quad in \quad V\} : Pbatt[i] = {} & \frac{T_{mg2}[i]W_{mg2}[i]}{e_{mg2}[i]}s4[i](1-z[i]) + \frac{T_{mg2}[i]W_{mg2}[i]}{e_{mg2}[i]}s4[i]z[i] + \\ & \frac{T_{mg2}[i]W_{mg2}[i]}{e_{mg2}[i]}s1[i]z[i] + \frac{T_{mg1}[i]W_{mg1}[i]}{e_{mg1}[i]}s1[i]z[i] + \frac{T_{mg2}[i]W_{mg2}[i]}{e_{mg2}[i]}s1[i](1-z[i]) + \\ & \frac{T_{mg2}[i]W_{mg2}[i]}{e_{mg2}[i]}s2[i](1-z[i]) + \frac{T_{mg2}[i]W_{mg2}[i]}{e_{mg2}[i]}s2[i]z[i] + \frac{T_{mg1}[i]W_{mg1}[i]}{e_{mg1}[i]}s2[i]z[i] + \\ & \frac{T_{mg1}[i]W_{mg1}[i]}{e_{mg1}[i]}s2[i](1-z[i]) + \frac{T_{mg2}[i]W_{mg2}[i]}{e_{mg2}[i]}s3[i](1-z[i]) + \frac{T_{mg2}[i]W_{mg2}[i]}{e_{mg2}[i]}s3[i]z[i]; \end{aligned} \tag{A.231}$$

$$SoC\_ode\{i \quad in \quad V \quad diff\{V\}\} : SOC[i+1] = SOC[i] - \frac{Pbatt[i]}{27000 \times 3600}; \tag{A.232}$$

$$acc\_eq\{i \quad in \quad V \quad diff\{1\}\} : acc[i] = \frac{vel[i] - vel[i-1]}{3.6}; \tag{A.233}$$

$$SOC\_init : SOC[1] = 0.80; \tag{A.234}$$
$$acc\_init : acc[1] = 0; \tag{A.235}$$
$$Shift1\_init : M_{shift}[1] = 0; \tag{A.236}$$
$$delta\_init : delta[1] = 0; \tag{A.237}$$
$$mode1\_init : s1[1] = 1; \tag{A.238}$$
$$mode2\_init : s2[1] = 0; \tag{A.239}$$
$$mode3\_init : s3[1] = 0; \tag{A.240}$$
$$mode5\_init : s5[1] = 0; \tag{A.241}$$
$$mode6\_init : s6[1] = 0; \tag{A.242}$$
$$mode7\_init : s7[1] = 0; \tag{A.243}$$
$$mode9\_init : s9[1] = 0; \tag{A.244}$$
$$constraint\_enginetorque\{i \quad in \quad V\} : T_e[i] = \frac{Teng[i]floor(W_e[i])}{W_e[i] + 10^{-6}}; \tag{A.245}$$
$$constraint\_enginespeed\{i \quad in \quad V\} : W_e[i] \geq 75 \times s2[i] + 75 \times s3[i] + 75 \times s5[i] + +75 \times s6[i] + +75 \times \tag{A.246}$$

$$\begin{aligned} delta\_shift\{i \quad in \quad V \quad diff\{1\}\} : delta[i] = abs(s1[i] - s1[i-1]) + \\ abs(s2[i] - s2[i-1]) + abs(s3[i] - s3[i-1]) + abs(s4[i] - s4[i-1]); \end{aligned} \tag{A.247}$$

$$\begin{aligned} Mode\_shift\{i \quad in \quad V \quad diff\{1\}\} : M_{shift}[i] = delta[i] \times alpha \times 0.5 \\ (I_e(W_e[i] - W_e[i-1])^2 + I_{mg1}(W_{mg1}[i] - W_{mg1}[i-1])^2); \end{aligned} \tag{A.248}$$

$$motor2\{i \quad in \quad V\} : T_{mg2}[i]W_{mg2}[i] \leq 60000; \tag{A.249}$$
$$motor1\{i \quad in \quad V\} : T_{mg1}[i]W_{mg1}[i] \leq 42000; \tag{A.250}$$
$$\tag{A.251}$$

$$\begin{aligned} engine1\{i \quad in \quad V\} : T_e[i] \leq max(0, (-3.002 \times 10^{(-14)} \times W_e[i]^6 + \\ +6.96 \times 10^{(-11)} \times W_e[i]^5 - 5.712 \times 10^{(-08)} \times W_e[i]^4 + \\ 1.885 \times 10^{(-05)} \times W_e[i]^3 - 0.001907 \times W_e[i]^2 + 0.05586 \times W_e[i] + 91.09; \end{aligned} \tag{A.252}$$

# Appendix B

# Look up tables

### B.0.1 1PG-1 topology

| Time | Velocity | WMG1 | TMG2 | TE | Mode |
|---|---|---|---|---|---|
| 1 | 0 | 0 | 0 | 0 | 4 |
| 2 | 0 | 0 | 0 | 0 | 4 |
| 3 | 0 | 0 | 0 | 0 | 4 |
| . | | | | | |
| . | | | | | |
| 12 | 22.3699 | -2.92895 | 107.168 | 81.2419 | 3 |
| 13 | 32.9916 | -2.87851 | 72.4122 | 81.688 | 3 |
| 14 | 41.3601 | -4.26484 | 87.3887 | 43.9901 | 3 |
| . | | | | | |
| . | | | | | |
| 594 | 3.54056 | -1.5E-22 | -78.5304 | 0 | 4 |
| 595 | 0 | -5.2E-21 | -40.0509 | 0 | 4 |
| 596 | 0 | 0 | 0 | 0 | 4 |
| 597 | 0 | 0 | 0 | 0 | 4 |
| 598 | 0 | 0 | 0 | 0 | 4 |
| 599 | 0 | 0 | 0 | 0 | 4 |
| 600 | 0 | 0 | 0 | 0 | 4 |

### B.0.2 2PG-1 topology

| Time | Velocity | WMG1 | TMG2 | TE | Mode |
|---|---|---|---|---|---|
| 1 | 0 | 0 | 0 | 0 | 4 |
| 2 | 0 | 0 | 0 | 0 | 4 |
| 3 | 0 | 0 | 0 | 0 | 4 |
| . | | | | | |
| . | | | | | |
| 8 | 1.12654 | 0 | 21.96257 | 0 | 4 |
| 9 | 1.77028 | 0 | 15.3694 | 0 | 4 |
| 10 | 2.73588 | 0 | 19.78111 | 0 | 4 |
| 11 | 9.65606 | -81.2312 | 48.8033 | 0 | 1 |
| 12 | 22.3699 | -188.186 | 87.7856 | 0 | 1 |
| 13 | 32.9916 | 1.10646 | 123.669 | 88.137 | 3 |
| 14 | 41.3601 | 1.63934 | 100.387 | 68.1747 | 3 |
| . | | | | | |
| . | | | | | |
| 594 | 3.54056 | 0 | -77.0291 | 0 | 4 |
| 595 | 0 | 0 | -36.673 | 0 | 4 |
| 596 | 0 | 0 | 0 | 0 | 4 |
| 597 | 0 | 0 | 0 | 0 | 4 |
| 598 | 0 | 0 | 0 | 0 | 4 |
| 599 | 0 | 0 | 0 | 0 | 4 |
| 600 | 0 | 0 | 0 | 0 | 4 |

### B.0.3 2PG-2 topology

| Time | Velocity | WMG1 | TMG2 | TE | Mode |
|---|---|---|---|---|---|
| 1 | 0 | 0 | 0 | 0 | 1 |
| 2 | 0 | 0 | 0 | 0 | 1 |
| 3 | 0 | 0 | 0 | 0 | 1 |
| . | | | | | |
| . | | | | | |
| 8 | 1.12654 | 11.0233 | 9.09009 | 0 | 1 |
| 9 | 1.77028 | -2.5E-25 | 13.1569 | 0 | 4 |
| 10 | 2.73588 | 0 | 16.8868 | 0 | 4 |
| 11 | 9.65606 | 0 | 84.7364 | 0 | 4 |
| 12 | 22.3699 | 0 | 150.969 | 0 | 4 |
| 13 | 32.9916 | 1.56E-21 | 91.5969 | 70.9251 | 2 |
| 14 | 41.3601 | 1.75E-21 | 66.5525 | 71.0428 | 2 |
| . | | | | | |
| . | | | | | |
| 594 | 3.54056 | 0 | -67.1625 | 0 | 4 |
| 595 | 0 | 0 | -34.2532 | 0 | 4 |
| 596 | 0 | 0 | 0 | 0 | 4 |
| 597 | 0 | 0 | 0 | 0 | 4 |
| 598 | 0 | 0 | 0 | 0 | 4 |
| 599 | 0 | 0 | 0 | 0 | 4 |
| 600 | 0 | 0 | 0 | 0 | 4 |

### B.0.4 3PG-1 topology

| Time | Velocity | WMG1 | TMG2 | TE | Mode |
|---|---|---|---|---|---|
| 1 | 0 | 3.52E-52 | 0 | 5.73E-22 | 4 |
| 2 | 0 | 3.52E-52 | 0 | 5.73E-22 | 4 |
| 3 | 0 | 3.52E-52 | 0 | 5.73E-22 | 4 |
| . | | | | | |
| . | | | | | |
| 8 | 1.12654 | 0 | 13.9453 | 0 | 4 |
| 9 | 1.77028 | 0 | 11.5162 | 0 | 4 |
| 10 | 2.73588 | 0 | 15.9822 | 0 | 4 |
| 11 | 9.65606 | 0 | 84.2666 | 0 | 4 |
| 12 | 22.3699 | 0 | 153.002 | 0 | 4 |
| 13 | 32.9916 | 205.3 | 75.0593 | 45.2546 | 5 |
| 14 | 41.3601 | 262.674 | 76.246 | 34.8528 | 5 |
| . | | | | | |
| . | | | | | |
| 594 | 3.54056 | 0 | -68.8863 | 0 | 4 |
| 595 | 0 | 0 | -35.1324 | 0 | 4 |
| 596 | 0 | 0 | 0 | 0 | 4 |
| 597 | 0 | 0 | 0 | 0 | 4 |
| 598 | 0 | 0 | 0 | 0 | 4 |
| 599 | 0 | 0 | 0 | 0 | 4 |
| 600 | 0 | 0 | 0 | 0 | 4 |

### B.0.5 3PG-2 topology

| Time | Velocity | WMG1 | TMG2 | TE | Mode |
|---|---|---|---|---|---|
| 1 | 0 | 3.52E-52 | 0 | 5.73E-22 | 1 |
| 2 | 0 | 3.52E-52 | 0 | 5.73E-22 | 1 |
| 3 | 0 | 3.52E-52 | 0 | 5.73E-22 | 1 |
| . | | | | | |
| . | | | | | |
| 8 | 1.12654 | 10.8102 | 18.6304 | 4.77E-27 | 1 |
| 9 | 1.77028 | 16.9875 | 12.3265 | 5.61E-13 | 1 |
| 10 | 2.73588 | 24.5232 | 43.247 | 8.73E-12 | 1 |
| 11 | 9.65606 | -2.7E-14 | 83.1283 | 94.1386 | 3 |
| 12 | 22.3699 | -4.8E-12 | 178.805 | 106.131 | 3 |
| 13 | 32.9916 | -102.483 | 115.68 | 78.2718 | 1 |
| 14 | 41.3601 | 0 | 105.929 | 78.9018 | 1 |
| . | | | | | |
| . | | | | | |
| 594 | 3.54056 | 33.97507 | -68.8863 | 0 | 1 |
| 595 | 0 | 0 | -35.1324 | 0 | 1 |
| 596 | 0 | 0 | 0 | 0 | 1 |
| 597 | 0 | 0 | 0 | 0 | 1 |
| 598 | 0 | 0 | 0 | 0 | 1 |
| 599 | 0 | 0 | 0 | 0 | 1 |
| 600 | 0 | 0 | 0 | 0 | 1 |